INFINITE DILUTION ACTIVITY COEFFICIENT MEASUREMENTS OF ORGANIC SOLUTES IN SELECTED DEEP EUTECTIC SOLVENTS BY GAS-LIQUID CHROMATOGRAPHY

by

Nkululeko Nkosi

[BTech. Eng. (Chem)]

Mangosuthu University of Technology, uMlazi

Submitted in fulfilment of the academic requirements for the degree of Master of Engineering in Engineering to the Faculty of Engineering, Department of Chemical Engineering, Durban University of Technology.

Supervisor: Mr Suresh Ramsuroop

Co-Supervisor (s): Dr Kaniki Armel Tumba

: Dr Khalid Osman

July 2017

In loving memory of my parents,

Siphiwe Doris Xulu (Mother)

and

Eric Mpiliza Mwandla (Father)

PREFACE

The work presented in this dissertation was performed in the Research Laboratory in the School of Chemical Engineering at the Durban University of Technology. Mr S. Ramsuroop supervised the work and co-supervised by Doctor K.A. Tumba and Doctor K. Osman.

This dissertation is submitted as the full requirement for the degree of Master of Engineering in Chemical Engineering. The contents presented in this dissertation is original, except where the work of others is stated in the text, the results presented have not been previously submitted to any tertiary institution as part of a degree.

I at this moment certify that the above statement is correct:

_____

N. Nkosi (Candidate)

_____

Date

DECLARATION

I, Nkululeko Nkosi, declare that:

i) The research in this dissertation, except where otherwise indicated or acknowledged, is my original work;
ii) This dissertation has not been submitted for any degree or examination at any other institution;
iii) This dissertation does not contain other person's data, graphs, pictures or other information unless specifically acknowledged as being sourced from other individuals;
iv) This dissertation does not include other individuals writing unless specifically recognised as being sourced from other researchers. Where other written sources have been quoted then:
    a) Their words have been re-written, but the general information attributed to them has been referenced;
    b) Where their exact words have been used, their writing has been placed inside quotation marks referenced.
v) This dissertation does not contain graphics, tables, or text copied and pasted from the internet unless specifically acknowledged and the source being detailed in the dissertation and the references section.

_____

N. Nkosi (Candidate)

_____

Date

As the candidate's supervisor, I approve this Dissertation for submission:

_____ _____

Mr S. Ramsuroop Date

As the candidate's co-supervisor, I approve this Dissertation for submission:

_____ / _____ _____ / _____

Dr K.A. Tumba Date Dr K. Osman Date

ABSTRACT

Many separation processes in the chemical and petrochemical industries are energy intensive, and unfortunately, involve a range of solvents that are environmentally harmful and destructive. Alternative, sustainable separation techniques are desired to replace these conventional methods used in the separation of azeotropic as well as close-boiling mixtures, with the intention of reducing energy costs and adverse impact on the environment.

In the present study, a new class of solvents called deep eutectic solvents (DESs) of Type III were investigated as alternatives to conventional solvents currently employed in separation processes. DESs are classified as 'green' solvents because of a range of favourable properties including lower cost, desirable solubility properties and reduced environmental impact (Abbott *et al.*, 2003b; Smith *et al.*, 2014). The infinite dilution activity coefficients (IDACs) values of 24 solutes – including alk-1-anes, alk-1-enes, alk-1-ynes, cycloalkanes, alkanols, alkylbenzenes, heterocyclics, esters, and ketones – were measured at 313.15, 323.15, 333.15 and 343.15 K by gas-liquid chromatography (GLC) in DESs. The four investigated DESs were as follows: 1) Tetramethylammonium chloride + Glycerol (DES1); 2) Tetramethylammonium chloride + Ethylene Glycerol (DES2); 3) Tetramethylammonium chloride + 1,6 Hexanediol (DES3); and 4) Tetrapropylammonium bromide + 1,6 Hexanediol (DES4).

This work focused on the performance of DESs as extractive solvents for selected azeotropic and close-boiling binary mixtures. The two key performance criteria for these extractive solvents – selectivity and capacity – were determined from experimental infinite dilution activity coefficients (IDACs) of various solutes. The effect of solute molecular structure on IDAC values was investigated. Moreover, the effect of varying the hydrogen bond donors (HBDs) in DESs on IDAC values was examined. Partial excess molar enthalpies at infinite dilution were determined from the experimental IDAC data. Moreover, common industrial separation problems were selected to investigate DES potential to separate various mixtures by determining selectivity and capacity at infinite dilution.

The results obtained in this study indicate that the use of a long carbon chain HBDs greatly decreases miscibility of DESs with organic solutes. For systems such as n-heptane - toluene, acetone - ethanol, cyclohexane - benzene and n-hexane - benzene systems, DES4 was the best solvent regarding the separation performance index.

However, further investigation for DES4 by measurements of vapour-liquid equilibria (VLE) and liquid-liquid equilibria (LLE) data is suggested, as these data would provide additional pertinent information regarding the separation of such mixtures using DES4. The data produced from this study can be used to extend the applicability range of predictive models such as Universal Quasi-Chemical Functional Group Activity Coefficients (UNIFAC) and modified UNIFAC (Do) which are already incorporated in some chemical engineering process simulators.

ACKNOWLEDGEMENTS

I would like to take this opportunity and express my sincerest gratitude to the following individuals and organisations, without whom contribution, this work would not have been possible:

- I would like to express my utmost gratitude to Mr Suresh Ramsuroop for his expert supervision and guidance of the research undertaken. Dr Kaniki A. Tumba and Dr Khalid Osman, the co-supervisors, are sincerely acknowledged for their support, wisdom, ideas and motivation during this work. Working with them has been a great learning experience in many fields;
- My colleagues in Chemical Engineering for their thoughts: S.E Msibi, S. Zondi, E. Tete, M. Chollom, M.S Ndebele, E.T. Ganda, B. Motsvene, P.T. Cherop,……..
- My friends, Nsindiso Nxumalo and Langelihle Masuku who have crossed over from being just my friends to my brothers. You have etched an indelible mark upon my soul, and I am richer knowing you;
- Ayanda Khanyile, The Thermodynamics Research Unit laboratory technician at UKZN by aiding in the building and setting up the equipment used for the research;
- The laboratory technicians at the Department of Chemical Engineering, the Durban University of Technology, in particular, Thokozani P. Ngema for his selfless sacrifice, support and encouragement;
- The financial assistance of the National Research Foundation (NRF) towards my Master's degree is acknowledged;
- Finally and most importantly of all, the Shabalala family, for being so supportive, encouraging and financial assistance, I have made it this far.

TABLE OF CONTENTS

LIST OF FIGURES

CHAPTER TWO: LITERATURE REVIEW

CHAPTER FOUR: EQUIPMENT DESCRIPTION AND EXPERIMENTAL PROCEDURE

CHAPTER FIVE: EXPERIMENTAL RESULTS

CHAPTER SIX: DISCUSSION

APPENDIX B: ORGANIC MOLECULAR STRUCTURE

LIST OF TABLES

CHAPTER TWO: LITERATURE REVIEW

CHAPTER FIVE: EXPERIMENTAL RESULTS

CHAPTER SIX: DISCUSSION

APPENDIX A: ORIGIN, PURITY AND PROPERTIES OF CHEMICALS

APPENDIX C: SAMPLE OF CALCULATIONS

NOMENCLATURE

English letters

A	Parameter (regressed) in the extended Antoine vapour pressure equation
a_t	Polar contribution parameter in correlation of Tsonopoulos (1974)
B	Parameter (regressed) in the extended Antoine vapour pressure equation
B^0	Parameter in the extended Antoine vapour pressure equation
B^1	Parameter in the Wagner vapour pressure equation
B_{ij}	Interaction second Virial coefficient [$cm^3.mol^{-1}$]
B_{virial}	Second Virial coefficient, density expansion [$cm^3.mol^{-1}$]
b_t	Polar contribution parameter in correlation of Tsonopoulos (1974)
C	Parameter (regressed) in the extended Antoine vapour pressure equation
C	Concentration [$mol.cm^{-3}$]
E_i	Ionaisation potential, species (i) [$kJ.mol^{-1}$]
f_i	Fugacity, pure species (i) [kPa]
$\hat{f}_i$	Fugacity, species (i) in solution [kPa]
$f^{(0)}$	Term in correlation of Tsonopoulos (1974), defined by Equation (3-59)
$f^{(1)}$	Term in correlation of Tsonopoulos (1974), defined by Equation (3-60)
$f^{(2)}$	Term in correlation of Tsonopoulos (1974), defined by Equation (3-61)
$f^{(3)}$	Term in correlation of Tsonopoulos (1974), defined by Equation (3-62)
H	Henry's Law constant
H_i	Partial excess molar enthalpy, species (i) in solution [$kJ.mol^{-1}$]
I_C	Criticlal ionaisation potential, [$kJ.mol^{-1}$]

j_2^3	Column pressure correction factor
K_{aw}	Air-water partitioning coefficient
k_i	Capacity
$k_{j,s}$	Capacity of solvent (s)
N_c	Number of carbon atoms in the solute molecule
n_i	Number of moles, species (i) [mol]
P	Pressure [Pa]
P_c	Critcal pressure [Pa]
P_i^{sat} or P_i^*	Saturation vapour pressure, species (i) [Pa]
P_w	Saturation vapour pressure (water), [Pa]
q	Volumetric flow rate [$m^3.s^{-1}$]
R	Universal gas constant [$J.mol.^{-1}.K^{-1}$]
$S_{ij,s}$	Selectivity of species (i) over species (j), in solvent (s)
T	Absolute temperature [K]
T_c	Critical temperature [K]
T_f	Ambient temperature [K]
t_R	Solute retention time (GLC) [s]
t_G	Carrier gas (unretained) retention time (GLC) [s]
U	Outlet voluemtric flow rate (GLC) [$m^3.s^{-1}$]
U_o	Outlet voluemtric flow rate (GLC), corrected [$m^3.s^{-1}$]
V	Volume [m^3]
V_G	Vapor phase volume [m^3]
V_L	Liquid phase volume [m^3]

V_N	Solute retention volume [m^3]
V_C	Critical molar volume [$cm^3.mol^{-1}$]
v_i^*	Solute (i) molar volume [$cm^3.mol^{-1}$]
v_i^∞	Partial molar volume, species (i) [$cm^3.mol^{-1}$]
x_i	Mole fraction, species (i), liquid phase
y_i	Mole fraction, species (i), vapour phase
Z	Compressibility factor

Greek letters

α	Relative volatility/Separation factor
$\alpha_{ij,s}$	Relative volatility of species (i) over species (j), in solvent (s)
γ_i	Activity coefficient, species (i) in solution
μ_i	Chemical potential, species (i)
ω_i	Acentric factor

Subscript

1	Denotes solutes
2	Denotes carrier gas
3	Denotes solvent
c	Denotes a critical property
G	Denote unretained component in equation (3-17)
G	Denote gas phase, except in equation (3-17)
i	Denote pure species
j	Denotes species
ij	Denote interaction properties

L	Denotes liquid phase
M	Denotes mobile phase
f	Denotes bubble flow meter
N	Denotes net retention
o	Denotes outlet
w	Denotes water
r	Denotes a reduce property
sol	Denote the solute property

Supercript

l	Denotes liquid phase
v	Denotes vapour phase
∞	Denotes a value at infinite dilution
sat	Denotes saturated value
exp	Denote experiemntally determined value
lit	Denotes literature value
L	Denotes the property in liquid phase
M	Denotes the propery at mobile phase

Notation

Δ	Denotes the difference

Abbreviations

IGS	Inert Gas Stripping
GLC	Gas-Liquid Chromatography
GC	Gas Chromatography

VLE	Vapour-Liquid Equilibrium
LLE	Liquid-Liquid Equilibria
DEM	Differential Ebulliometry Method
GCM	Group Contribution Method
TCD	Thermal Conductivity Detector
FID	Flame Ionasation Detector
HBD	Hydrogen Bond Donor
DES	Deep Eutectic Solvent
COSMO-RS	Conductor-like Screening Model for Real Solvents
ILs	Ionic Liquids
R.D	Relative Deviation
IDAC	Infiite Dilution Activity Coeffieicient
QAS	Quantanery Ammonium Salt
OCs	Organic Compounds
ChCl	Choline Chloride
ASOG	Analytical Solution of Groups
UNIFAC	Universal Quasi-Chemical Functional Group Activity Coefficients
[HMIM][BTI]	1-hexy-3-methyl-imidazolium bis(trifluormethylsulfonyl)imide
[BMIM][SCN]	1-butyl-3-methyl-imidazolium thiocyanate
[EMIM][SCN]	1-ethyl-3-methyl-imidazolium thiocyanate
[OMIM][PF_6]	1-octyl-3-methyl-imidazolium hexafluorophosphate
[NMP]	*N*-Methyl-2-pyrrolidone
[BMIM][SbF_6]	1-butyl-3-methyl-imidazolium hexafluoroantimonate
[$COC_2N_{1,1,2}$][FAP]	ethy-dimethyl-(2-methoxyethyl)ammonium trifuortris(perfluoroethyl) phosphate
[EMIM][CH_3SO_3]	1-ethyl-3-methyl-imidazolium methanesulfonate
[EPY][BTI]	*N*-ethyl-pyridinium bis(trifluoromethylsulfonyl)imide

CHAPTER ONE

INTRODUCTION

The fundamental importance of the chemical and petrochemical industries towards the growth of the world economy cannot be overstated, as evidenced by the economic value of chemicals produced by these sectors. The vast majority of these chemicals are produced either from reactions or separation processes. In these sectors, accurate and reliable phase equilibrium data is of particular interest as this type of data forms the basis for the design and optimisation of separation processes.

In chemical and petrochemical industries, most separation processes are energy intensive and require the use of solvents. Proper separation solvent selection not only safeguards the environment and minimises expenses for pollution remediation but can also improve the process economics. To optimise these processes, thermodynamic data that quantify the key performance criteria of solvent like selectivity and capacity of extractants at infinite dilution – are required to assess the effectiveness of separation processes.

An activity coefficient is a quantitative indicator of the deviation of a solution behaviour from ideality. At infinite dilution, while there is a high notable intensity of solute-solvent interactions, solute-solute interactions are negligible. These interactions play a fundamental role in the separation of binary mixtures, especially in the separation of azeotropic mixtures and mixtures with close-boiling points. Activity coefficient at infinite dilution is a key parameter in the production of high purity chemicals that use solvents to aid with the separation process.

1.1. Problem statement

Industrial separation processes such as extraction/azeotropic distillation and liquid-liquid extraction use a large volumes of organic compounds (OCs). However, used solvents from separation processes are often toxic and volatile, rendering them environmentally ‘unfriendly’. Therefore, the solution is to pursue better, green solvents for new and existing processes. An effort has been made to investigate an alternative green solvent to improve the following: minimising environmental impact and energy costs, and refining the efficiency of existing extraction processes of close-boiling as well as azeotropic mixtures. Ionic liquids (ILs) as alternative solvents to OCs are currently under extensive investigation due to their properties favourable to the environment such as non-reactive with water, more biodegradable and less toxic. However, the processes to synthesise and purify ILs

are expensive and difficult to achieve. Such disadvantages which have limited their large-scale industrial applications (Xu *et al.*, 2015).

1.2. Scope of the study

This study focuses on deep eutectic solvents (DESs) as alternative green solvents to ILs and organic solvents for liquid-liquid extraction or extractive distillation of certain key close-boiling or azeotropic systems that have, as of yet, not been studied. DESs are cheaper and more environmentally friendly because they are sometimes derived from renewable and non-toxic bio-resources, and they share similar properties with ILs.

In this study, interactions between DES and solutes with the following functional groups, were investigated and analysed by gas-liquid chromatography (GLC): alk-1-anes, alk-1-enes, alk-1-ynes, cycloalkanes, alkanols, alkylbenzenes, heterocyclic, ketones and esters.

To date, no investigation has been conducted on activity coefficients at infinite dilution in the four different DESs examined in the study. From experimental IDAC data, selectivities and capacities were obtained for systems, which are of particular interest to the petrochemical and chemical industries. The following solvents were used during this study:

- Tetramethylammonium chloride + Glycerol; and the molar ratio is [1:2]
- Tetramethylammonium chloride + Ethylene Glycol; and the molar ratio is [1:2]
- Tetramethylammonium chloride + 1,6 Hexanediol; and the molar ratio is [1:1]
- Tetrapropylammonium bromide + 1,6 Hexanediol; and the molar ratio is [1:2]

In this study, IDAC measurements were conducted at temperatures ranging from 313.15 to 343.15 K in order to compare and justify the benefits of using DESs in industrial separation processes. The selected hydrocarbon combinations for which DES performance was compared and listed are as follows: n-hexane/hex-1-ene, n-hexane/benzene, methanol/benzene, cyclohexane/benzene, cyclohexane/ethanol, acetone/ethanol and n-heptane/toluene.

However, before using above solvents, the test systems were measured to verify the experimental setup and procedure in measuring activity coefficients at infinite dilution. The test systems used were n-hexane, cyclohexane, toluene, and benzene in hexadecane solvent at temperatures ranging from 323.15 to 333.15 K.

1.3. Aim and objectives of the study

The aim of this study was as followed:

- to carry out preliminary assessment of selected DESs as potential agents to enhance a broad range of separation processes, including those involving close-boiling and azeotropic binary mixtures.

Objectives were as follows:

- to measure the infinite dilution activity coefficient of selected organic solutes in a specific type of DESs at various temperatures;
- to analyse these data so as to determine the separation performance by determining the selectivity and capacity of the DESs as solvents; and
- to benchmark DESs against currently used industrial solvents and ILs.

1.4. Outline of the thesis

The outline of this thesis is as follows:

Chapter One presents an introduction to the study.

Chapter Two continues with a detailed review of techniques and solvents that have been used previously by scientific researchers for the measurement of activity coefficients at infinite dilution.

Chapter Three presents a consideration of thermodynamic fundamentals relevant to this study.

Chapter Four focuses on the experimental equipment and procedures used in this current study.

Chapter Five presents the measured results for test systems that are used to verify the experimental setup and procedure. Moreover, new IDAC data of investigated DESs are reported.

Chapter Six presents the discussion of the results and proceeds to compare the separation performance of the investigated DESs to that of other industrial solvents.

Chapter Seven presents the conclusions of this study and offers recommendations based on the research findings.

CHAPTER TWO

LITERATURE REVIEW

Chapter Overview

This chapter reviews deep eutectic solvents in general and includes, inter alia, including the general naming of Deep Eutectic Solvents (DESs); a brief history detailing the development of DESs classification; and some interesting properties of DESs.

There is a myriad of techniques and equipment available for the measurement of infinite dilution activity coefficients (IDACs). As a result, it is important that the correct technique is employed for the purpose for which it is intended. The purpose of this chapter is not to present an exhaustive review of all experimental methods for the determination of IDACs; rather, it will consider the methods that are most widely used today. The most widely used techniques for measuring IDACs include gas-liquid chromatography method; differential ebulliometry method; and inert gas stripping method.

For an excellent review of the other methods in the determination of IDACs, other publications are available (Muhlbauer, 1997; Tumba, 2010).

A detailed examination of the gas-liquid chromatography method, the technique used in this work, follows.

2.1 Deep eutectic solvents

2.1.1 Definition

DESs are compounds formed from a mixture of organic salts, typically simple quaternary ammonium salts (QAS) and metal salt hydrates, or a hydrogen bond donor (HBD), that melts at or below 100 ^{o}C (Abbott *et al.*, 2003b). They are synthesised into Class I, II, and III DESs respectively, as shown in Table 2-1, with their general formulae presented in Table 2-2. The term eutectic mixture relates to a lower melting temperature of a mixture than that of individual components, as depicted in Figure 2-1.

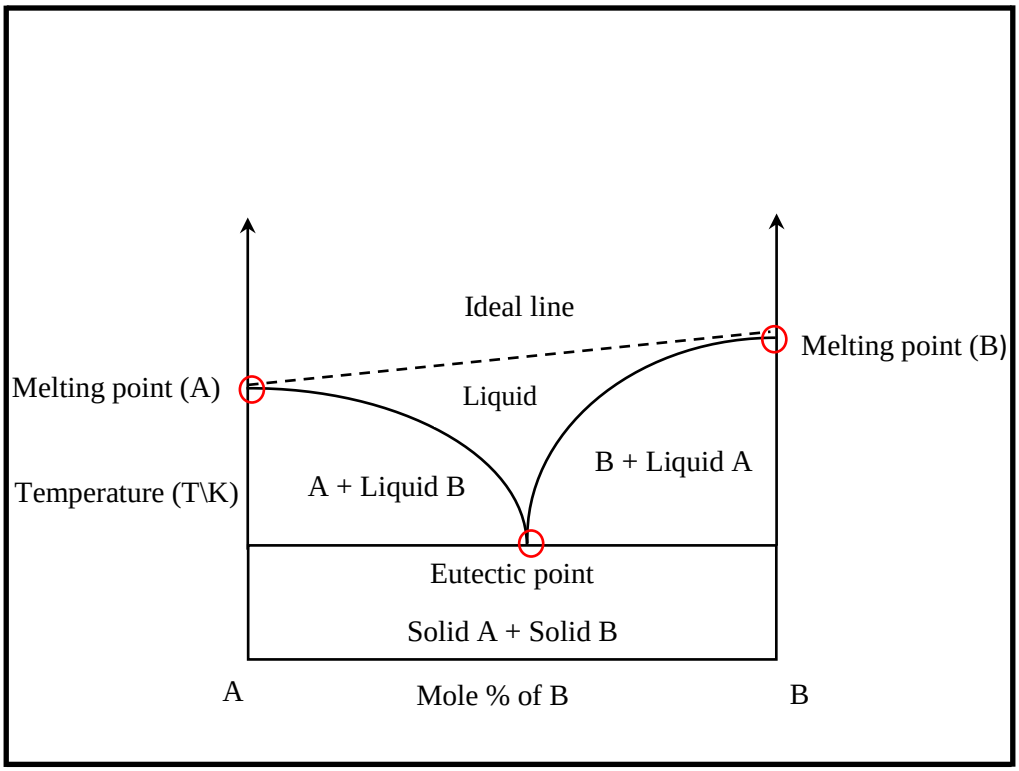

Figure 2-1: The solid-liquid phase diagram for a DES forming components A and B.

2.1.2 Background

In 2001, Abbott *et al.* (2003b) reported DESs as new potential 'green' alternative solvents as compared to ILs. This was due to issues surrounding ILs such as the high cost of synthesis and the costly starting materials, and also the problems associated with sensitivity to water, especially impurities. According to the literature, DESs could be considered an extension of the ILs because they share similar physical properties and characteristics (Abbott *et al.*, 2003b). DESs are a category of ionic solvents that are formed from an eutectic mixture of Brønsted/Lewis acids and bases containing a variety of anionic and cationic species (Abbott *et al.*, 2003b).

Another class (Type IV) of DESs could also be prepared by mixing metal salt hydrates as a replacement for the organic salts used in Type I, II, and III DESs with hydrogen bond donors (HBDs). Tables 2-1 and 2-2 show the classification of DESs and their general formulae (Abbott *et al.*, 2003b).

Table 2-1: The classification of DESs (Abbott *et al.*, 2014; Smith *et al.*, 2014)

Classification	Solvents
Type I	Organic salt + metal salt
Type II	Organic salt + metal salt hydrate
Type III	Organic salt + HBD
Type IV	Metal salt + HBD

Table 2-2: The general formulae of all DESs classes (Abbott *et al.*, 2014; Smith *et al.*, 2014)

Classification	Formulae	Terms
Type I	$Cat^+X^-•zMCl_x$	M = Zn, Sn, Fe, Al
Type II	$Cat^+X^-•zMCl_x•yH_2O$	M = Cr, Co, Cu, Ni, Fe
Type III	$Cat^+X^-•zRZ$	Z = COOH, $CONH_2$, OH
Type IV	$zMCl_{x-1}•RZ+MCl^+_{x+1}$	Z = $CONH_2$, OH
		M = Zn, Al, Cr

where X, is a halide anion; z, refers to the number of Y molecules that interact with the anion: R, Alkyl group.

The present study will assess Type III DESs. The first use of this class of solvents was proposed and reported by Abbott *et al.* (2003b) who investigated a DES having a melting temperature of 12 ^{o}C. They synthesised a DES consisting of choline chloride (ChCl) and Urea in a 1:2 respective molar ratio. Various components used to synthesise DESs are shown in Figures 2-2 and 2-3. They can also be constituted by using other HBDs such as alcohols, acids, amines, sugars, and polyols (Abbott *et al.*, 2003b; Xu *et al.*, 2015). An extensive literature survey reveals that the most reported DESs are organic solvents from ChCl-based in combination with the different type of HBDs (Abbott *et al.*, 2003b; Hua Zhao, 2013; Ghareh Bagh *et al.*, 2015; Mohsenzadeh *et al.*, 2015; Radosevic *et al.*, 2015; Verevkin *et al.*, 2015; Wen *et al.*, 2015; Xu *et al.*, 2015).

Abbott *et al.* (2003b) also investigated monocarboxylic acids in an attempt to form DESs, but the solvent formation was impossible as the melting point of Type III DESs depends on the interaction between the salt and the HBD, and the magnitude of the lattice energy of organic salt and HBD. According to recent research, the strong salt-HBD interaction results in a weaker interaction between the cation and the anion of the organic salt, giving rise to a more disordered system, and thus a lower melting point (Abbott *et al.*, 2003b).

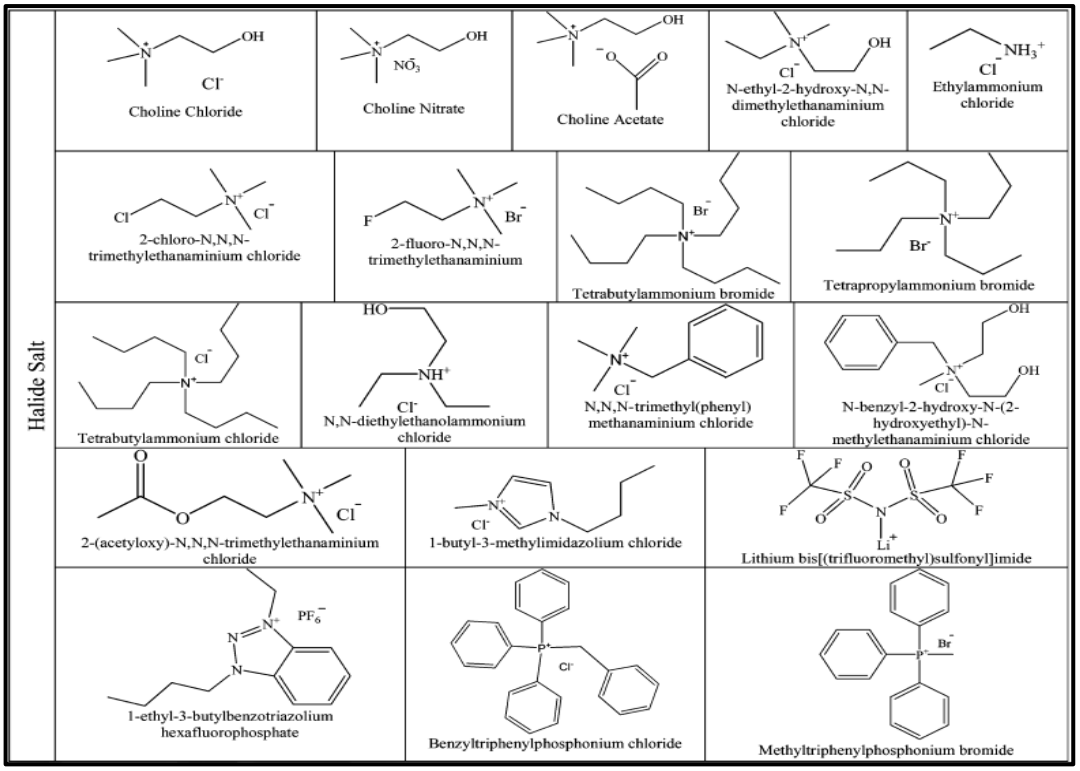

Figure 2-2: Examples of commonly used organic salts structures in the preparation of DESs (García *et al.*, 2015).

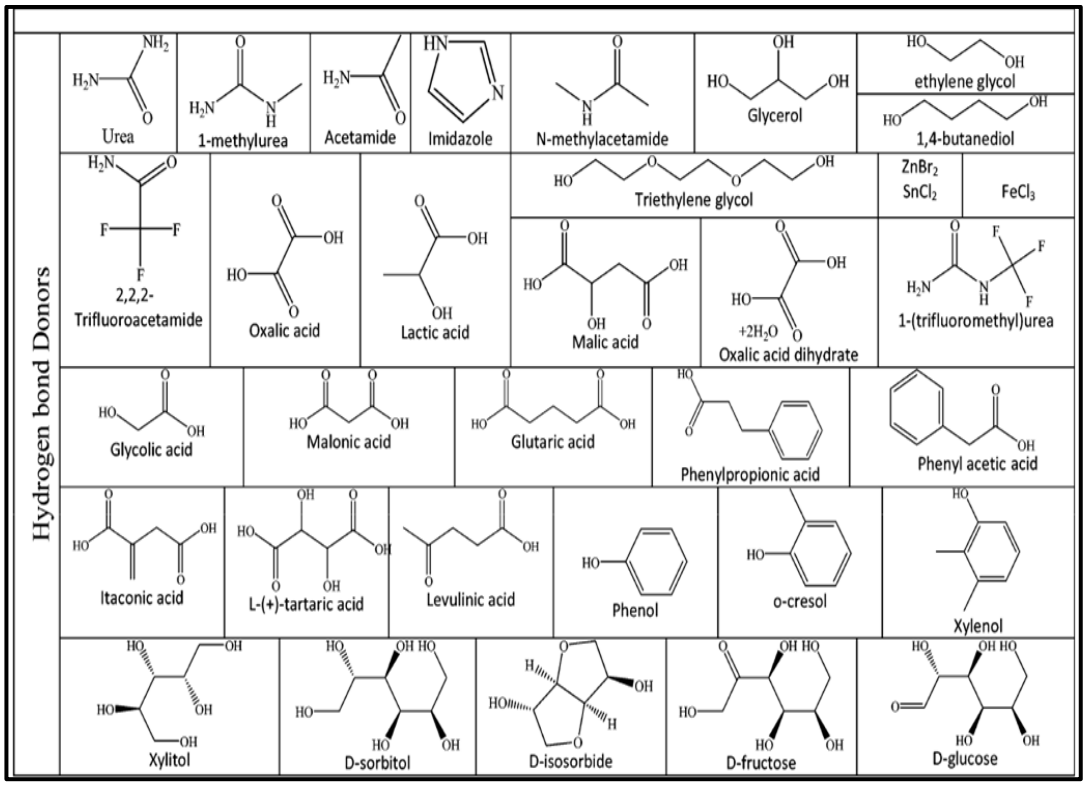

Figure 2-3: Examples of commonly used HBD structures in the preparation of DESs (García *et al.*, 2015).

2.1.3 Properties of deep eutectic solvents

Physicochemical and thermodynamic properties of substances – such as density, viscosity, freezing point or conductivity – are important as they help to identify their limitations in industrial applications. Most organic solvents have an adverse effect on the environment as they are toxic and hazardous. Organic compounds are considered unsafe for the environment as they contribute to ozone layer depletion (Anastas and Kirchhoff, 2002; Clark and Tavener, 2007). Consequently, an effort to substitute OCs has been made to investigate some potential alternative solvents that are more environmentally benign for use in chemical processes. In this regard, solvents such as water, supercritical fluids, ILs, or solvent-free processes, have been investigated (Clark and Tavener, 2007). However, it is still difficult to find suitable 'green' solvents as an alternative to OCs. For a solvent to be considered 'green' with respect to the environment, there are certain criteria that must be met (Anastas and Kirchhoff, 2002), as depicted in Table 2-3:

Table 2-3: Criteria in selecting a 'green' solvents (Plechkova and Seddon, 2008)

Criteria	Reasons
Price	Ensure stability of the chemical process; solvent should be cost effective
Grade	In purification, to prevent energy consumption, technical grade solvents are preferred
Availability	Ensuring a constant availability, the solvent should be available in bulk
Recyclability	Using eco-efficient procedures, spent solvent should be fully recycled in a chemical process
Synthesis	The preparation of solvent should be through an energy saving process, and the synthetic reaction should be highly atom-efficient
Performance	Solvents should show similar or superior performances to be eligible over currently used solvents
Flammability	To ensure safety, solvents should be non-flammable
Stability	In a chemical process, the solvent needs to be chemically and thermally stable
Storage	To adhere with all legislations to be transported by any means of transport, solvent storage should be viable
Renewability	Concerning carbon emissions, renewable raw materials are to be used when synthesising the solvent
Biodegradability	The solvent should be biodegradable and not produce any toxic metabolites
Toxicity	Solvents have to exhibit a negligible toxicity to reduce the risk to nature or humans

In reality, a solvent that meets all these criteria is difficult to find. However, DESs meet the most of the said criteria. Abbott *et al.* (2003b) and Smith *et al.* (2014), have intensively investigated the properties of DESs. These researchers reported that DESs exhibit similar properties to those of room temperature ILs suggesting that they may be alternative solvents to OCs due to their attractive properties (Abbott *et al.*, 2003b):

- higher biodegradability and biocompatibility as ‘green‘ solvent;
- high chemical and thermal stability;
- negligible vapour pressure;
- non-flammability;
- low toxicity;
- wide liquid range; and
- chemical compatibility with water.

Abbott *et al.* (2003b) and Smith *et al.* (2014) reported that DESs lead to a vast number of eutectic mixtures with different properties, by simply changing one or both components. The properties of DESs are discussed in the following sub-sections.

2.1.3.1 Density

In general, density is one of the most important fluid properties in industrial processes. The effect of pressure and temperature on density is a prerequisite to the development of suitable equations for the design of industrial separation processes (Smith *et al.*, 2001).

DESs generally exhibit higher density values than water, and their density is similar to that of ILs which vary between 1.1 $g.cm^{-3}$ and 2.4 $g.cm^{-3}$ (Shahbaz *et al.*, 2011b). DESs similar to ILs are thought to be composed of unfilled vacancies and holes that govern density behaviour (García *et al.*, 2015). To date, an extensive literature survey reveals little data on DESs that are available at atmospheric conditions.

The factors that affect DES density are temperature, the composition of water by mass, and organic salt to the HBDs molar ratio (Shahbaz *et al.*, 2011b; Leron *et al.*, 2012). In general, DES density increases with decreasing temperature. Furthermore, DES density increases with decreasing percentages of water content, and increases with a decreasing chain length of the anion (García *et al.*, 2015).

The practical importance of DES density in separation processes and the very large number of organic salts-HBDs mixtures justify the need to develop predictive models - such as structure-property relationships - that will allow effective screening of DESs in view of industrial applications (García *et al.*, 2015).

2.1.3.2 Melting point

The melting point is an inverse process of freezing. The melting point of a DES depends on the choice of the HBD, organic halide salt, and the mixture composition (Xu *et al.*, 2015). Most of the available literature concerns binary systems more than ternary systems. The solid-liquid phase diagram for these binary systems is illustrated in Figure 2-1.

The melting point of DESs is the most remarkable and perhaps their most valuable property. If a predictive method is to be developed, the relationship between melting point and the structure of DESs is of great value. Organic salts exhibit far lower melting, whereas metal salts have a high melting point (Sarwono M.M., 2013; Mohsenzadeh *et al.*, 2015; Xu *et al.*, 2015). For instance, the DES synthesis, first reported by Abbott *et al*., (2003b) was a mixture of ChCl and Urea, in a 1:2 respective molar ratio. However, the melting points for pure individual components (ChCl and Urea) are 134 ^{o}C and 302 ^{o}C, respectively.

There is no clear correlation between the melting point of the pure component, and the freezing point of the components that could be drawn. The lattice energy of the DES depends on the changes that arise from the interactions of entropy, anion or HBD to form a clear liquid (Abbott *et al.*, 2003b; Leron *et al.*, 2012).

2.1.3.3 Viscosity

Mixture viscosity is crucial for practical applications as it determines mass transfer rate in industrial processes. This property depends on ions size (Abbott *et al.*, 2003b; Hayyan *et al.*, 2013; García *et al.*, 2015). Although DESs are reported to have favourable properties, they exhibit vast viscosities at ambient temperature (higher than 100 cP) as compared to organic solvent.

Extremely large viscosities will give rise to process design problems in liquid-liquid extraction and extractive distillation which rely on efficient mass transfer. These viscous DESs will lead to high pumping costs requiring equipment oversizing and resulting in higher costs for separation processes

(Mohsenzadeh *et al.*, 2015). However, DESs formed by using small quaternary ammonium salts (QASs) and fluorinated HBD such as ethylammonium and trifluoroacetamide, exhibit low viscosity (García *et al.*, 2015). The very attractive option to lower DES viscosity and pumping costs is an addition of a controlled amount of water, a method which must be done with caution as it could affect other properties of DESs.

Viscosity is affected by the intensive hydrogen-bond network (for example, longer fluorinated chains), temperature, mixture composition, and water content (Shahbaz, 2013; Liu *et al.*, 2014; García *et al.*, 2015). The viscosity of DESs follows an Arrhenius-like behaviour as it increases with decreasing temperature. Furthermore, DESs have larger viscosity than water as the value increases with decreasing moisture content, where the forces such as van der Waals and electrostatic interactions lead to higher viscosity.

For practical purposes, high viscosities are not desirable due to high-energy requirements (Sarwono M.M., 2013).

DESs are likely to be cross-contaminated in reactions or separation by other chemicals (Abbott *et al.*, 2003b; Hua Zhao, 2013). This could affect the physicochemical properties of DESs, so it is necessary to know what and how much is contaminated as this will be essential for design system tolerances.

2.1.3.4 Conductivity

The ability of a material to conduct electrical current depends on the valence, free ions, and their mobility. Conductivity is primarily evaluated using Hole theory (Smith *et al.*, 2014), a method which allows the evaluation of activation energy, resulting in conclusions similar to those reported for viscosity. Abbott *et al.* (2003b), adopted this method to predict the conductivity of the DES consisting of an organic halide salt mixed with Urea as HBD in a molar ratio of 1:2.

Deep eutectic solvent conductivity and viscosity have a strong correlation due to their exhibited Arrhenius-like behaviour. These solvents show poor conductivity (at ambient condition, conductivities are lower than 1 $mS.cm^{-1}$) due to their excessive viscosities. The addition of organic halide salts to HBDs increases conductivity and lowers viscosity due to the additional available carriers in increasingly less viscous DESs.

2.1.3.5 Surface tension

Surface tension is an important physicochemical property for the purpose of mass transfer operations. Highly viscous DESs exhibit higher surface tension due to strong intermolecular force between HBDs and corresponding organic halide salts (Dávila *et al.*, 2007; Aparicio *et al.*, 2009). The surface tension of DESs is greater than that of ILs, a property which is a measure of the strength of DESs (Smith *et al.*, 2014). Further, DESs surface tension is higher in comparison with pure organic compounds (i.e. benzene and hexane) but lower than water. However, these ranges of DESs and organic components are necessary for separation processes (such as a liquid-liquid extraction). The cation type has a significant effect on the surface tension because of its hydrogen-bond ability. Moreover, surface tension increases with decreasing temperature, and increases with decreasing salt concentration (Abbott *et al.*, 2011; Francisco *et al.*, 2013; Jibril *et al.*, 2014; Ventura *et al.*, 2014).

2.1.4 Applications of DESs

To date, DESs applications and research are in their infancy even though they are liquid at ambient condition and show some interesting advantages. However, they might be an alternative to ILs that have been proposed for many applications as they significantly contribute to a reduction of environmental impact in many processes. Table 2-4 presents an overview of potential applications of DESs in the chemical industry.

Table 2-4: Potential use of DESs in the chemical industry (Plechkova and Seddon, 2008).

Chemical industry	Application
Electrochemistry	The electrolyte in batteries, electro-optics, solar panels, fuel cells and metal plating
Biological uses	Embalming, drug delivery, biocides, personal care and biomass processing
Analysis	The stationary phase for GC columns, HPLC and the matrices for mass spectrometry.
Solvents and catalysis	Synthesis, catalysis, nano-chemistry, multiple reactions, extractions and catalysis
Engineering	A dispersing agent, plasticisers, lubricants, coatings, and plasticisers

DESs are economically viable and highly attractive to a broad range of industries specifically because of desirable properties. This was observed when a relatively small amount of DES added

in a catalyst synthesis showed significant improvements in activity, selectivity, and a lifetime of some homogeneous catalysts (Shahbaz *et al.*, 2011a; De Santi *et al.*, 2012; Gu *et al.*, 2015). As a result, DESs-based processes can certainly be considered as alternatives to some large-scale industrial processes.

An in-depth study conducted by Smith *et al.* (2014) on the applications of DESs inspired researchers to investigate industrial separation processes based on these solvents. To date, DESs have been studied in a wide range of applications related to the chemical industry including the following (Abbott *et al.*, 2003a; Jhong *et al.*, 2009; Morrison *et al.*, 2009; Skopek *et al.*, 2009; Lawes *et al.*, 2010; Gutiérrez *et al.*, 2011; Serrano *et al.*, 2012):

- use in analytical devices;
- alternative electrolyte to water and organic solvents for the study of conducting polymers;
- drug solubilization vehicles;
- synthesis of carbon electrodes for capacitors;
- electrolyte for dye-sensitised solar cells; and
- lubrication of steel/steel contacts.

This present study has focused on the assessment of some DESs as potential solvents to replace OCs in separation processes. Emphasis was placed on industrial systems that exhibit azeotropes or close-boiling systems as such systems are difficult to separate by conventional means. In recent years, investigations into DESs as alternative solvents for many industrial processes have proliferated, motivated by an in-depth study by Smith *et al.* (2014) for applications of DESs. However, to date, there is no thorough extensive investigation on assessment of DESs in azeotropic and close-boiling mixtures.

2.2 Activity coefficient at infinite dilution

2.2.1 Definition

Activity coefficient (γ_i) is a measurement of the non-ideality of the solute in the mixture (Smith *et al.*, 2001). Thus, activity coefficient accounts for the deviation in the behaviour of real systems from ideal systems. It can be defined by the following equation:

$$\gamma_i = \frac{\hat{f}_i}{x_i f_i} \tag{2-1}$$

where: x_i, is the molar fraction of the component i in the mixture;

$\hat{f}_i$, is the fugacity of the component i in the mixture; and

f_i, is the fugacity of pure component i.

For an ideal solution, $\gamma_i = 1$. Departure from ideality can also be expressed in terms of activity (a_i) defined as a ratio of fugacity to fugacity of component i (mixture and pure) at its standard state (Smith *et al.*, 2001).

$$a_i = x_i \gamma_i \tag{2-2}$$

2.2.2 Importance of IDACs

Infinite dilution activity coefficient, (γ_i^{∞}) is an important property playing a critical role in environment and chemical engineering. It is defined as the limiting value of activity coefficient when the concentration tends to zero (Seader *et al.*, 2011). In the chemical industry, IDACs can provide accurate and useful phase equilibria data for systems that are in the dilute region (Seader *et al.*, 2011). Furthermore, IDAC data aid in the design of various separation units for high purity chemicals. This is significant as the last traces of impurities require the greatest separation effort for removal, to achieve high purity chemicals.

Infinite dilution activity coefficient measurements can guide in pre-selecting a suitable solvent for a specific separation process. This property permits the calculation of parameters necessary for the commercial design of separation processes. Hence, one of the most important applications of activity coefficient at infinite dilution includes the description of the behaviour of mixtures in their dilute regions. This is relevant to the following areas:

- environmental pollution remediation: the effort to remove last traces of impurities, is difficult, costly and energy intensive.
- industrial processes: the production of high purity products by raising the purity of chemicals at lower costs.

The investigation of the dilute region is important for both practical and theoretical purposes. The following sub-section discusses applications of activity coefficients at infinite dilution in Chemical

Engineering.

2.2.3 Practical and theoretical applications of IDACs

The practical and theoretical applications of IDACs in chemical engineering include the following:

- improvement of the understanding of theory for liquid solutions (Smith *et al.*, 2001);
- predictions of the existence of azeotropes (Seader *et al.*, 2011);
- screening of solvents for solvent extraction and extractive distillation processes (Seader *et al.*, 2011);
- characterisation of the behaviour of liquid mixtures (Weir and de Loos, 2005);
- calculation of partition coefficient and Henry's Law constants (Smith *et al.*, 2001);
- prediction of retention volumes in gas chromatography, (Weir and de Loos, 2005); and
- determination of molar enthalpies of solutions, (Smith *et al.*, 2001).

2.2.3.1 Screening of solvents for extraction and extractive distillation processes

The potential solvent in separation processes can be determined on the basis of experimental activity coefficients at infinite dilution data (Tumba, 2010). From IDAC data the selectivity ($S_{ij,s}^{\infty}$) and the capacity ($k_{j,s}^{\infty}$) of the solvent can be calculated. These two parameters have an important role in selecting the suitable solvent as an entrainer in azeotropic extractive distillation, as well as, liquid-liquid extraction columns for the separation of any systems, including for mixtures that form azeotropes or close-boiling mixtures. The appropriate entrainer should exhibit high values of selectivity and capacity. Equations (2-3) and (2-4) are used to calculate selectivity and capacity.

$$S_{ij,s}^{\infty} = \frac{\gamma_i^{\infty}}{\gamma_j^{\infty}} \tag{2-3}$$

and

$$k_{j,s}^{\infty} = \frac{1}{\gamma_j^{\infty}} \tag{2-4}$$

where ($S_{ij,s}^{\infty}$), is the selectivity at infinite dilution of solvent (s) for a particular system consisting of *i* and *j*, while ($k_{j,s}^{\infty}$), the capacity of solvent (s) at infinite dilution, is the measure of the amount

of component (j) that is capable of dissolving in the solvent (Smith *et al.*, 2001).

2.2.3.2 The predictions of existence of azeotropes

Activity coefficients at infinite dilution data can be used to predict if an azeotropic exists and the condition at which a binary mixture azeotrope occurs. For mixtures that indicate positive deviation from Raoult's Law ($\gamma_i^{\infty} > 1$), an azeotrope with a pressure-maximum (minimum temperature) occurs. However, for mixtures that indicate negative deviation from Raoult's Law ($\gamma_i^{\infty} < 1$), an azeotrope with the binary pressure-minimum (maximum-temperature) occurs. In such cases, the equations below apply (positive and negative deviations), Equations (2-5) and (2-6).

$$\left(\ln \gamma_j^{\infty}\right) > \ln\left(\frac{P_i^{sat}}{P_j^{sat}}\right) > -\left(\ln \gamma_i^{\infty}\right) \tag{2-5}$$

and

$$\left(\ln \gamma_j^{\infty}\right) < \ln\left(\frac{P_i^{sat}}{P_j^{sat}}\right) < -\left(\ln \gamma_i^{\infty}\right) \tag{2-6}$$

where ($\gamma_{i,j}^{\infty}$) is the activity coefficient of component (i) and (j) at infinite dilution and (P^{sat}) saturation vapour pressure for both components (i) and (j).

This prediction is necessary as it prevents an over design of the distillation column and minimises both investment and operating costs (Seader *et al.*, 2011).

2.2.3.3 The calculation of partition coefficient and Henry's Law constant

In the chemical industry, environmental pollution is posed by discharges through wastewater effluents, evaporation and spills. Most of these pollutants have carcinogenic potential and are toxic. Thus, in waste water treatment, activity coefficients at infinite dilution can be used to characterise air-water partitioning coefficients (K_{aw}) for pollutants. Moreover, they can be used as a qualitative measure of the volatility of a substance and its whereabouts in nature. These parameters are closely related to Henry's Law constant H_{ij} under the assumption that the vapour phase behaves as an ideal gas. In this case, Equation (2-7) relates Henry's law constant to infinite dilution activity

coefficient:

$$\gamma_{sol}^{\infty} = \frac{H_{ij}}{P_{sol}^{sat}} \tag{2-7}$$

and

$$H_{ij} = \gamma_{sol}^{\infty} P_{sol}^{sat} \tag{2-8}$$

It follows that:

$$K_{aw} = \frac{\gamma_{sol}^{\infty} P_{sol}^{sat} v_w^{L}}{RT} \tag{2-9}$$

where, P^{sat}, v_w^{L} and R are the saturation vapour pressure of pure liquid solute, the molar volume of pure water, and the ideal gas constant, respectively; whereas, T is the absolute temperature.

2.2.3.4 Characterisation of the behaviour of liquid mixtures

The activity coefficient data determined at infinite dilution provides useful information about the behaviour of a given mixture. At infinite dilution region, the molecular interaction that is occurring is only those between solute and solvents, whereas those of solute and solute can be ignored (Alessi *et al.*, 1991). Activity coefficient values at infinite dilution are used to demonstrate the maximum deviation from ideality. The liquid will be ideal when the activity coefficient value is equal to unity ($\gamma_i^{\infty} = 1$); however, activity coefficients for a non-ideal liquid at infinite dilution are either greater or less than unity.

2.2.3.5 The prediction of retention volumes in a gas chromatograph (GC)

The success of GC analysis depends, to a considerable degree on the choice of stationary phase and identification parameters. In stationary phase selection, it is crucial to take into account the nature of the substance to be measured. Polarity and selectivity, for example, are of decisive importance in the choice of stationery phase. Gas-liquid chromatography (GLC) utilises the changes of three necessary thermodynamic parameters of chemical and physical processes involved in a system, such as IDACs.

However, the measurements of the amount of stationary phase in a capillary column are difficult. To overcome this, indirect ways are recommended to estimate specific retention volumes from capillary columns. This could be obtained by determining the mass of stationary phase from specific retention volumes obtained on packed column, or using a standard solute with partition data measured on packed column.

2.2.3.6 Determination of excess molar enthalpies of solutions

The effect of temperature change on activity coefficient is presented by Gibbs-Helmholtz Equation (2-10).

$$\left[\frac{\partial\left(G^E/RT\right)}{\partial T}\right]_{p,x} = -\frac{H^E}{RT^2} \tag{2-10}$$

The excess properties are related to the activity coefficient by the Gibbs-Duhem Equation which leads to the following relations:

$$\left(\frac{\partial \ln \gamma_i}{\partial T}\right)_{p,x} = -\frac{H_i^E}{RT^2} \tag{2-11}$$

and

$$\left(\frac{\partial \ln \gamma_i^{\infty}}{\partial\left(1/T\right)}\right)_{p,x} = -\frac{\Delta H_i^{E,\infty}}{R} \tag{2-12}$$

where $\Delta H_i^{E,\infty}$ and R are the slope of the fitted line partial excess molar enthalpy at an infinite dilution that can be obtained directly from the straight line (derived from Equation (2-12)) and ideal gas constant; and (T) is the experimental temperature.

The model of the form below (Equation (2-13)) was fitted to the experimental IDAC data of selected solutes (Heintz *et al.*, 2001). Heintz *et al.* (2001) suggested the use of this equation to determine the standard deviation of measured values from the fitted line.

$$\ln \gamma_i^{\infty} = A + B/T \tag{2-13}$$

In this study, the above equation was used to determine excess molar enthalpies of solution from

experimental data, through linear regression.

2.2.4 Experimental and predictive methods for the determination of IDACs

Activity coefficients at infinite dilution can be measured either by direct or indirect methods. Indirect methods involve the extrapolation directly from existing vapour-liquid equilibrium data (VLE). The use of these methods has always led to results of dubious quality when care is not taken (Palmer, 1987). Direct methods involve measurements in the dilute region and usually provide more accurate results than indirect methods.

2.2.4.1. Predictive methods used to determine IDACs

The measurement of phase equilibrium data for multi-component systems is costly and time-consuming. However, the prediction of phase equilibrium data without any available experimental data is becoming possible. This is attainable through some reliable thermodynamic predictive models. Furthermore, this predicted data allows for the possibility of estimating residual lines for ternary systems and for the development of simulators as well as for the efficient design of extraction processes. These methods include the following:

- Group Contribution Methods GCMs;
- Solvatochromic Parameters for Activity Coefficient Estimation (SPACE);
- Conductor-like Screening Model for Real Solvents methods (COSMO-RS);
- Quantitative Structure-Property Relationship (QSPR);
- Group Contribution Solvation Model (GCS);
- Linear Solvation Relationships (LSR); and
- Modified Separation of Cohesive Energy Density (MOSCED).

A brief description of GCMs and COSMO-RS as the most widely employed methods by researchers will be discussed in the following sub-sections.

Group Contribution Methods (GCMs)

GCM is an efficient and successful predictive method as far as predicting IDACs is concerned, is one of the simplest forms in estimating IDACs as it requires only molecular structure knowledge. This concept considers each molecule as the sum of the functional groups that constitute molecules.

Also, the IDAC of the solution is correlated not regarding molecules but regarding the functional groups contained in the mixture (Fredenslund *et al.*, 1975).

The major models such as UNIFAC (Universal Quasi-Chemical Functional Group Activity Coefficients), modified UNIFAC, and ASOG (Analytical Solution of Groups) are most commonly used models by researchers to predict IDAC in the liquid phase. These models contain the group interaction parameters which are commonly predicted from experimental data. A large number of experimental data is required to fit the group interaction parameters.

The fundamental assumption of GCMs states that any interaction made by one group to another is assumed to be of independent material properties. However, this assumption will only be considered if the interaction of groups in a molecule does not affect the nature of each other within that molecule (Fredenslund *et al.*, 1975; Prausnitz, 1980).

Despite their common use and a wide range of applications, these methods have several disadvantages due to the undetermined group proximity effects which view molecules as a collection of individual groups (Fredenslund *et al.*, 1975). This results in a poor performance for systems whose components differ in size and when predicting IDACs.

Application of UNIFAC Method

The UNIFAC method was originally published by Fredenslund *et al.* (1975). The group interaction parameters matrix of this model is continuously updated so as to improve model performance and expand its use. This model provides an accurate and reliable method to predict VLE data based on group contributions.

This method can calculate the IDACs of the non-electrolyte and non-polymeric liquid phase mixtures. Different GCMs are used to calculate these properties. However, its application is limited by input variables that should range from low to moderate pressures and temperatures between and 152 ^{o}C (Fredenslund *et al.*, 1975; Fredenslund *et al.*, 1977).

The UNIFAC method is regarded by far as the most successful model, and applicable in various areas such:

- to calculate vapor-liquid (VLE), solid-liquid (SLE), liquid-liquid (LLE) equilibrium data;

- to predict thermodynamics properties (such as excess enthalpies, gas solubility and pure component vapour pressure); and
- to determine flashpoints of solvent mixtures.

The advantages and limitations of the UNIFAC method are expounded in Table 2-5.

Table 2-5: Potential benefits and disadvantages of using UNIFAC method (Fredenslund *et al.*, 1975)

Advantages	Disadvantages
Capable of producing accurate and reliable VLE data for binary systems.	Limited to a specific range of temperature (between 303.15 and 425.15 K)
Represent mixtures of widely different molecular sizes.	For mixtures containing polymers, the UNIFAC method does not apply
Uses only two adjustable parameters.	UNIFAC method only considers condensable components
	Limited to available group- interaction parameters for LLE data
	Limited to moderate pressure.

Applications of ASOG

The ASOG model was originally published by Wilson and Deal (1962) to evaluate VLE data of a binary system. While this model has common thermodynamics basis as UNIFAC, the ASOG model has been widely superseded by the UNIFAC method because it is limited to temperatures near ambient (Wilson and Deal, 1962; Kojima and Tochigi, 1979).

COSMO-RS

The COSMO-RS model originally published by Klamt (1995), is an extension of a dielectric continuum solvation model to liquid phase thermodynamics. The main objective of introducing this model was to determine a new approach for describing the dependence of IDAC on the mixture temperature and composition (Klamt, 1995).

This predictive model is a viable alternative to traditional GCMs as it requires quantum mechanical (QM) calculations instead of experimental data. Moreover, this model is suitable for predicting IDAC in an extensive variety of systems where a limited number of input variables are required.

The approach of QM calculations starts from the computation of a molecular surface based on unimolecular of individual species in the system instead of a mixture itself. This method combines the statistical thermodynamics methodology with an electrostatic theory of locally interacting molecular surfaces. The model parameters must be optimised so that they can be used in the prediction of IDACs and the properties of a system.

2.2.4.2. Experimental methods used to determine the IDACs

In the last 50 years, a substantial number of experimental methods have been developed to determine activity coefficients at infinite dilution, including the following:

- Differential Ebulliometry Method (DEM) (Gautreaux and Coates, 1955);
- Inert Gas Stripping Method (IGS) (Leroi *et al.*, 1977);
- Gas-Liquid Chromatography Method (GLC) (Letcher, 1980);
- Inverse Solubility Method (ISM) (Letcher, 1980);
- Head-Space Chromatography Method (HSC) (Hussam and Carr, 1985);
- Rayleigh Distillation Method (RDM) (Dohnal and Horáková, 1991);
- Differential Static Cell Method (DSC) (Pividal *et al.*, 1992); and the
- Dew Point Method (DPM) (Suleiman and Eckert, 1994);

Each of these methods is only applicable with certain conditions, and some are outmoded because they generate poor results. A brief description of GLC, DEM and IGS methods which - defined by Abbott (1986) and summarised by Muhlbauer (1997) as the most important and widely used methods for measurements and predictions of IDACs - are expounded below.

Gas-liquid Chromatography Method (GLC)

GLC is the most widely used method for the measurements of activity coefficients partition coefficients, complex formation constants, adsorption, and second viral coefficients of gas mixtures (Letcher, 1980). This IDAC measurement method is accurate and reliable when the criteria below are met (Guiochon and Guillemin, 1988):

- The solvent must be in a liquid phase at the selected experimental temperature.
- The solvent vapour pressure must be negligible at selected experimental temperature to

prevent evaporation of the column.

- For reasonable retention times, the solute must be volatile.
- The carrier gas must be insoluble in the solvent.
- The mixture must have negligible adsorption effect.

GLC can be used for systems in which the solvent has a moderate volatility, but with less accuracy (Thomas *et al.*, 1982). Table 2-6 represents the potential advantages and disadvantages of GLC method. The schematic diagram of the GLC method is presented in Figure 2-4.

Table 2-6: The potential advantages and disadvantages of the GLC method (Weir and de Loos, 2005).

Advantages	**Disadvantages**
Solutes of high purity not required.	The IDAC of the solvent in the solute cannot be determined.
Possibility of injecting multiple solutes at once.	The method is suited to low volatility or non-volatile solvents only.
Allows measuring reactive systems.	Limited to specific experimental temperature ranges.
Requires small volumes of solvent and solutes for measurements.	Shorter distance of solvent through which the carrier gas travelled.
	Interfering adsorption effects.

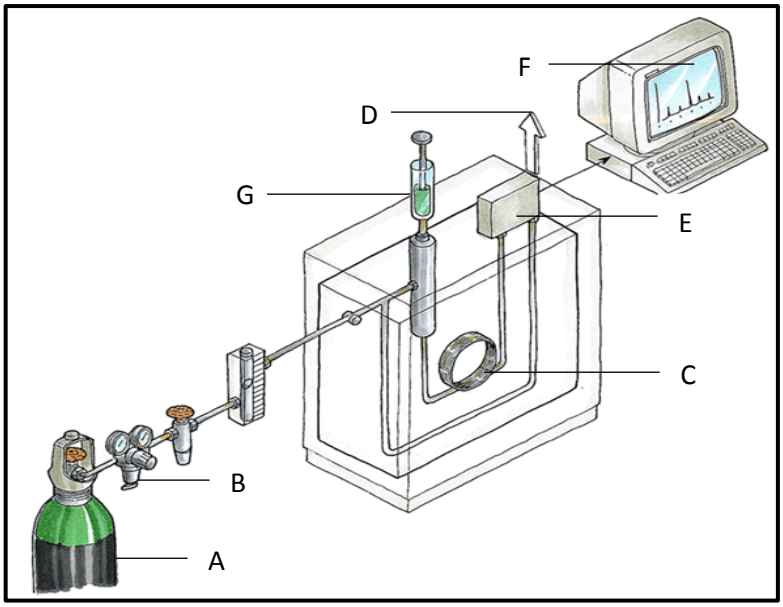

Figure 2-4: Gas-liquid chromatography schematic diagram.

A – Helium (carrier gas); B – Carrier gas flow regulator valve; C – Packed column (oven); D – Effluent bubble flow metre (waste gases); E – Thermal conductivity detector (TCD); F – Retention time analysis (Chart recorder); G – Sample injection (solute).

Differential Ebulliometry Method (DEM)

DEM (Figure 2-5), first developed by Gautreaux and Coates (1955) derived four equations for measuring and predicting VLE data. It obtains VLE data for binary systems by measuring system boiling temperature difference. These measurements are made either isothermally or isobarically.

For accurate VLE data, components should have similar relative volatilities. This method has been identified out by many researchers as the best and most suitable method for systems that involve water. Table 2-7 presents the advantages and disadvantages of DEM.

Table 2-7: Potential advantages and disadvantages of the DEM (Weir and de Loos, 2005).

Advantages	Disadvantages
Capable of measuring multiple systems at once	Inaccurate for binary systems with too high boiling temperature difference
Capable of measuring systems where the solute and the solvent have similar volatility	Time-consuming
	For accurate measurements, it requires a considerable amount of expertise
	The equipment setup (construction) and maintenance are excessively costly

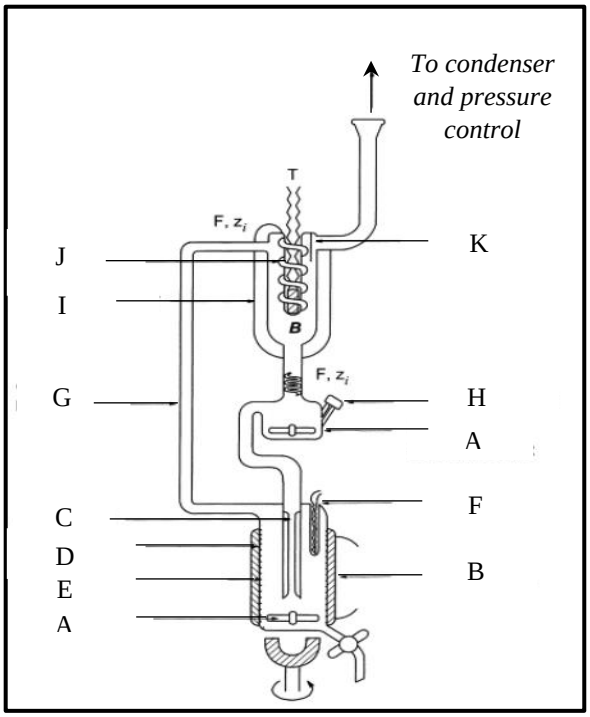

Figure 2-5: Differential ebulliometer schematic diagram (Richon, 2011).

A – Magnetic Stirring bar; B – Heating coil; C – Capillary; D – Reboiler; E – Fused ground glass; F – Temperature sensor (Pt 100); G – Cottrell pump; H – Sample septum (mixing spiral); I – vacuum jacket; J – Fussed glass spiral; K – Splash guard

Inert Gas Stripping Method

The idea behind this approach originates from a technique developed by Fowlis and Scott (1963) for the calibration of chromatographic detectors. In 1977, Leroi *et al.* (1977) developed the experimental procedure for this method which involves a constant bubbling flow of a carrier gas into a dilutor cell that is passed through a liquid mixture such that it 'stripped' a highly diluted solution of a volatile solute in a heavier solvent. A gas chromatograph then analyses the traces of a volatile solute. The resulting successive peak areas from this analysis are then used to determine activity coefficients at infinite dilution from the solute vapour concentration versus stripping time profile.

Originally, these measurements were time-consuming and quite delicate. However, researchers have simplified and accelerated the IGS method (Tumba, 2010). The dilutor technique has various advantages, such as the capability of measuring both small and large values of activity coefficients in pure or mixed solvents (Atik *et al.*, 2004). The benefits and disadvantages of this method are presented in Table 2-8.

Table 2-8: Potential benefits and disadvantages of the IGS method (Weir and de Loos, 2005)

Advantages	Disadvantages
GC detector need not be calibrated	Partial condensation should be avoided
Equipment is fairly straightforward	Charging and discharging of the dilutor cell
The mixture of solvents can be measured	Only applicable for highly volatile solutes
Capable of investigating multiple solutes at once	Requires a good liquid contact to obtain reliable data
Allows measuring systems with high volatility solvents	

For more details on the IGS method, the reader is referred to the work by Tumba (2010) and Leroi *et al.* (1977), amongst others where the in-depth review of the IGS method is well expounded. Figure 2-6 presents a typical flow diagram of the IGS method, similar to the one described by Coquelet and Richon (2005) and Krummen *et al.* (2000). Figure 2-7 presents the original dilutor cell proposed by Leroi *et al.* (1977).

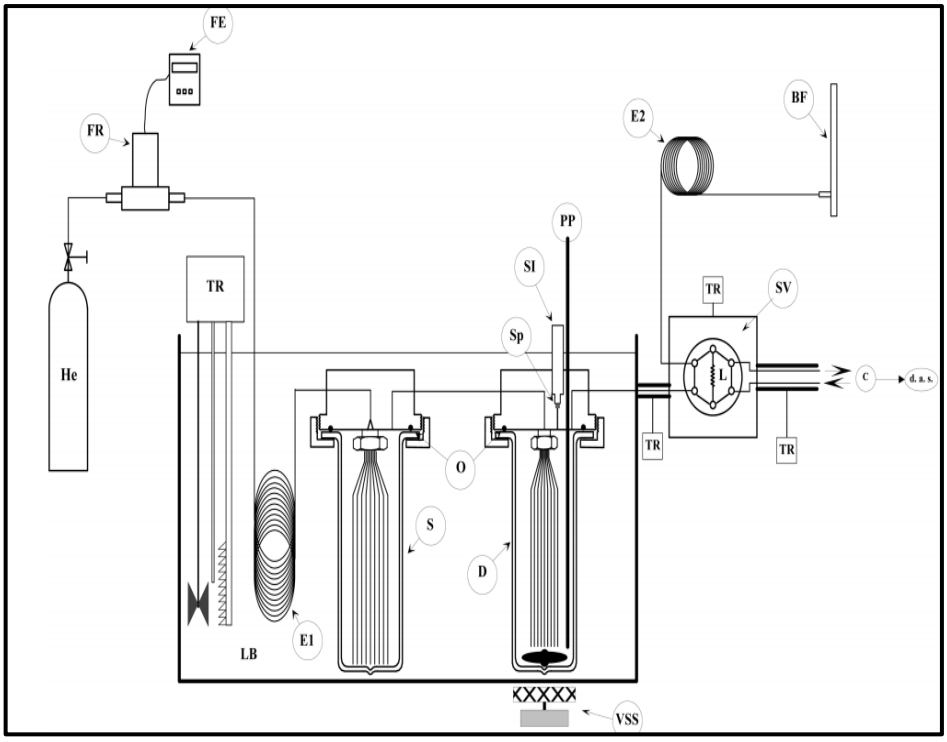

Figure 2-6: Flow diagram of the IGS method.

BF - Bubble flow metre; C - Chromatograph; D - Dilutor cell; d.a.s data acquisition system; He - Helium; E1 & E2 - Coil tube heat exchangers; FE - Flow meter electronic; FR - Flow regulator; L - Sampling loop; LB - Liquid bath; PP - Platinum resistance thermometer; S - Saturator; SI - Solute injector; Sp - Septum; SV - Sampling valve; TR - Temperature regulator; VSS - Variable speed stirrer.

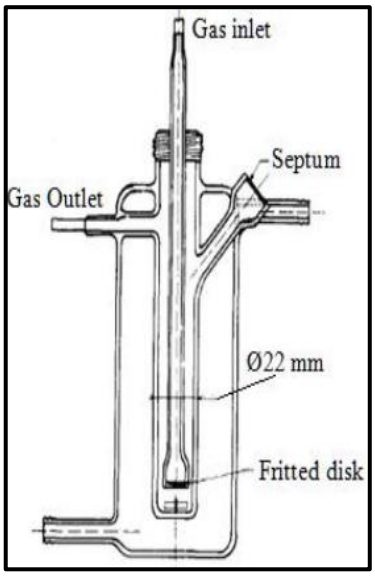

Figure 2-7: Dilutor flask as proposed by (Leroi *et al.*, 1977).

In this study, the solvent-solute relationship considered for binary systems was categorised based on their volatilities in the classes of low and high volatility. The appropriate equipment readily available for the determination of activity coefficients at infinite dilution for selected binary systems was a gas-liquid chromatograph.

2.2.5 Gas-Liquid Chromatography (GLC)

The GLC method was proposed in the early 1950s, gradually improving throughout the 1960s, (Dohnal and Horáková, 1991). This method has been enhanced by Everett (1965) to be easy to use, cost effective and with simple experimental procedure and setup. These improvements included the derivation of improved calculations for the determination of the infinite dilution activity coefficient from experimental data by researchers such as Everett (1965) and Cruickshank *et al.* (1966). Dohnal and Horáková (1991) noted that comprehensive accounts of the theory and practice of GLC had been presented by Conder and Young (1979) and Letcher (1978). According to Dohnal and Horáková (1991), the GLC method has not been altered much in the last 35 years, with major changes being the integration of new technologies, such as new on-line gas chromatographs, into the existing technique.

In this method, a carrier gas (helium) is used to transport a minuscule volume of injected mobile phase (solute) in the packed column where it equilibrates with a stationery-coated phase (solvent). Thus, when equilibrium is achieved the eluted solutes is detected to provide retention times and other parameters that relate to γ_i^{∞} of the solutes in a solvent (Guiochon and Guillemin, 1988). The detector used is usually either a flame ionisation (FID) or thermal conductivity (TCD).

The popularity of this method amongst researchers is confirmed by the database compiled Bastos *et al.* (1984) for the measurements of activity coefficient at infinite dilution. Of the 2097 experiments done, 1849 (88.2%) of activity coefficients values were measured using the GLC method.

2.3 Review of activity coefficients at infinite dilution data in DESs

To date, Verevkin *et al.* (2015) presented the first and only research which is an investigation similar to this study. The focus of the work of Verevkin *et al.* (2015) was to assess the separation performance of a DES consisting (Choline Chloride: Glycerol) in a 1:1 and 1:2 respective molar ratios. Activity coefficients at infinite dilution for common solutes were measured and predicted

over the temperatures range of 298.15 to 353.15 K. Gas-liquid chromatography was used as measurement technique and PC-SAFT model for data correlation.

The results from Verevkin *et al.* (2015) determined that the values of activity coefficients at infinite dilution increased with an increasing carbon chain length for all systems measured. The effect of the molar ratio in IDACs values was observed where IDAC drastically decreased with an increase in carbon chain length. It was noted from selectivity and capacity values that the DES was suitable for the separation of polar and non-polar solutes. It was noted that IDACs values were in fair agreement with the predicted values within 30% deviation (Verevkin *et al.*, 2015).

This work by Verevkin *et al.* (2015) has motivated further investigation into the DES-based separation of difficult common industrial binary mixtures in this study.

CHAPTER THREE

THERMODYNAMICS FUNDAMENTALS

Chapter Overview

The objective of this chapter is to briefly provide insight into the fundamental thermodynamic principles required to undertake the theoretical treatment of infinite dilution activity coefficient data obtained from measurements. The development of equations associated with the gas-liquid chromatography technique (GLC) is considered. These equations have also been discussed in detail by many researchers such as Smith *et al.* (2001), Muhlbauer (1997) and Walas (1985).

3.1. Equations for IDAC computation

3.1.1. Derivation of infinite dilution activity coefficient equation from phase equilibria

Principles for measurements of infinite dilution activity coefficients using gas-liquid chromatography are well detailed by Letcher (1978). James and Martin (1952) demonstrated the idea of using net retention volumes measurable by the GLC to yield the physicochemical data. Porter *et al.* (1956) then expanded the idea of James and Martin (1952) to relate the net retention volumes to γ_i^{∞} of the solute (1) in the solvent (3) (γ_{13}^{∞}).

Conder and Young (1979) define the partition coefficient (K_L) of the solute between two phases by the equations:

$$K_L = \frac{q}{c} = \frac{C_L}{C_M} \tag{3-1}$$

where

$$C_L = \frac{x_1 n_3}{V_L} \tag{3-2}$$

and

$$C_M = \frac{y_1 n_2}{V_G} \tag{3-3}$$

where C_M (and c) is the concentration of solute in the mobile phase; C_L (and q) is the concentration of the solute in the liquid phase when the solute occurs as a vapour or liquid at equilibrium; x_1 and y_2 are the mole fraction of solute in the liquid and vapour phases; V_L and V_G are the volume of the liquid phase and the vapour phase; n_2 is the number of moles of carrier gas component in the vapour phase and n_3 is the number of moles of solvent in the liquid phase.

From the criterion of phase equilibrium, if the mobile phase is in equilibrium with the stationary phase (L), then the chemical potentials in both phases are equal.

$$\mu_i^L = \mu_i^M \tag{3-4}$$

where the chemical potential (μ_i) is given by:

$$\mu_i = \mu_i{}^o + RT \ln \alpha_i \tag{3-5}$$

where α_i and T are the activity and system temperature, constant in the above expression.

Taking into account Equation (3-4) and substituting concentrations (C_L and C_M) to activities in Equations (3-4) and (3-5) can be written as follows:

$$\mu_i{}^{o,L} + RT \ln C_L = \mu_i{}^{o,M} + RT \ln C_M , \tag{3-6}$$

This leads to:

$$\ln \frac{C_L}{C_M} = \frac{\mu_i^{o.M} - \mu_i^{o,L}}{RT} \tag{3-7}$$

and,

$$K_L = \frac{C_L}{C_M} = \exp\left(\frac{\Delta \mu_i^o}{RT} \right) \tag{3-8}$$

The net retention volume (V_N) is related to K_L, and the volume of the stationary phase by the equation:

$$V_N = K_L V_L \tag{3-9}$$

Laub and Pecsok (1978) suggested that the above expression is used to obtain K_L at low column pressures.

Equation (3-9) can be re-written in a simplified form in terms mole fractions and number of moles as follows:

$$K_L = \frac{x_1 n_3 V_G}{y_1 n_2 V_L} \tag{3-10}$$

Considering that the vapour phase (V_G) is an ideal gas its volume is given as follows:

$$V_G = \frac{n_2 RT}{P} \tag{3-11}$$

Assuming that the solute activity coefficient is dependent on pressure, the modified Raoult's law is obtained as:

$$yP = x\gamma_{13}^{\infty} P_i^* \tag{3-12}$$

where P is the solute pressure and P_i^* is the saturated vapour pressure.

Now, combining Equation (3-12) into Equation (3-10) yields:

$$K_L = \frac{n_3 V_G P}{\gamma_{13}^{\infty} P_i^* n_2 V_L} \tag{3-13}$$

Re-writing this expression when the ideal gas law is assumed and rearranging factors, the following equation suggested by Porter *et al.* (1956) is then obtained:

$$\gamma_{13}^{\infty} = \frac{n_3 RT}{V_L K_L P_i^*} \tag{3-14}$$

and

$$\gamma_{13}^{\infty} = \frac{n_3 RT}{V_N P_i^*} \tag{3-15}$$

where V_N is the net retention volume. For greater accuracy, Everett (1965) and Cruickshank *et al.* (1966) further developed Equation (3-15) to derive an equation that accounts for solute-solute and solute-carrier gas imperfections and compressibility, as well as pressure drop through the column. The derived equation, then used by Letcher (1978), is given by:

$$\ln \gamma_{13}^{\infty} = \ln\left(\frac{n_3 RT}{V_N P_1^*}\right) - \frac{\left(B_{11} - v_1^*\right)P_1^*}{RT} + \frac{\left(2B_{12} - v_1^{\infty}\right)J_2^3 P_o}{RT} \tag{3-16}$$

where P_o is the column outlet pressure and is the same as the atmospheric pressure; P_1 is the column inlet pressure; P_1^* is the saturated vapour pressure of the solute at temperature T, obtained through Antoine Equation (Poling *et al.*, 2001); $P_o J_2^3$ is the mean column pressure; v_1^* is the molar volume of the solute; and v_1^{∞} is the partial molar volume of the solute at infinite dilution.

In this study, the net solute retention volume (V_N) was calculated using the equation given by Letcher (1978):

$$V_N = \left(J_2^3\right)^{-1} U_o \left(t_R - t_G\right) \tag{3-17}$$

where J_2^3 is the pressure correction term; t_R is the retention times for the solutes; t_G is the retention time for the un-retained gas and; U_o is the corrected column outlet volumetric flow rate of the carrier gas that was measured with a soap bubble flow meter.

The determination of the pressure correction term (J_2^3) was detailed by Everett (1965), calculated as:

$$J_2^3 = \left(\frac{2}{3}\right)\left[\frac{\left(\frac{P_i}{P_o}\right)^3 - 1}{\left(\frac{P_i}{P_o}\right)^2 - 1}\right] \tag{3-18}$$

where P_i the column inlet pressure calculated from the column pressure drop displayed by the equipment. The corrected column outlet volumetric flow rate from bubble flow meter is given by:

$$U_o = U\left(1 - \frac{P_w}{P_o}\right)\frac{T}{T_f} \tag{3-19}$$

where T_f is the temperature of the flow meter; P_w is the vapour pressure of water at T_f; and U is the volumetric flow rate of the measured carrier gas by bubble soap flow meter at the column outlet. The vapour pressures of water and solutes involved in both methods of Laub and Pecsok (1978) and Everett and Powl (1976) were calculated using the Antoine Equation (Antoine, 1988) that was detailed by Poling *et al.* (2001).

3.1.2. Estimation of virial coefficients

The second virial coefficients of the pure solutes (B_{11}) was calculated using the equation detailed by McGlashan and Potter (1962):

$$B/V_c = 0.43 - 0.886\left(\frac{T_c}{T}\right) - 0.694\left(\frac{T_c}{T}\right)^2 - 0.0375(n-1)\left(\frac{T_c}{T}\right)^{4.5} \tag{3-20}$$

where V_c is the critical volume; T_c is the critical temperature; and n is the number of carbon atoms. The same Equation (3-20) was used to determine the mixed viral coefficients, B_{12}. The mixed critical properties were calculated using the mixing rules of Hudson and McCoubrey (1960) Equations (3-21, 3-22, and 3-24) and those detailed by Lorentz given by Equation (3-23) (Conder and Young, 1979).

$$T_c = 128 \cdot \left(T_{c11} \cdot T_{c22}\right)^{\frac{1}{2}} \cdot \left(I_{c11} \cdot I_{c22}\right)^{\frac{1}{2}} \cdot \left(V_{c11} \cdot V_{c22} / I_{c12}\right) \tag{3-21}$$

where

$$I_{c12} = \left(I_{c11} + I_{c22}\right) \cdot \left(V_{c11}^{\frac{1}{3}} + V_{c22}^{\frac{1}{3}}\right)^6 \tag{3-22}$$

and

$$V_{c12} = \frac{1}{8} \cdot \left(V_{c11}^{\frac{1}{3}} + V_{c22}^{\frac{1}{3}} \right)^3 \tag{3-23}$$

and

$$n_{12} = \frac{n_1 + n_2}{2} \tag{3-24}$$

From the above four equations, critical properties (T_c and V_c) as well as I_c, the ionisation potential were taken from the literature (Poling *et al.*, 2001; Lide, 2004). It is worth nothing that the McGlashan and Potter (1962) equation is only applicable to non-polar alkanes, alkenes, alkynes and aromatics (Poling *et al.*, 2001).

Saturated molar volumes, (v_1^*) were determined using Modified Rackett Equation of Poling *et al.* (2001) proposed by Spencer and Danner (1972) as follows (Rackett, 1970):

$$v_1^* = V_c\left(0.29056 - 0.08775\omega\right) Exp\left(1 - \frac{T}{T_c}\right)^{\frac{2}{7}} \tag{3-25}$$

where ω is the acentric factor of the solute.

In this study, the v_1^∞ of the solute was assumed to be the same as the v_1^* of the solute for the purpose of calculations (Letcher and Whitehead, 1997).

It is very difficult to evaluate the real second virial coefficients from the experimental data because they are temperature dependent. Poling *et al.* (2001) suggested that the most reliable correlation that can be utilised in the determination of the second virial coefficient is the following equation proposed by Tsonopoulos *et al.* (1989) given by:

$$\frac{B_{virial} P_c}{RT_c} = f^{(0)}(T_r) + \omega f^{(1)}(T_r) + a_t f^{(2)}(T_r) + b_t f^{(3)}(T_r) \tag{3-26}$$

where

$$f^{(0)}(T_r) = 0.1445 - \frac{0.330}{T_r} - \frac{0.1385}{T_r^2} - \frac{0.0121}{T_r^3} - \frac{0.000607}{T_r^8} \tag{3-27}$$

and

$$f^{(1)} = 0.0637 + \frac{0.331}{T_r^2} - \frac{0.423}{T_r^3} - \frac{0.008}{T_r^8} \tag{3-28}$$

and

$$f^{(2)}(T_r) = \frac{1}{T_r^{\,6}} \tag{3-29}$$

and

$$f^{(3)}(T_r) = -\frac{1}{T_r^8} \tag{3-30}$$

Poling *et al.* (2001) utilised these correlations to approximate the experimental second virial coefficients of pure components as well as for mixtures of polar and non-polar systems at a given temperature based on the critical properties of the components. The correlations of Tsonopoulos *et al.* (1989) apply to species such as ketones, water and alcohols that exhibit hydrogen bonds. For non-polar alkanes, alkenes, alkynes, and aromatics, the simplified Tsonopoulos *et al.* (1989) equation proposed by Smith *et al.* (2001) (a_t and b_t set to zero) is given by:

$$\frac{B_{virial} P_c}{RT_c} = f^{(0)}(T_r) + \omega f^{(1)} \tag{3-31}$$

Moreover, re-arranging Equation (3-31) yields the following correlation:

$$B_{ii} = B^0 + \omega_i B^1 = \left[0.083 - \frac{0.422}{T_r^{1.6}}\right] + \omega_i \left[0.139 - \frac{0.172}{T_r^{4.2}}\right] \tag{3-32}$$

Poling *et al.* (2001) suggested that the second virial coefficients determined by this simplified equation by Smith and co-authors are only true when $T_r > 0.6$ and $\omega < 0.4$.

For polar components, the original equation proposed by Tsonopoulos *et al.* (1989) was utilised to

determine the second virial coefficients. The same equation was used to determine the mixed second virial coefficient with T_c, P_c, ω, a_t, and b_t given by:

$$(T_c)_{12} = \sqrt{(T_c)_1 (T_c)_2 (1 - k_{12})} \tag{3-33}$$

$$(P_c)_{12} = 4(T_c)_{12} \left[\frac{\left(\frac{P_c V_c}{T_c} \right)_1 + \left(\frac{P_c V_c}{T_c} \right)_2}{\left[\left(V_c^{\frac{1}{3}} \right)_1 + \left(V_c^{\frac{1}{3}} \right)_2 \right]^3} \right] \tag{3-34}$$

$$\omega_{12} = \frac{(\omega)_1 + (\omega)_2}{2} \tag{3-35}$$

where k_{12}, is an empirical binary interaction parameter obtained by using the guidelines provided by Tarakad and Danner (1977).

Moreover, for polar components, a_t and b_t are given by:

$$(a_t)_{12} = \frac{(a_t)_1 + (a_t)_2}{2} \tag{3-36}$$

and

$$(b_t)_{12} = \frac{(b_t)_1 + (b_t)_2}{2} \tag{3-37}$$

CHAPTER FOUR

EQUIPMENT DESCRIPTION AND EXPERIMENTAL PROCEDURE

Chapter Overview

There are various techniques and equipment available for the measurement of activity coefficient at infinite dilution. It is imperative that a researcher use the correct method in accordance with the study purpose. Moreover, to obtain experimental data with high levels of accuracy, the experimental apparatus and procedure must be properly operated and calibrated. Furthermore, it must be ensured that the most relevant variables – such as chemical purity, pressure, temperature, sample composition and sample quantity – are accurately measured.

As the technique utilised in this study has been identified in previous chapters, this section highlights the description of materials used, including the experimental setup and procedures for the measurements of activity coefficient at infinite dilution. This chapter further discusses the synthesis of DESs, as this was done before undertaking experimental measurements. The uncertainties on the experimental parameters and variables were taken into consideration and are duly reported in this section.

4.1. Materials

4.1.1. Purity of materials

In this study, all the materials used (gaseous: helium and liquid: DESs and GLC solvent) were found to be within an acceptable purity margin (above 98%) and were utilised without any further purification.

4.1.2. Helium

Helium, used as carrier gas for gas-liquid chromatographical purposes, was supplied by Afrox South Africa (Pty) Ltd in a 9.1 m^3 cylinder (at 20 ^{o}C and 1 atm) with a certified minimum purity of 99.999%. Impurities consisted mainly of moisture, oxygen, nitrogen and methane at quantities less than 10.5 ppm.

4.1.3. Deep eutectic solvents

In this study, two different salts (namely, tetramethylammonium chloride ($C_4H_{12}NCl$) [TMAC] and tetrapropylammonium bromide ($C_{16}H_{36}BrN$) [TPAB]) and three separate HBDs (namely, glycerol ($C_3H_{16}O_3$), ethylene glycol ($C_2H_{14}O_2$) and 1,6 hexanediol ($C_6H_{14}O_2$)) were selected for the synthesis of four DESs. All chemicals above were supplied from Sigma-Aldrich Chemicals (New Germany, South Africa) with a minimum purity of 98 %. These DESs were selected because activity coefficients at infinite dilution measurements for difficult industrial separations are rare. The details of used DESs can be found in Appendix A (Table A-1).

4.1.4. DES Preparation

All salts were mixed with HBDs in a selected molar ratio utilising a magnetic stirrer bar in a tightly sealed beaker at a selected temperature ranging from 353.15 K to 393.15 K until a colourless liquid was formed. For reliability and accuracy for DES synthesis, it is mixed for an extended period (4 - 8 hours) until a homogenous mixture is formed perfectly. Before use, DESs were heated for eight hours (373.15 K) in the oven to remove any contained moisture.

4.1.5. Solute used in gas-liquid chromatography

Solute suppliers with quoted purities, which were utilised in GLC for activity coefficient measurements at infinite dilution are, listed in Appendix A (Table A-2). Since it is well known that the GLC technique can separate the solute from any impurities, these were not purified further. Solutes, include alk-1-anes, alk-1-enes, alk-1-ynes, cycloalkanes, alkanols, alkylbenzenes, ketones, heterocyclics, and esters.

4.2. Activity coefficient at infinite dilution measurements from GLC

4.2.1. Experimental setup

Figure 4-1, shows the experimental setup for the GLC technique for the determination of activity coefficients at infinite dilution. A Shimadzu GC-2014 gas chromatograph equipped with thermal conductivity detectors (TCD) was utilised for experimental measurements. This experimental setup is similar to those used by other researchers (Letcher, 1978; Tumba, 2010).

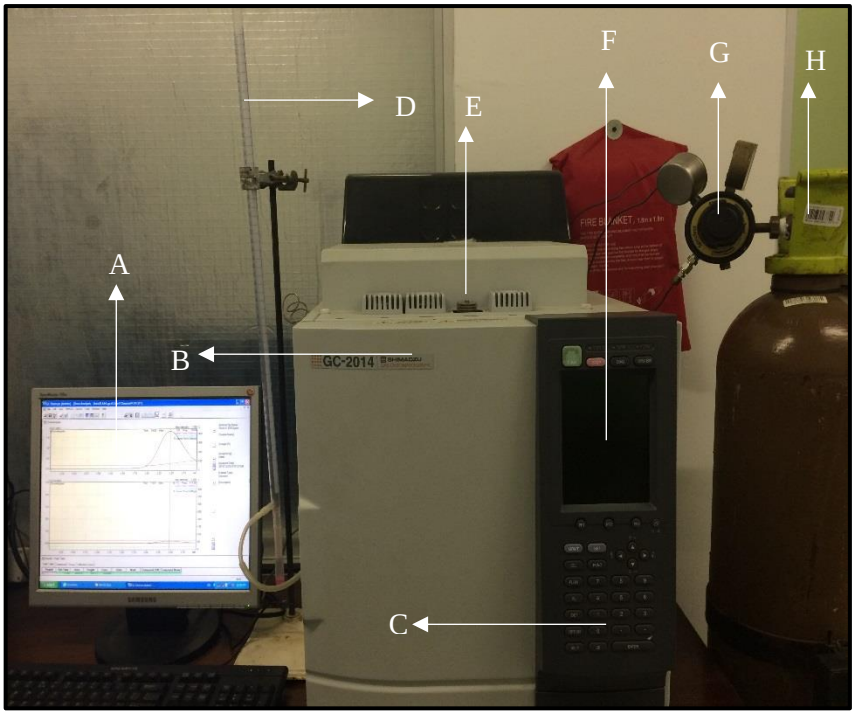

Figure 4-1: Experimental setup for the measurement of IDACs

A – PC monitor; B – Column oven; C – Operation panel; D – Bubble flow meter; E – Manual injector; F – GC screen monitor; G – Pressure regulator; H – Helium (carrier gas)

4.2.2. Experimental procedure

Two different stainless-steel columns of 1 m length and 4.1 mm diameter were washed with hot soapy water and rinsed with hot water. Both columns were prepared with two different required solvent loadings to monitor adsorption effects during the experiment. The freshly made columns were weighed and installed into the oven and conditioned for at least two hours. This conditioning ensures that the pressure drop across the column remains the same. Additionally, this assisted in the removal of any contained moisture in the initially prepared columns. The columns were repeatedly removed from the oven and weighed to monitor the changes in masses. When there were no further changes on the prepared columns, it was considered that no loss of solvent occurred.

For all measurements undertaken, the gas chromatography detector and injector temperatures were both set to T = 523.15 K. Activity coefficient at infinite dilution experimental measurements of different solutes were done at different temperatures; 313.15 K, 323.15 K, 333.15 K, and 343.15 K. One solute was injected at a time (0.1 - 0.2 µl), and the output signal from TCD was recorded on the desktop computer for calculation purposes. For consistency in experimental data, at least three injections were made for each solute. Relevant parameters such as temperatures, pressures and flow

rate were also recorded at regular intervals. More detailed experimental parameters and variables needed to determine activity coefficient at infinite dilution by utilising Equation (3-16) are briefly discussed below.

4.2.2.1. Experimental parameters

To measure and predict infinite dilution activity coefficients, defined parameters must be controlled or determined experimentally. The following parameters were determined from the experiments and used in Equation (3-16).

Determination of inlet and outlet pressures (P_i and P_o)

The outlet pressure was the same as atmospheric pressure, as the end of the column was open to atmosphere. The atmospheric pressure was measured by a digital barometer with an uncertainty of ±10 Pa. Depending on the inlet gas flow set by the operator, the equipment fixed the pressure drop through the packed column. The inlet pressure was calculated by:

$$P_i = P_o + \Delta P \tag{4-1}$$

where P_i and P_o are the inlet and outlet pressure (Pa), with an uncertainty of ±5.0 Pa.

Determination of flow rate

The measurement of a gas flow rate was carried out with a simple calibrated soap-bubble meter that consisted of a 50 ml calibrated cylinder. This direct method is easy to operate, is inexpensive and has high accuracy. Thus, the gas flow rate was set and maintained at a range of 15 ml.min^{-1} to 40 ml.min^{-1} with an accuracy of $\pm 0.50\%$.

Determination of number of moles of solvents (n_3)

The determination of infinite dilution activity coefficient is extremely sensitive to the amount of solvent accommodated in the column. Thus, care is required to determine the number of moles of solvent with the utmost accuracy. The following procedure was employed:

a) **Mixture preparation:**

- An empty, clean and dry round bottom flask was carefully weighed using a digital balance with a precision of ± 0.0001 g.

- Chromosorb, the solid support for solvent, was carefully added to the round bottom flask and weighed.
- The amount of purified solvent was added on the basis of the required percent to give a loading of approximately 27 - 34% by mass of solvent.
- The solvent was added to the solid support and weighed carefully.

b) Coating solid support with solvent:

- Dichloromethane was added to the flask and mixed with mixture (solid-solvent) to evenly distribute the solvent over the solid support, and the total mass was carefully weighed.
- The flask containing the mixture was tightly sealed with a hollow rubber stopper and carefully weighed.

c) Evaporation (Dichloromethane):

- The flask, which contained mixture, was inserted into the incubator (oven with shaker) at 60 ^{o}C with a shaker rotational speed of 80 rounds per minutes.
- Dichloromethane was continually removed from the round bottom flask sealed with hollow rubber stopper using a vacuum pump at approximately 60 kPa.

d) Column packing:

- The solid support coated with solvent was carefully loaded into a known mass of the empty column (stainless-steel) with the aid of vacuum pump and funnel until the mixture was equally distributed inside the column. The weight of the packed column was measured.

From these measurements, it was possible to determine the number of moles of the solvent contained in the packed column. This solid support is hygroscopic. As the exposure to air might add to inaccurate results, it was important to perform the packing procedure in a fume hood and seal the ends of the column.

Determination of real retention times (t_r and t_G)

Experimentally, the determination of different retention times was observed and registered on a chromatogram as a peak. However, retention time from the chromatogram ruler is inaccurate. It is important to determine the actual retention time from peak properties to achieve an effective infinite

dilution activity coefficient. The detector (Thermal Conductivity Detector) responded when a carrier gas or solute passed it with time. This emitted a signal, which was registered on a chromatogram as a peak. Therefore, the exact retention times were determined from the chromatogram as the time from injection to the intersection of the baseline, with tangents to the peak (Letcher, 1978). With respect to retention times (t_r and t_G) the estimated uncertainty was ±0.3 seconds. Figure 4-2 illustrates the procedure used to attain accurate retention times using peak properties.

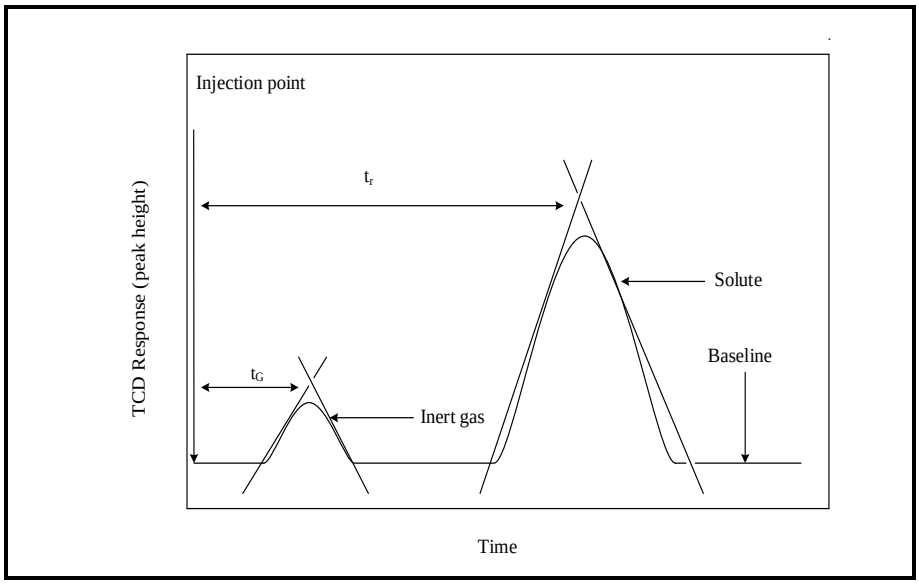

Figure 4-2: The illustrative diagram of chromatogram showing TCD response as a function of time (Letcher, 1978).

Injected solute volumes

The typical injection volume of 0.1 to 0.2 µl was used as defined by infinite dilution region, where the mole fraction is 10^{-5}. If considering n-hexane (0.1 µl) as a solute, this corresponds to 7.6×10^{-7} mole. From this measurement, it was reasonable to assume that the solute was exposed to 30 % of the solvent at any instant.

CHAPTER FIVE

EXPERIMENTAL RESULTS

Chapter Overview

This chapter first presents the results for the n-hexadecane test systems. This was done to confirm the reliability of the experimental set up as well as the accuracy of the experimental procedure used in this study. The test systems included n-hexadecane as a solvent and four solutes i.e. n-hexane, cyclohexane, benzene, and toluene at 313.15 K and 323.15 K.

Experimental activity coefficients at infinite dilution were therefore measured at T = [313.15, 323.15 333.15 and 343.15] K.

Partial excess enthalpies for the new measured systems as calculated from equation (3-16) and Gibbs-Helmholtz equation are reported. The plots and correlations of experimental infinite dilution activity data with temperature and number of carbons of solutes are also presented at infinite dilution.

5.1. Experimental infinite dilution activity coefficients

5.1.1. Infinite dilution activity coefficient data in n-hexadecane (Test systems)

It was necessary before the beginning of experiments to assess the performance of the equipment, i.e. to verify its ability to accurately measure activity coefficients at infinite dilution. The data for the chosen test systems were measured at 313.15 K and 323.15 K (Table 5-1). The data measured (Table 5-1) in this work were found to deviate within 2.63 % from the various literature data.

Table 5-1: Experimental and literature data of infinite dilution activity coefficients of selected test systems.

Solutes	**Temperature** / K	**Experimental** γ_{13}^{∞}	**Literature** γ_{13}^{∞}	**R.D.**[#] /%
n-Hexane	313.15	0.90	0.870-0.910 [a, c, d, e]	1.10
	323.15	0.88	0.860-0.905 [a, b, c, f]	2.21
Cyclohexane	313.15	0.78	0.778 [c]	0.54
	323.15	0.77	0.739-0.787 [a, b,]	2.63
Benzene	313.15	1.01	1.006-1.051 [a, b, c]	0.80
	323.15	0.97	0.932-0.995 [a, b,]	2.30
Toluene	323.15	0.94	0.941[a, b]	0.06

[a]Tumba et al. (2013); [b]Schult et al. (2001); [c]Chien et al. (1981); [d]Laub and Pecsok (1978); [e]Parcher and Hussey (1973); [f]Castells et al. (1999)

The relative deviation from the literature was calculated using Equation (5-1).

$$R.D. = \frac{\gamma_{13}^{\infty(Exp)} - \gamma_{13}^{\infty(Lit)}}{\gamma_{13}^{\infty(Lit)}} \times 100\% \tag{5-1}$$

As can be seen from the above results (Table 5-1) with small deviations, it can be assumed that the experimental set-up and the experimental procedure used were reliable. Therefore, further research for new systems could be pursued with confidence.

5.1.2. Infinite dilution activity coefficient for new systems

Experimental infinite dilution activity coefficients were measured at atmospheric conditions. The experimental data are listed in Tables 5.2 to 5.17 and plotted in Figures 5.1 to 5.40.

5.1.2.1. Tetramethylammonium chloride + Glycerol; (DES1)

Table 5-2: Measured activity coefficients at infinite dilution for selected organic solutes (1) in DES1 (3) at T = (313.15, 323.15, 333.15 and 343.15) K with solvent column loading n_3 = 7.1213 mmol (30.21 wt. %).

Experimental activity coefficient at infinite dilution at T [K]				
Solute	**T=313.15**	**T=323.15**	**T=333.15**	**T=343.15**
n-hexane	223.968	248.573	276.874	314.705
n-heptane	218.483	243.115	264.250	309.556
n-octane	213.060	235.453	260.658	301.793
cyclopentane	193.061	238.171	260.360	298.043
cyclohexane	190.881	215.745	237.418	262.707
cycloheptane	187.485	204.023	225.641	247.864
cyclooctane	185.226	199.473	218.328	230.768
hex-1-ene	286.515	345.338	379.122	431.878
hept-1-ene	209.837	235.706	253.510	287.712
hept-1-yne	69.635	71.867	73.108	74.720
oct-1-yne	51.082	55.052	58.181	61.641
ethanol	3.216	3.133	2.929	2.827
methanol	1.222	1.202	1.189	1.168
propan-1-ol	6.568	6.114	5.815	5.565
propan-2-ol	6.674	6.487	6.214	6.043
isobutyl alcohol	29.086	21.787	18.697	17.310
benzene	54.998	48.094	45.077	42.036
toluene	98.171	89.228	85.327	84.163
ethylbenzene	146.232	139.617	137.210	133.959
acetone	10.691	10.350	10.033	9.828
butan-2-one	23.498	22.652	21.466	20.159
thiophene	2.520	2.567	2.584	2.635
pyridine	0.607	0.636	0.680	0.705
methyl acetate	2.658	2.729	2.941	2.947
ethyl acetate	5.393	5.257	5.146	5.039

Table 5-3: Measured activity coefficient at infinite dilution for selected organic solutes (1) in DES1 (3) at T = (313.15, 323.15, 333.15 and 343.15) K with solvent column loading n_3 = 8.0029 mmol (33.95 wt. %).

Experimental activity coefficient at infinite dilution at T [K]				
Solute	**T=313.15**	**T=323.15**	**T=333.15**	**T=343.15**
n-hexane	222.139	250.022	278.741	315.254
n-heptane	218.483	243.115	265.250	309.556
n-octane	210.651	235.672	261.389	300.431
cyclopentane	197.699	235.148	270.709	303.343
cyclohexane	194.811	223.494	240.703	258.850
cycloheptane	188.366	218.917	226.885	243.981
cyclooctane	184.301	202.216	211.453	238.751
hex-1-ene	284.207	344.175	364.709	426.263
hept-1-ene	206.412	236.233	253.169	287.598
hept-1-yne	68.821	71.023	72.973	74.687
oct-1-yne	53.636	56.944	58.646	62.004
ethanol	3.216	3.133	2.929	2.827
methanol	1.245	1.239	1.207	1.186
propan-1-ol	6.391	6.146	5.900	5.577
propan-2-ol	6.660	6.5173	6.208	6.061
isobutyl alcohol	28.568	23.523	19.686	17.066
benzene	55.279	50.688	47.765	43.165
toluene	98.517	90.124	85.237	84.052
ethylbenzene	147.960	139.398	136.463	132.475
acetone	10.690	10.419	9.813	9.657
butan-2-one	23.874	22.453	21.121	20.396
thiophene	2.659	2.652	2.672	2.743
pyridine	0.630	0.649	0.672	0.702
methyl acetate	2.660	2.724	2.822	2.933
ethyl acetate	5.439	5.343	4.687	4.662

Table 5-4: Calculated average activity coefficients at infinite dilution for selected organic solutes (1) in DES1 (3) at T = (313.15, 323.15, 333.15, and 343.15) K.

Experimental activity coefficient at infinite dilution at T [K]				
Solute	**T=313.15**	**T=323.15**	**T=333.15**	**T=343.15**
n-hexane	223.053	249.298	277.807	314.979
n-heptane	218.483	243.115	264.750	309.556
n-octane	211.856	235.562	261.023	301.112
cyclopentane	195.380	236.660	265.535	300.693
cyclohexane	192.846	219.620	239.060	260.779
cycloheptane	187.925	211.470	226.263	245.922
cyclooctane	184.764	200.845	214.891	234.759
hex-1-ene	285.361	344.757	371.916	429.070
hept-1-ene	208.124	235.970	253.339	287.655
hept-1-yne	69.228	71.445	73.041	74.703
oct-1-yne	52.359	55.998	58.413	61.823
ethanol	3.216	3.133	2.929	2.827
methanol	1.233	1.220	1.198	1.177
propan-1-ol	6.480	6.130	5.858	5.571
propan-2-ol	6.667	6.502	6.211	6.052
isobutyl alcohol	28.827	22.655	19.192	17.188
benzene	55.138	49.391	46.421	42.601
toluene	98.344	89.676	85.282	84.107
ethylbenzene	147.096	139.508	136.836	133.217
acetone	10.690	10.384	9.923	9.742
butan-2-one	23.686	22.552	21.294	20.278
thiophene	2.590	2.610	2.628	2.689
pyridine	0.618	0.643	0.676	0.704
methyl acetate	2.659	2.727	2.881	2.940
ethyl acetate	5.416	5.300	4.916	4.850

Table 5-5: The partial excess enthalpy at infinite dilution for selected organic solutes in DES1 obtained from the Gibbs-Helmholtz equation.

Excess Enthalpy	
Solute	$\Delta H_i^{E,(\infty)}$ = **kJ.mol^{-1}**
n-hexane	-10.203
n-heptane	-10.068
n-octane	-10.314
cyclopentane	-12.614
cyclohexane	-8.865
cycloheptane	-7.828
cyclooctane	-7.016
hex-1-ene	-11.629
hept-1-ene	-9.303
hept-1-yne	-2.241
oct-1-yne	-4.834
ethanol	4.051
methanol	1.410
propan-1-ol	4.455
propan-2-ol	3.002
isobutyl alcohol	15.405
benzene	7.478
toluene	4.680
ethylbenzene	2.842
acetone	2.898
butan-2-one	4.674
thiophene	-1.063
pyridine	-3.904
methyl acetate	-3.184
ethyl acetate	3.629

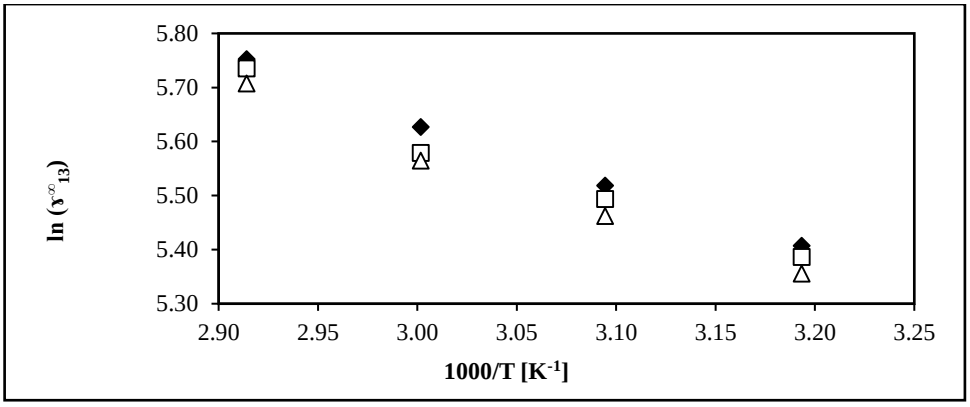

Figure 5-15: Plots of ln (γ_{13}^{∞}) against 1/T for alkanes; n-hexane (♦), n-heptane (□), and n-octane (Δ) (1) in DES1 (3).

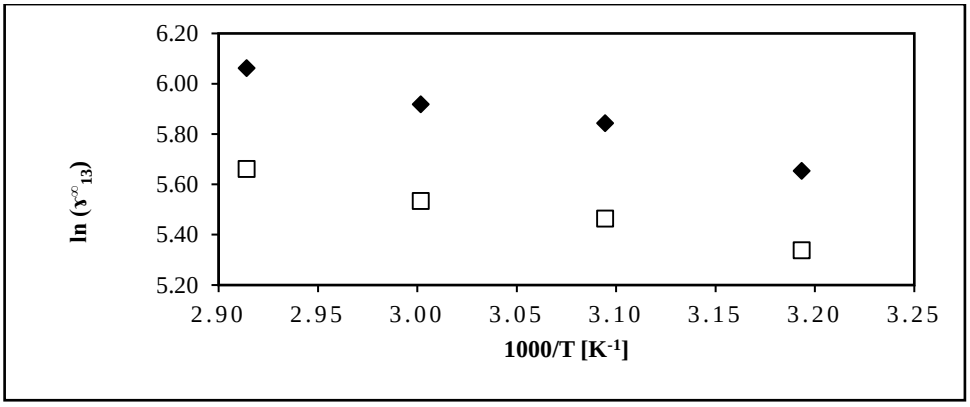

Figure 5-1: Plots of ln (γ_{13}^{∞}) against 1/T for alk-1-enes; hex-1-ne (♦) and hept-1ene (□), (1) in DES1 (3).

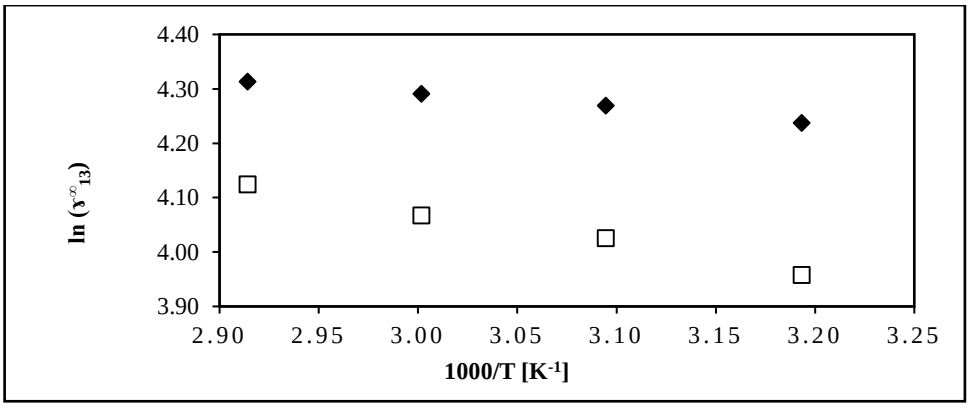

Figure 5-2: Plots of ln (γ_{13}^{∞}) against 1/T for alk-1-ynes; hep-1-yne (♦), and oct-1-yne (□), (1) in DES1 (3).

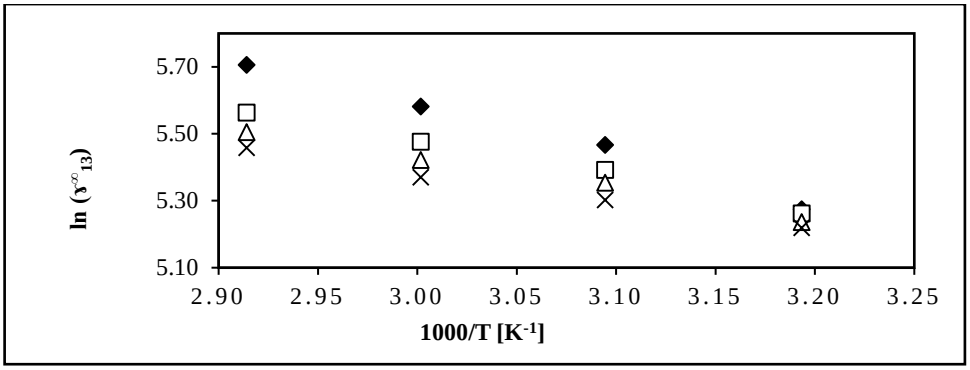

Figure 5-3: Plots of ln (γ_{13}^{∞}) against 1/T for cycloalkanes; cyclopentane (♦), cyclohexane (□), cycloheptane (Δ), and cyclooctane (x), (1) in DES1 (3).

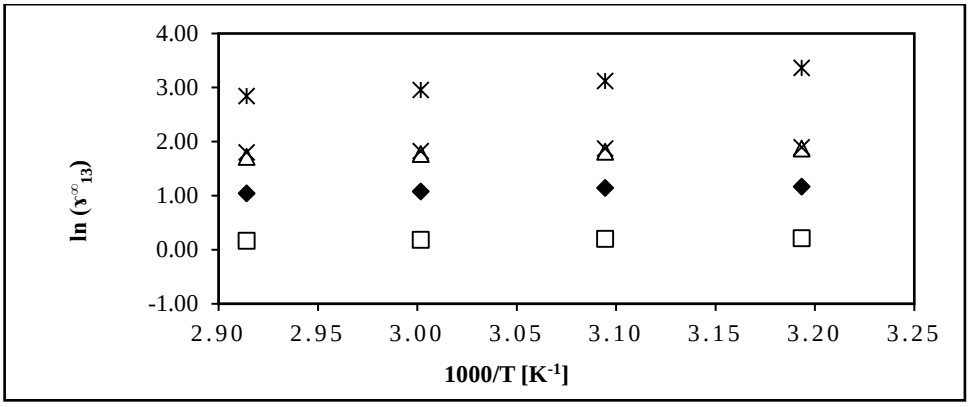

Figure 5-4: Plots of ln (γ_{13}^{∞}) against 1/T for alkanols; methyl alcohol (□), ethyl alcohol (♦), propan-1-ol (Δ), propan-2-ol (x), and isobutyl alcohol (∗), (1) in DES1 (3).

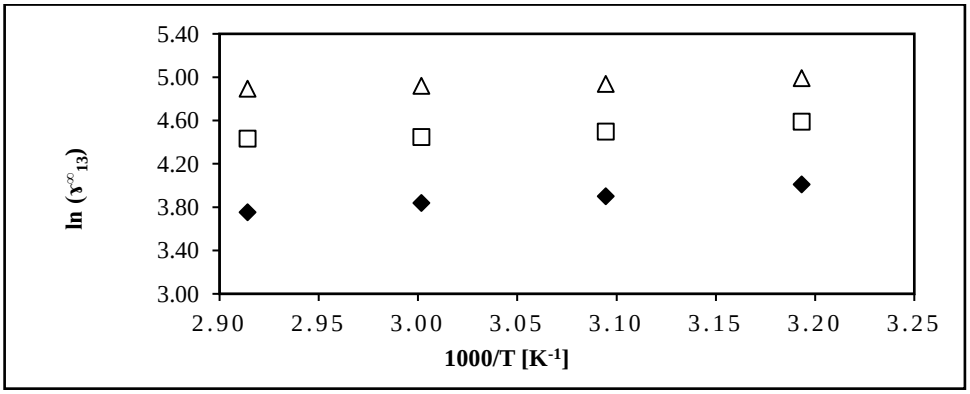

Figure 5-5: Plots of ln (γ_{13}^{∞}) against 1/T for alkylbenzenes; benzene (♦), toluene (□), and ethylbenzene (Δ), (1) in DES1 (3).

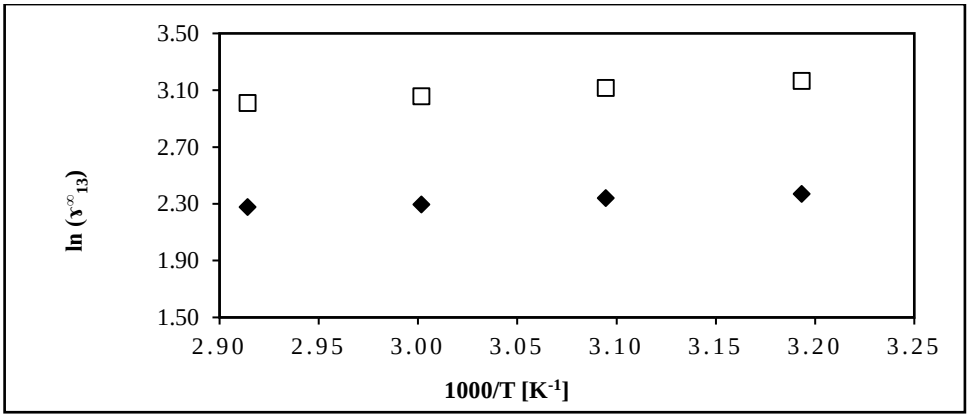

Figure 5-6: Plots of ln (γ_{13}^{∞}) against 1/T for ketones; acetone (♦) and butan-2-one (□), (1) in DES1 (3).

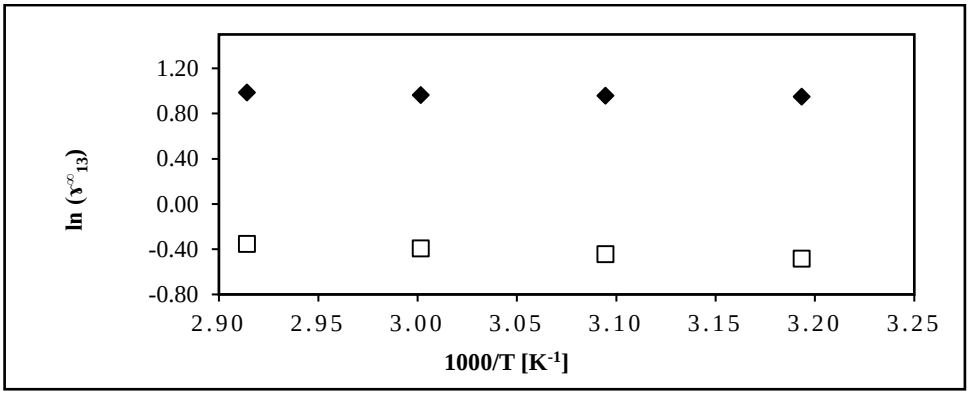

Figure 5-7: Measured ln (γ_{13}^{∞}) against 1/T for heterocyclic; thiophene (♦) and pyridine (□), (1) in DES1 (3).

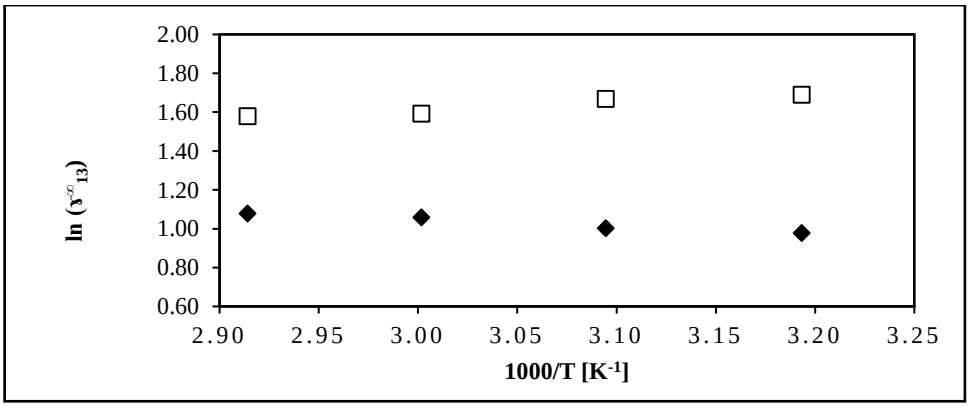

Figure 5-8: Plots of ln (γ_{13}^{∞}) against 1/T for ester; methyl acetate (♦) and ethyl acetate (□), (1) in DES1 (3).

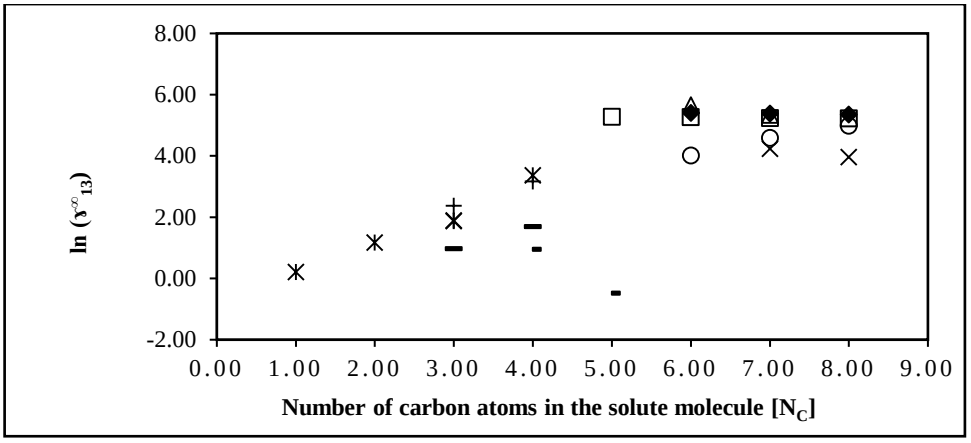

Figure 5-9: Plots of ln (γ_{13}^{∞}) against N_c for alkanes (♦), alk-1-enes (∆), alk-1-ynes (x), cycloalkanes (□), alkanols (∗), alkyl benzenes (o), heterocyclic (-), ketones (+), and ester (–), (1) in DES1 (3).

5.1.2.2. Tetramethylammonium chloride + Ethylene Glycol; (DES2)

Table 5-6: Measured activity coefficients at infinite dilution for selected organic solutes (1) in DES2 (3) at T = (313.15, 323.15, 333.15 and 343.15) K with solvent column loading n_3 = 21.5117 mmol (30.02 wt. %).

Experimental activity coefficient at infinite dilution at T [K]				
Solute	**T=313.15**	**T=323.15**	**T=333.15**	**T=343.15**
n-hexane	1780.112	1670.539	1554.798	1435.144
n-heptane	1565.295	1490.629	1426.685	1353.412
n-octane	1207.450	1169.605	1130.022	1085.122
cyclopentane	212.041	203.351	187.403	166.489
cyclohexane	313.405	295.530	295.273	276.371
cycloheptane	475.779	428.745	370.768	326.704
cyclooctane	612.092	552.644	521.868	509.870
hex-1-ene	596.789	383.948	271.383	201.820
hept-1-ene	1093.129	694.502	392.154	253.420
hept-1-yne	41.284	40.655	37.014	34.664
oct-1-yne	52.707	50.781	45.675	42.208
ethanol	2.253	2.194	2.052	2.005
methanol	0.726	0.659	0.603	0.577
propan-1-ol	2.786	2.568	2.307	2.288
propan-2-ol	2.877	2.719	2.625	2.533
isobutyl alcohol	11.478	9.441	7.997	6.921
benzene	20.489	18.372	17.022	16.171
toluene	42.998	40.526	38.122	36.488
ethylbenzene	86.216	76.678	69.201	63.546
acetone	5.279	4.953	4.811	4.677
butan-2-one	9.724	9.5996	9.176	8.514
thiophene	1.082	1.073	1.045	1.011
pyridine	0.426	0.410	0.410	0.396
methyl acetate	1.118	1.138	1.143	1.227
ethyl acetate	2.0996	2.144	2.214	2.240

Table 5-7: Measured activity coefficients at infinite dilution for selected organic solutes (1) in DES2 (3) at T = (313.15, 323.15, 333.15 and 343.15) K with solvent column loading n_3 = 9.2635 mmol (33.11 wt. %).

Experimental activity coefficient at infinite dilution at T [K]				
Solute	**T=313.15**	**T=323.15**	**T=333.15**	**T=343.15**
n-hexane	1837.492	1742.233	1628.822	1461.935
n-heptane	1565.295	1490.629	1426.685	1363.412
n-octane	1228.210	1196.976	1154.124	1095.373
cyclopentane	211.383	203.770	186.219	167.410
cyclohexane	317.546	306.514	298.290	277.921
cycloheptane	477.365	429.221	375.121	322.051
cyclooctane	652.730	592.235	535.686	488.323
hex-1-ene	592.661	404.221	271.879	199.216
hept-1-ene	1073.227	641.693	384.388	276.587
hept-1-yne	41.036	39.129	37.743	35.848
oct-1-yne	52.858	49.255	45.448	42.092
ethanol	2.253	2.194	2.052	2.005
methanol	0.715	0.648	0.608	0.587
propan-1-ol	2.798	2.571	2.320	2.307
propan-2-ol	2.890	2.745	2.649	2.556
isobutyl alcohol	10.302	8.543	7.225	6.420
benzene	18.979	17.978	16.792	15.349
toluene	41.369	38.642	37.523	36.005
ethylbenzene	83.158	77.195	70.307	65.003
acetone	5.057	4.952	4.708	4.562
butan-2-one	9.8995	9.509	8.957	8.826
thiophene	1.051	1.046	1.014	1.008
pyridine	0.406	0.395	0.393	0.385
methyl acetate	1.121	1.141	1.144	1.240
ethyl acetate	2.049	2.071	2.193	2.240

Table 5-8: Calculated average activity coefficients at infinite dilution for selected organic solutes (1) in DES2 (3) at T = (313.15, 323.15, 333.15, and 343.15) K.

Experimental activity coefficient at infinite dilution at T [K]				
Solute	**T=313.15**	**T=323.15**	**T=333.15**	**T=343.15**
n-hexane	1808.802	1706.386	1591.810	1448.540
n-heptane	1565.295	1490.629	1426.685	1358.412
n-octane	1217.830	1183.291	1142.073	1090.247
cyclopentane	211.712	203.561	186.811	166.950
cyclohexane	315.475	301.022	296.782	277.146
cycloheptane	476.572	428.983	372.944	324.377
cyclooctane	632.411	572.439	528.777	499.096
hex-1-ene	594.725	394.084	271.631	200.518
hept-1-ene	1083.178	668.098	388.271	265.004
hept-1-yne	41.160	39.892	37.379	35.256
oct-1-yne	52.782	50.018	45.561	42.150
ethanol	2.253	2.194	2.052	2.005
methanol	0.721	0.654	0.605	0.582
propan-1-ol	2.792	2.570	2.314	2.297
propan-2-ol	2.883	2.732	2.637	2.545
isobutyl alcohol	10.890	8.992	7.611	6.670
benzene	19.734	18.175	16.907	15.760
toluene	42.183	39.584	37.822	36.246
ethylbenzene	84.687	76.936	69.754	64.274
acetone	5.168	4.953	4.759	4.620
butan-2-one	9.812	9.554	9.066	8.670
thiophene	1.067	1.059	1.030	1.009
pyridine	0.416	0.402	0.401	0.391
methyl acetate	1.120	1.140	1.144	1.233
ethyl acetate	2.074	2.107	2.203	2.240

Table 5-9: The partial excess enthalpy at infinite dilution for selected organic solutes in DES2 obtained from the Gibbs-Helmholtz equation.

Excess Enthalpy	
Solute	$\Delta H_i^{E,(\infty)}$ = **kJ.mol^{-1}**
n-hexane	6.551
n-heptane	4.189
n-octane	3.272
cyclopentane	7.089
cyclohexane	3.585
cycloheptane	11.537
cyclooctane	7.073
hex-1-ene	32.504
hept-1-ene	42.614
hept-1-yne	4.714
oct-1-yne	6.846
ethanol	3.726
methanol	6.423
propan-1-ol	6.202
propan-2-ol	3.673
isobutyl alcohol	14.651
benzene	6.676
toluene	4.481
ethylbenzene	8.271
acetone	3.366
butan-2-one	3.772
thiophene	1.723
pyridine	1.715
methyl acetate	-2.592
ethyl acetate	-2.456

.

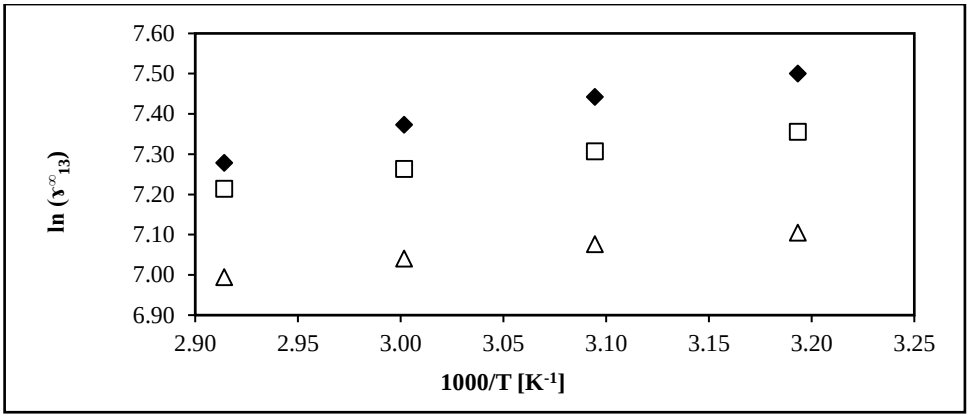

Figure 5-10: Plots of ln (γ_{13}^{∞}) against 1/T for alkanes; n-hexane (♦), n-heptane (□), and n-octane (Δ) (1) in DES2 (3).

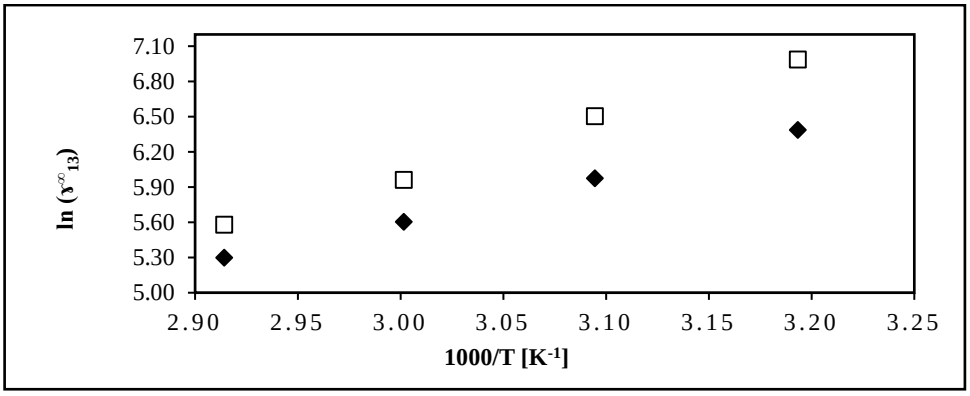

Figure 5-11: Plots of ln (γ_{13}^{∞}) against 1/T for alk-1-enes; hex-1-ne (♦) and hept-1ene (□), (1) in DES2 (3).

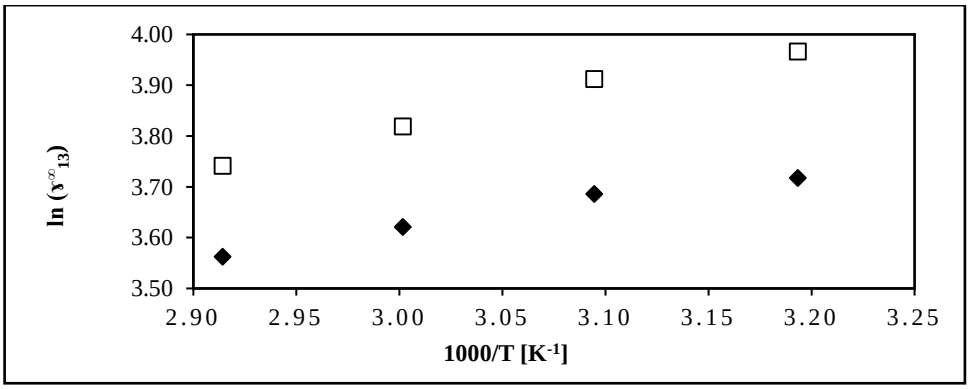

Figure 5-12: Plots of ln (γ_{13}^{∞}) against 1/T for alk-1-ynes; hep-1-yne (♦), and oct-1-yne (□), (1) in DES2 (3).

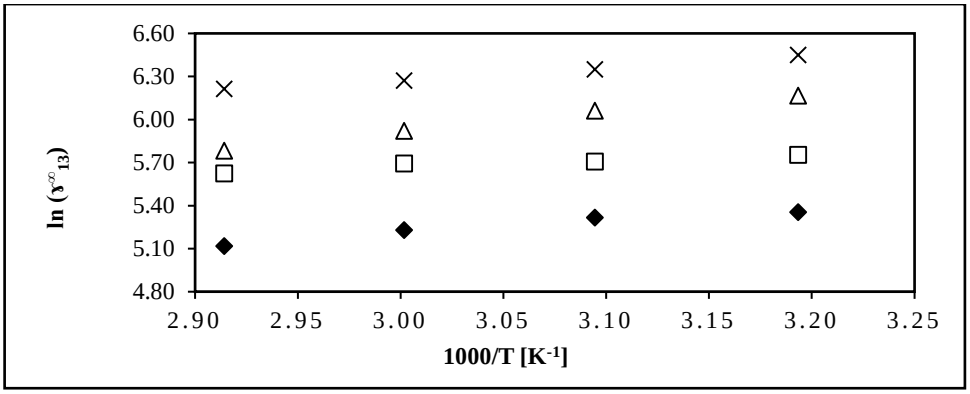

Figure 5-13: Plots of ln (γ_{13}^{∞}) against 1/T for cycloalkanes; cyclopentane (♦), cyclohexane (□), cycloheptane (∆), and cyclooctane (x), (1) in DES2 (3).

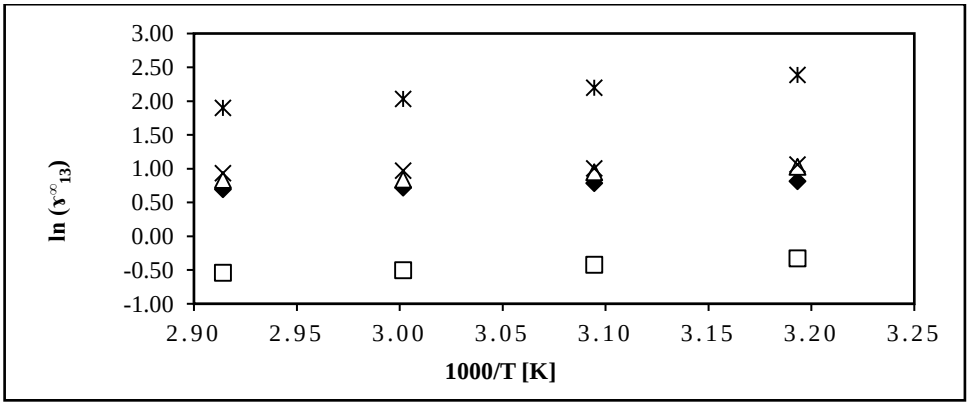

Figure 5-14: Plots of ln (γ_{13}^{∞}) against 1/T for alkanols; methyl alcohol (□), ethyl alcohol (♦), propan-1-ol (∆), propan-2-ol (x), and isobutyl alcohol (✶), (1) in DES2 (3).

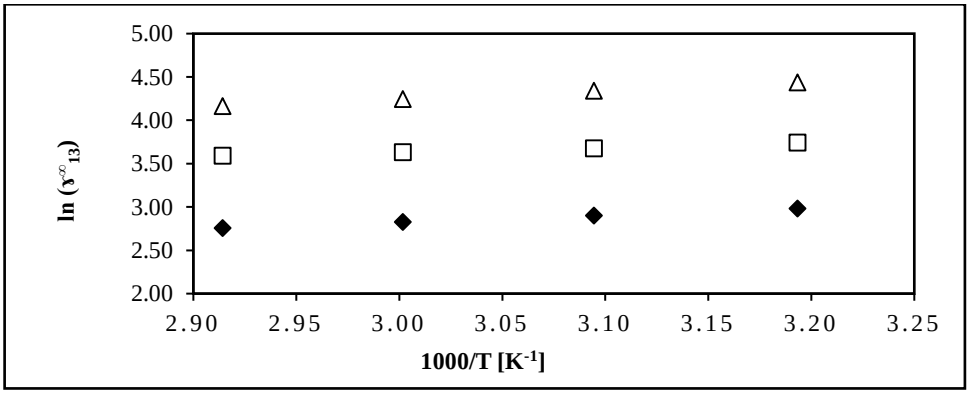

Figure 5-15: Plots of ln (γ_{13}^{∞}) against 1/T for alkylbenzenes; benzene (♦), toluene (□), and ethylbenzene (∆), (1) in DES2 (3).

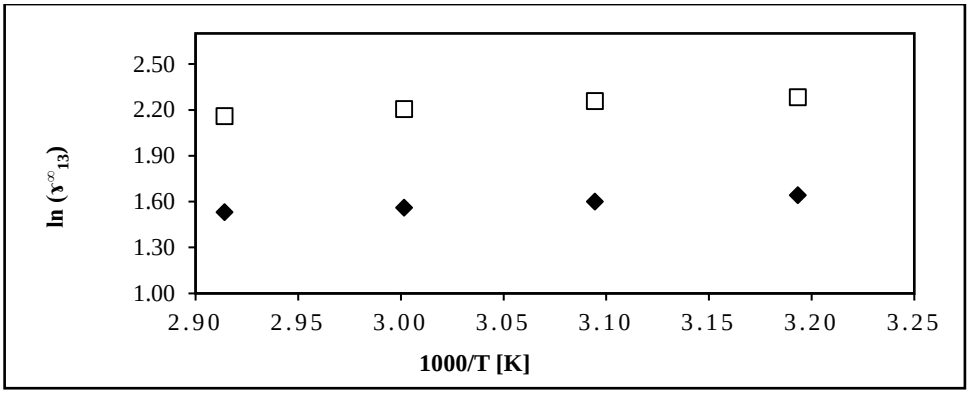

Figure 5-16: Plots of ln (γ_{13}^{∞}) against 1/T for ketones; acetone (♦) and butan-2-one (□), (1) in DES2 (3).

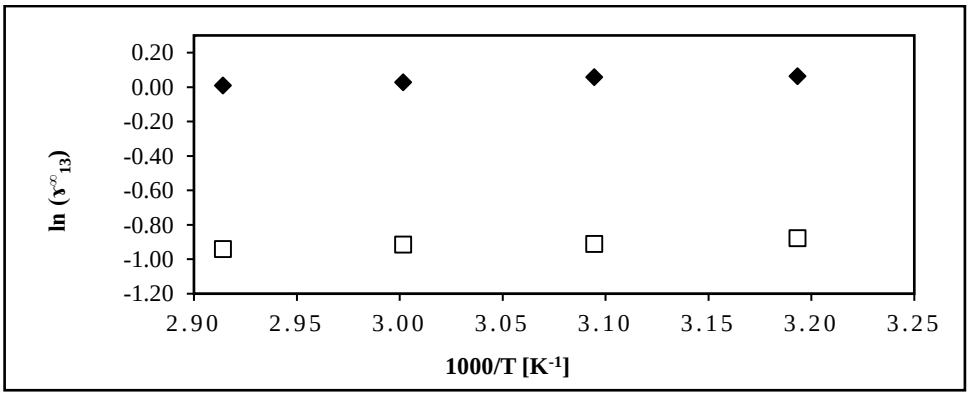

Figure 5-17: Plots of ln (γ_{13}^{∞}) against 1/T for heterocyclic; thiophene (♦) and pyridine (□), (1) in DES2 (3).

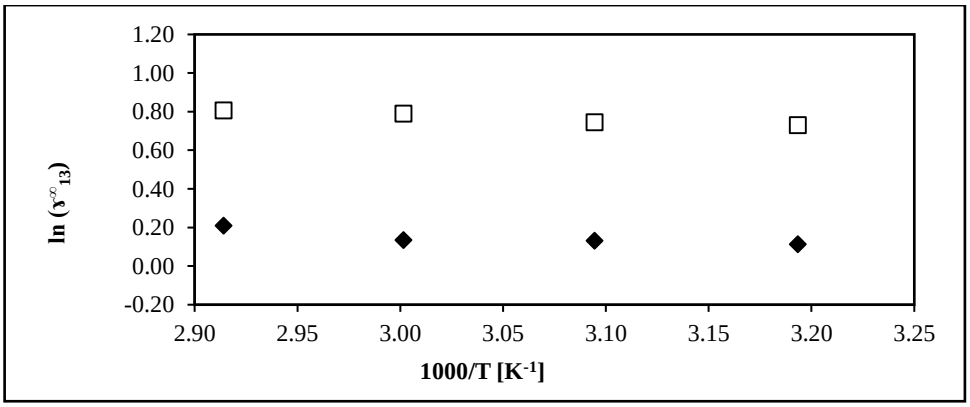

Figure 5-18: Plots of ln (γ_{13}^{∞}) against 1/T for ester; methyl acetate (♦) and ethyl acetate (□), (1) in DES2 (3).

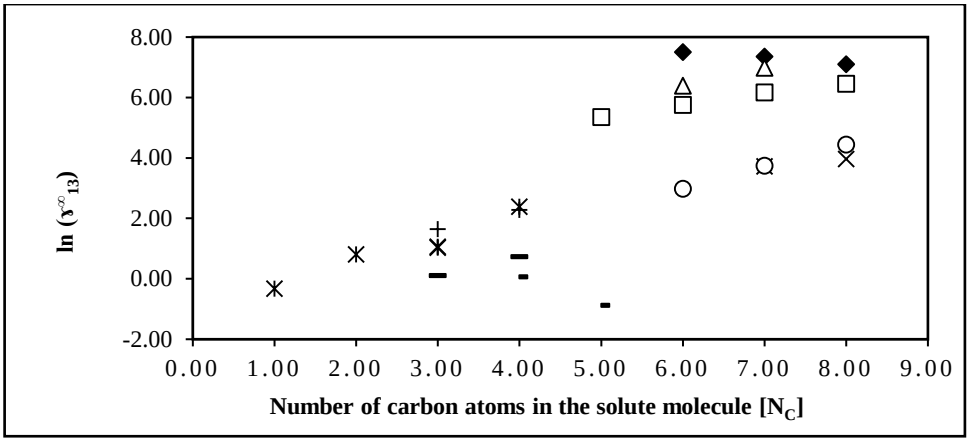

Figure 5-19: Plots of ln (γ_{13}^{∞}) against N_c for alkanes (♦), alk-1-enes (Δ), alk-1-ynes (x), cycloalkanes (□), alkanols (∗), alkyl benzenes (o), heterocyclic (-), ketones (+), and ester (–), (1) in DES2 (3).

5.1.2.3. Tetramethylammonium chloride + 1,6 Hexanediol; (DES3)

Table 5-10: Measured activity coefficients at infinite dilution for selected organic solutes (1) in DES3 (3) at T = (313.15, 323.15, 333.15 and 343.15) K with solvent column loading n_3 = 13.128 mmol (32.71 wt. %).

Experimental activity coefficient at infinite dilution at T [K]				
Solute	**T=313.15**	**T=323.15**	**T=333.15**	**T=343.15**
n-hexane	68.377	70.380	72.400	75.454
n-heptane	95.949	94.827	93.673	96.020
n-octane	119.607	122.432	123.738	129.465
cyclopentane	26.344	26.550	27.462	28.469
cyclohexane	32.289	36.507	37.375	37.9997
cycloheptane	42.571	42.832	42.991	43.901
cyclooctane	51.649	52.181	52.459	53.626
hex-1-ene	51.529	52.649	53.638	54.473
hept-1-ene	60.178	61.673	62.508	63.643
hept-1-yne	7.9996	8.151	8.241	8.472
oct-1-yne	7.369	7.500	7.614	7.865
ethanol	1.768	1.726	1.668	1.635
methanol	1.289	1.238	1.206	1.150
propan-1-ol	2.208	2.057	2.034	1.991
propan-2-ol	2.181	2.169	2.181	2.128
isobutyl alcohol	2.445	2.164	1.943	1.838
benzene	9.863	9.725	9.599	9.424
toluene	13.916	13.902	13.855	13.807
ethylbenzene	19.859	19.880	19.899	20.537
acetone	5.188	4.906	4.702	4.616
butan-2-one	6.201	6.073	5.920	5.770
thiophene	0.766	0.783	0.806	0.844
pyridine	0.212	0.228	0.251	0.273
methyl acetate	1.018	1.010	0.997	0.986
ethyl acetate	1.084	1.056	1.046	1.036

Table 5-11: Measured activity coefficients at infinite dilution for selected organic solutes (1) in DES3 (3) at T = (313.15, 323.15, 333.15 and 343.15) K with solvent column loading n_3 = 6.1564 mmol (30.05 wt. %).

Experimental activity coefficient at infinite dilution at T [K]				
Solute	**T=313.15**	**T=323.15**	**T=333.15**	**T=343.15**
n-hexane	69.115	70.591	72.727	74.479
n-heptane	98.511	94.962	78.243	78.414
n-octane	116.258	120.526	122.779	127.382
cyclopentane	28.961	27.800	25.927	27.429
cyclohexane	36.612	34.785	37.139	38.347
cycloheptane	39.176	38.458	38.040	37.803
cyclooctane	50.595	52.914	53.345	53.021
hex-1-ene	51.714	52.497	53.297	53.847
hept-1-ene	59.639	62.305	62.676	63.758
hept-1-yne	7.794	8.166	8.208	8.336
oct-1-yne	6.928	7.415	7.539	7.534
ethanol	1.746	1.728	1.652	1.601
methanol	1.299	1.233	1.190	1.118
propan-1-ol	2.108	2.047	2.029	1.951
propan-2-ol	2.177	2.153	2.172	2.138
isobutyl alcohol	2.405	2.074	1.902	1.727
benzene	9.788	9.504	9.421	9.331
toluene	13.435	13.238	13.328	13.110
ethylbenzene	18.902	18.620	18.642	18.392
acetone	5.321	4.938	4.810	4.552
butan-2-one	6.241	6.023	5.912	5.739
thiophene	0.764	0.768	0.789	0.801
pyridine	0.212	0.225	0.246	0.265
methyl acetate	1.015	1.008	0.997	0.989
ethyl acetate	1.080	1.060	1.049	1.035

Table 5-12: Calculated average activity coefficients at infinite dilution for selected organic solutes (1) in DES3 (3) at T = (313.15, 323.15, 333.15, and 343.15) K.

Experimental activity coefficient at infinite dilution at T [K]				
Solute	**T=313.15**	**T=323.15**	**T=333.15**	**T=343.15**
n-hexane	68.746	70.486	72.563	74.967
n-heptane	97.230	94.895	85.958	87.217
n-octane	117.933	121.479	123.259	128.423
cyclopentane	27.652	27.175	26.694	27.949
cyclohexane	34.451	35.646	37.257	38.173
cycloheptane	40.874	40.645	40.516	40.852
cyclooctane	51.122	52.547	52.902	53.323
hex-1-ene	51.621	52.573	53.467	54.160
hept-1-ene	59.909	61.989	62.592	63.700
hept-1-yne	7.897	8.158	8.224	8.404
oct-1-yne	7.149	7.457	7.576	7.699
ethanol	1.757	1.727	1.660	1.618
methanol	1.294	1.236	1.198	1.134
propan-1-ol	2.158	2.052	2.031	1.971
propan-2-ol	2.179	2.161	2.177	2.132
isobutyl alcohol	2.425	2.119	1.923	1.782
benzene	9.826	9.614	9.510	9.378
toluene	13.675	13.570	13.592	13.458
ethylbenzene	19.380	19.250	19.270	19.464
acetone	5.255	4.922	4.756	4.584
butan-2-one	6.221	6.048	5.916	5.755
thiophene	0.765	0.776	0.797	0.822
pyridine	0.212	0.226	0.249	0.269
methyl acetate	1.017	1.009	0.997	0.988
ethyl acetate	1.082	1.058	1.047	1.035

Table 5-13: The partial excess enthalpy at infinite dilution for selected organic solutes in DES3 obtained from the Gibbs-Helmholtz equation.

Excess Enthalpy	
Solute	$\Delta H_i^{E,(\infty)}$ = **kJ.mol^{-1}**
n-hexane	-2.576
n-heptane	3.814
n-octane	-2.407
cyclopentane	-0.092
cyclohexane	-3.149
cycloheptane	0.050
cyclooctane	-1.201
hex-1-ene	-1.440
hept-1-ene	-1.739
hept-1-yne	-1.745
oct-1-yne	-2.143
ethanol	2.559
methanol	3.809
propan-1-ol	2.527
propan-2-ol	0.506
isobutyl alcohol	9.153
benzene	1.351
toluene	0.413
ethylbenzene	0.116
acetone	3.979
butan-2-one	2.285
thiophene	-2.164
pyridine	-7.140
methyl acetate	0.885
ethyl acetate	1.279

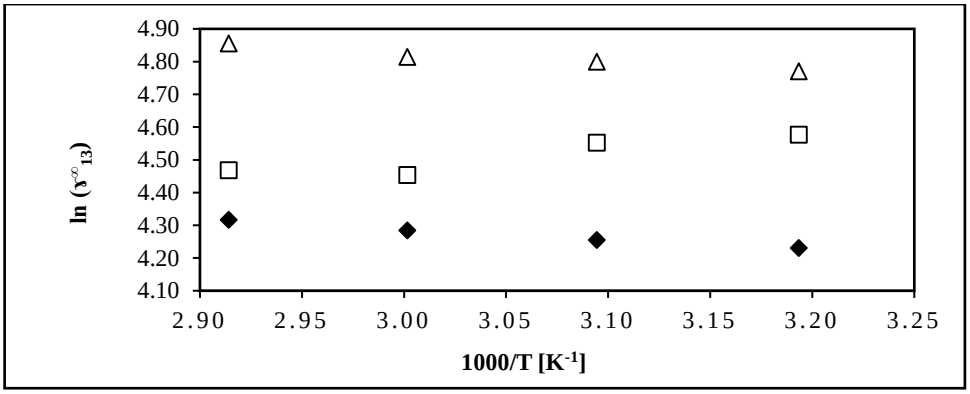

Figure 5-20: Plots of ln (γ_{13}^{∞}) against 1/T for alkanes; n-hexane (♦), n-heptane (□), and n-octane (Δ) (1) in DES3 (3).

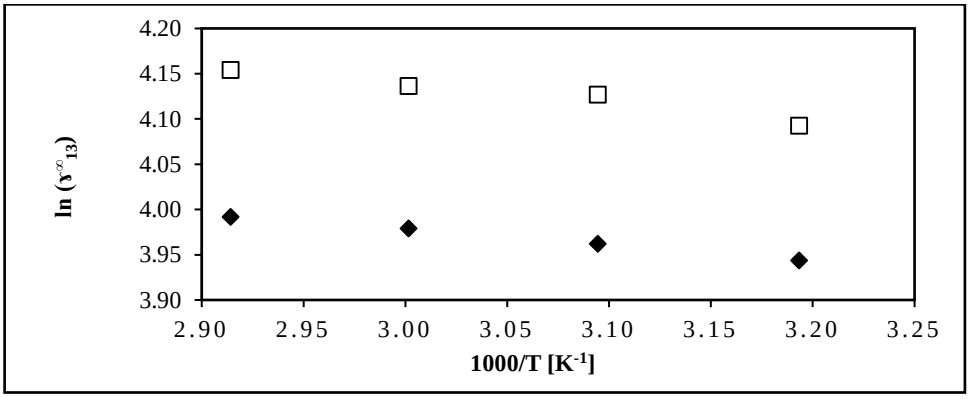

Figure 5-21: Plots of ln (γ_{13}^{∞}) against 1/T for alk-1-enes; hex-1-ne (♦) and hept-1ene (□), (1) in DES3 (3).

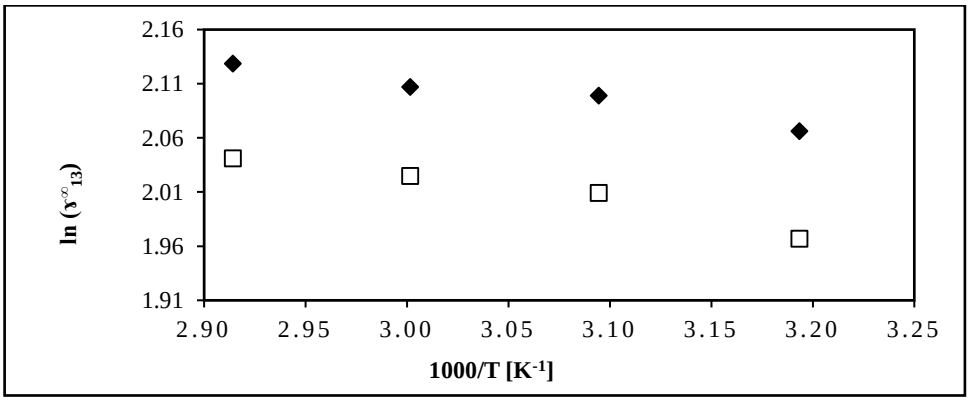

Figure 5-22: Plots of ln (γ_{13}^{∞}) against 1/T for alk-1-ynes; hep-1-yne (□), and oct-1-yne (Δ), (1) in DES3 (3).

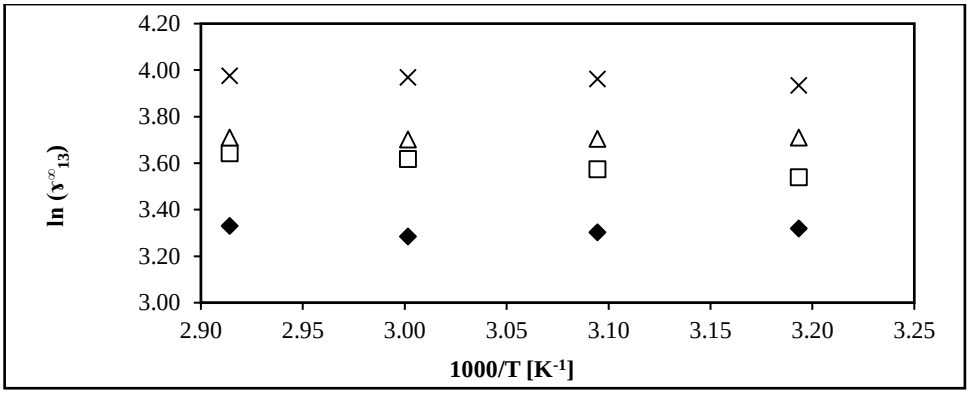

Figure 5-23: Plots of ln (γ_{13}^{∞}) against 1/T for cycloalkanes; cyclopentane (♦), cyclohexane (□) cycloheptane (∆), and cyclooctane (x), (1) in DES3 (3).

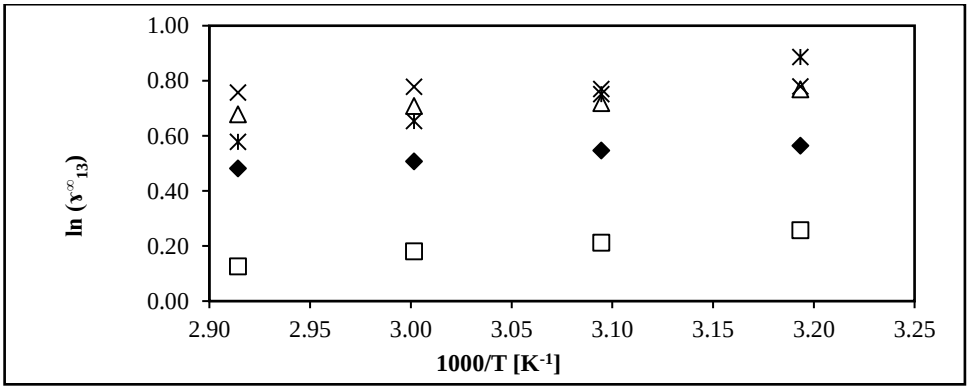

Figure 5-24: Plots of ln (γ_{13}^{∞}) against 1/T for alkanols; methyl alcohol (□), ethyl alcohol (♦), propan-1-ol (∆), propan-2-ol (x), and isobutyl alcohol (∗), (1) in DES3 (3).

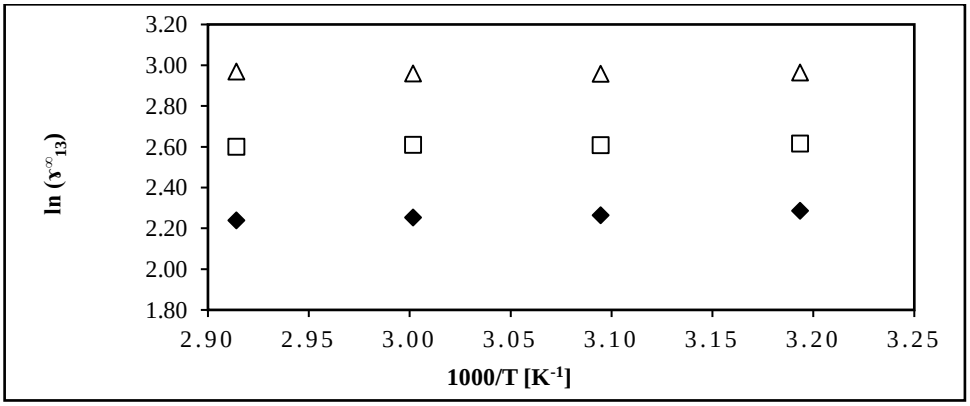

Figure 5-25: Plots of ln (γ_{13}^{∞}) against 1/T for alkylbenzenes; benzene (♦), toluene (□), and ethylbenzene (∆), (1) in DES3 (3).

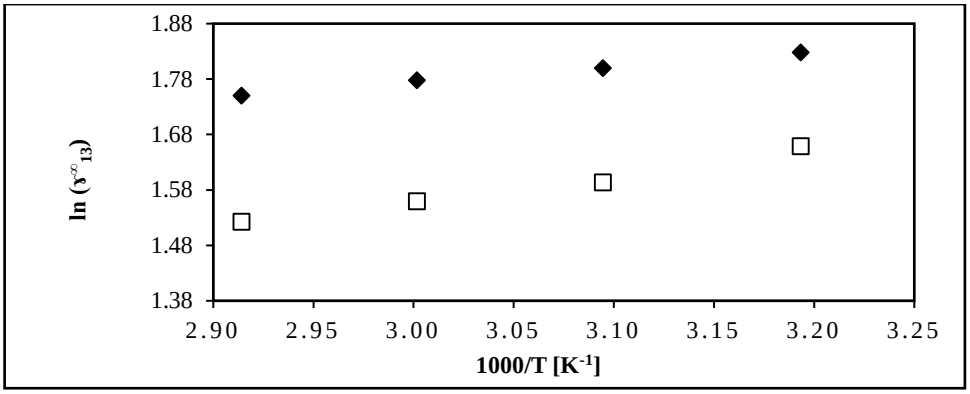

Figure 5-26: Plots of ln (γ_{13}^{∞}) against 1/T for ketones; acetone (□) and butan-2-one (♦), (1) in DES3 (3).

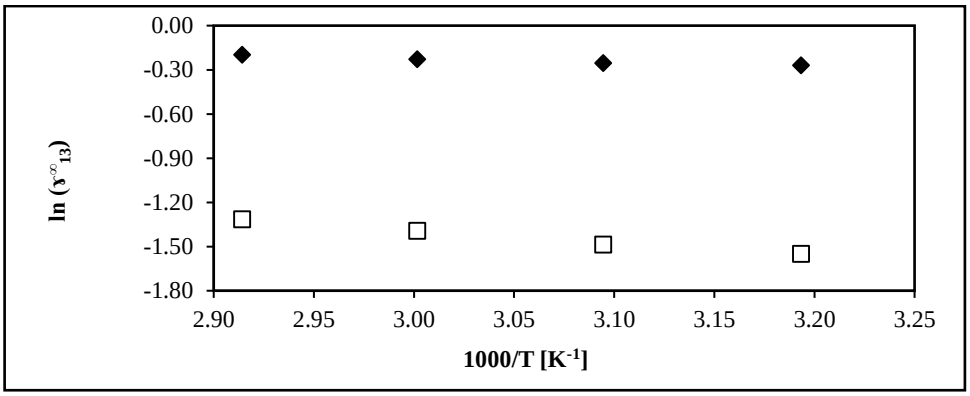

Figure 5-27: Plots of ln (γ_{13}^{∞}) against 1/T for heterocyclic; thiophene (♦) and pyridine (□), (1) in DES3 (3).

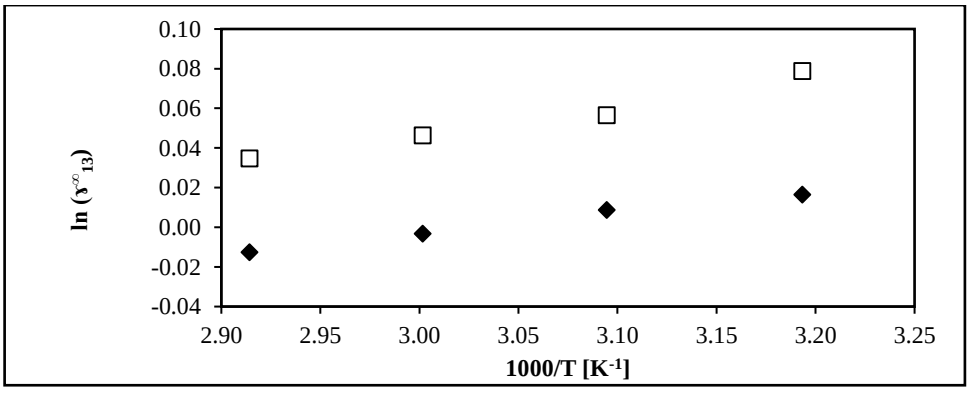

Figure 5-28: Plots of ln (γ_{13}^{∞}) against 1/T for ester; methyl acetate (♦) and ethyl acetate (□), (1) in DES3 (3).

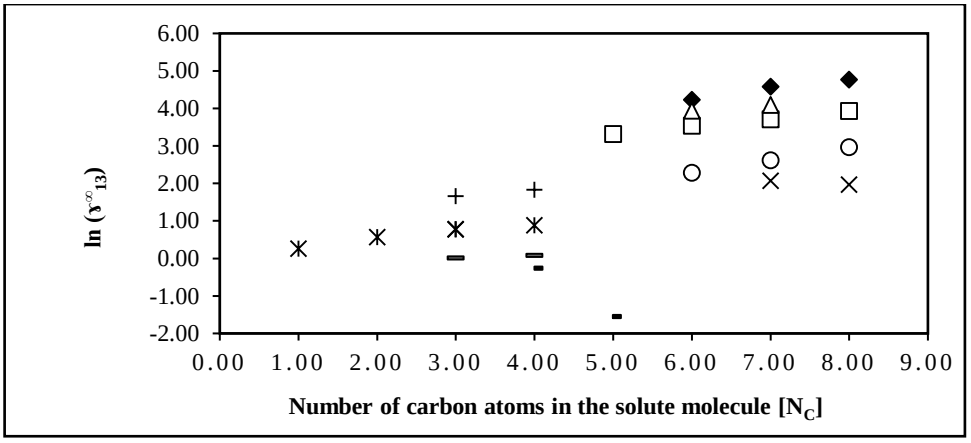

Figure 5-29: Plots of ln (γ_{13}^{∞}) against N_c for alkanes (♦), alk-1-enes (Δ), alk-1-ynes (x), cycloalkanes (□), alkanols (✶), alkylbenzenes (o), heterocyclic (-), ketones (+), and ester (–), (1) in DES3 (3).

5.1.2.4. Tetrapropylammonium bromide + 1,6 Hexanediol; (DES4)

Table 5-14: Measured activity coefficients at infinite dilution for selected organic solutes (1) in DES4 (3) at T = (313.15, 323.15, 333.15 and 343.15) K with solvent column loading n_3 = 6.441 mmol (27.41 wt. %).

Experimental activity coefficient at infinite dilution at T [K]				
Solute	**T=313.15**	**T=323.15**	**T=333.15**	**T=343.15**
n-hexane	27.829	21.052	18.584	18.015
n-heptane	30.405	28.277	25.556	23.278
n-octane	41.117	38.528	35.309	32.356
cyclopentane	9.762	8.047	7.662	8.895
cyclohexane	12.380	11.043	10.644	9.402
cycloheptane	13.973	13.021	12.111	11.279
cyclooctane	16.707	15.663	14.647	13.571
hex-1-ene	15.327	12.955	11.937	11.722
hept-1-ene	19.191	17.761	16.415	16.880
hept-1-yne	1.911	1.918	1.826	1.768
oct-1-yne	1.746	1.729	1.687	1.642
ethanol	0.552	0.530	0.521	0.494
methanol	0.357	0.332	0.345	0.327
propan-1-ol	0.671	0.638	0.609	0.575
propan-2-ol	0.788	0.760	0.736	0.698
isobutyl alcohol	0.814	0.698	0.605	0.541
benzene	2.176	2.120	2.033	1.952
toluene	3.192	3.155	3.040	2.903
ethylbenzene	4.774	4.598	4.458	4.244
acetone	1.667	1.642	1.520	1.440
butan-2-one	1.980	1.902	1.835	1.803
thiophene	0.156	0.170	0.170	0.172
pyridine	0.082	0.084	0.087	0.088
methyl acetate	0.324	0.333	0.323	0.333
ethyl acetate	0.372	0.359	0.345	0.331

Table 5-15: Measured activity coefficients at infinite dilution for selected organic solutes (1) in DES4 (3) at T = (313.15, 323.15, 333.15 and 343.15) K with solvent column loading n_3 = 2.8675 mmol (29.04 wt. %).

Experimental activity coefficient at infinite dilution at T [K]				
Solute	**T=313.15**	**T=323.15**	**T=333.15**	**T=343.15**
n-hexane	28.224	21.450	19.818	18.605
n-heptane	31.085	28.401	26.817	25.119
n-octane	39.027	36.735	36.196	32.761
cyclopentane	8.868	8.711	8.255	8.053
cyclohexane	11.604	11.008	11.511	9.992
cycloheptane	13.194	12.407	11.832	11.451
cyclooctane	15.731	14.846	14.182	13.528
hex-1-ene	14.552	13.573	14.250	14.192
hept-1-ene	19.798	17.626	16.899	16.812
hept-1-yne	1.739	1.731	1.769	1.797
oct-1-yne	1.574	1.587	1.616	1.642
ethanol	0.510	0.504	0.496	0.496
methanol	0.327	0.327	0.325	0.327
propan-1-ol	0.588	0.588	0.577	0.576
propan-2-ol	0.714	0.706	0.682	0.637
isobutyl alcohol	0.767	0.659	0.588	0.541
benzene	1.971	1.958	2.006	2.010
toluene	2.919	2.899	2.904	2.933
ethylbenzene	4.3545	4.304	4.257	4.262
acetone	1.563	1.524	1.508	1.487
butan-2-one	1.844	1.828	1.797	1.783
thiophene	0.141	0.1565	0.163	0.173
pyridine	0.078	0.081	0.085	0.089
methyl acetate	0.304	0.309	0.342	0.347
ethyl acetate	0.358	0.344	0.347	0.339

Table 5-16: Calculated average activity coefficients at infinite dilution for selected organic solutes (1) in DES4 (3) at T = (313.15, 323.15, 333.15, and 343.15) K.

Experimental activity coefficient at infinite dilution at T [K]				
Solute	**T=313.15**	**T=323.15**	**T=333.15**	**T=343.15**
n-hexane	28.026	21.251	19.201	18.310
n-heptane	30.745	28.339	26.187	24.198
n-octane	40.072	37.632	35.752	32.559
cyclopentane	9.315	8.379	7.958	8.474
cyclohexane	11.992	11.026	11.078	9.697
cycloheptane	13.583	12.714	11.972	11.365
cyclooctane	16.219	15.254	14.414	13.549
hex-1-ene	14.940	13.264	13.093	12.957
hept-1-ene	19.494	17.693	16.657	16.846
hept-1-yne	1.825	1.825	1.798	1.782
oct-1-yne	1.660	1.658	1.651	1.642
ethanol	0.531	0.517	0.509	0.495
methanol	0.342	0.330	0.335	0.327
propan-1-ol	0.629	0.613	0.593	0.576
propan-2-ol	0.751	0.733	0.709	0.668
isobutyl alcohol	0.790	0.679	0.596	0.541
benzene	2.073	2.039	2.020	1.981
toluene	3.055	3.027	2.972	2.918
ethylbenzene	4.564	4.451	4.357	4.253
acetone	1.615	1.583	1.514	1.464
butan-2-one	1.912	1.865	1.816	1.793
thiophene	0.148	0.163	0.167	0.173
pyridine	0.080	0.083	0.086	0.089
methyl acetate	0.314	0.321	0.333	0.340
ethyl acetate	0.365	0.351	0.346	0.335

Table 5-17: The partial excess enthalpy of mixing at infinite dilution for selected organic solutes in DES4 obtained from the Gibbs-Helmholtz equation.

Excess Enthalpy	
Solute	$\Delta H_i^{E,(\infty)}$ = **kJ.mol^{-1}**
n-hexane	12.435
n-heptane	6.003
n-octane	7.120
cyclopentane	3.084
cyclohexane	5.620
cycloheptane	5.322
cyclooctane	5.323
hex-1-ene	3.989
hept-1-ene	4.510
hept-1-yne	0.762
oct-1-yne	0.330
ethanol	2.023
methanol	1.073
propan-1-ol	2.666
propan-2-ol	3.418
isobutyl alcohol	11.339
benzene	1.303
toluene	1.388
ethylbenzene	2.083
acetone	3.023
butan-2-one	1.969
thiophene	-4.265
pyridine	-3.193
methyl acetate	-2.448
ethyl acetate	2.457

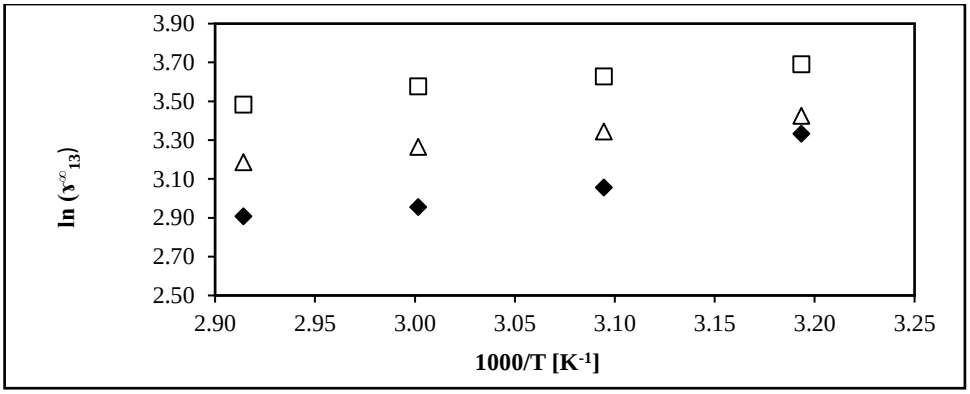

Figure 5-30: Plots of ln (γ_{13}^{∞}) against 1/T for alkanes; n-hexane (♦), n-heptane (□), and n-octane (Δ) (1) in DES4 (3).

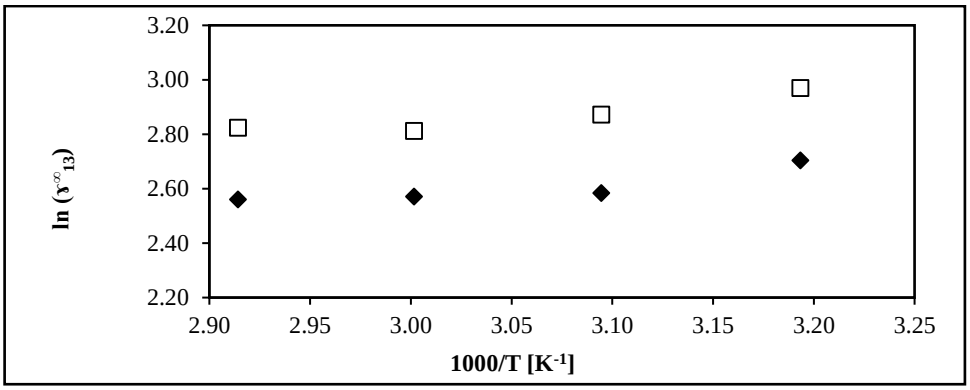

Figure 5-31: Plots of ln (γ_{13}^{∞}) against 1/T for alk-1-enes; hex-1-ne (♦) and hept-1ene (□), (1) in DES4 (3).

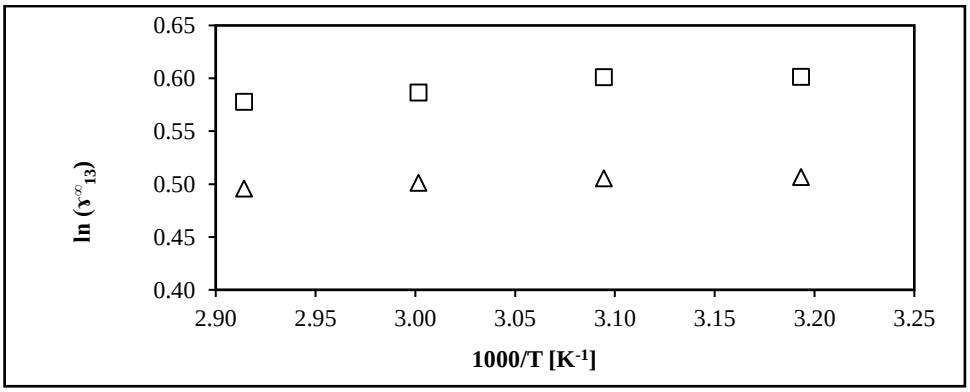

Figure 5-32: Plots of ln (γ_{13}^{∞}) against 1/T for alk-1-ynes; hep-1-yne (□), and oct-1-yne (Δ), (1) in DES4 (3).

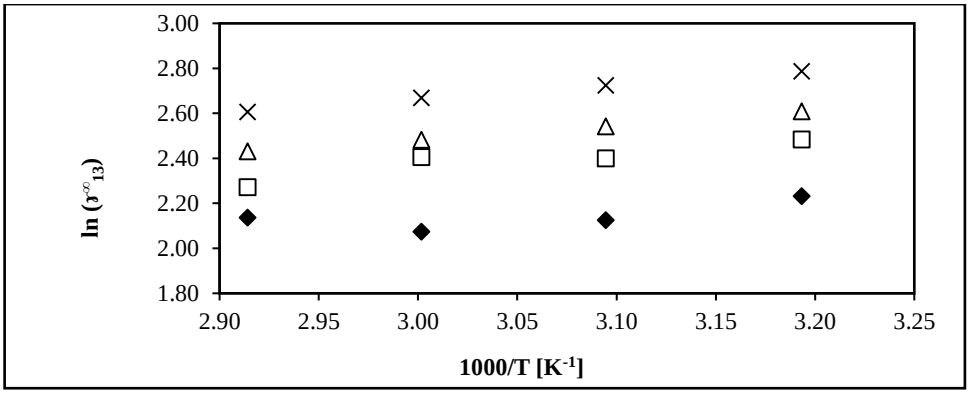

Figure 5-33: Plots of ln (γ_{13}^{∞}) against 1/T for cycloalkanes; cyclopentane (♦), cyclohexane (□) cycloheptane (∆), and cyclooctane (x), (1) in DES4 (3).

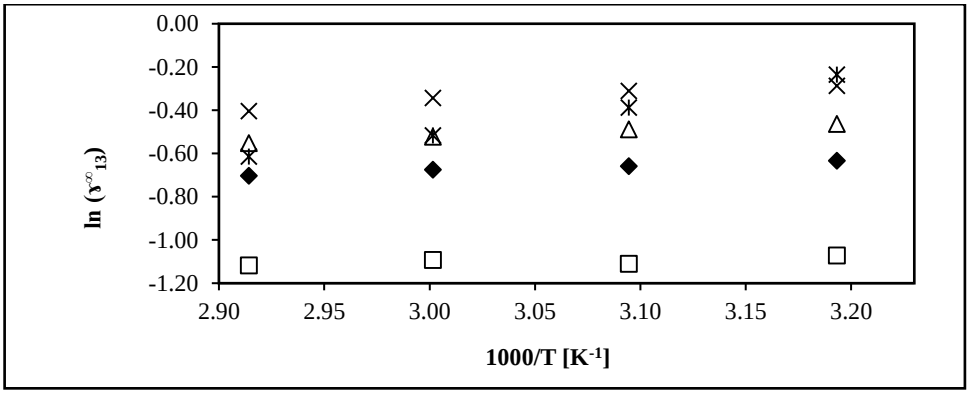

Figure 5-34: Plots of ln (γ_{13}^{∞}) against 1/T for alkanols; methyl alcohol (□), ethyl alcohol (♦), propan-1-ol (∆), propan-2-ol (x), and isobutyl alcohol (✶), (1) in DES4 (3).

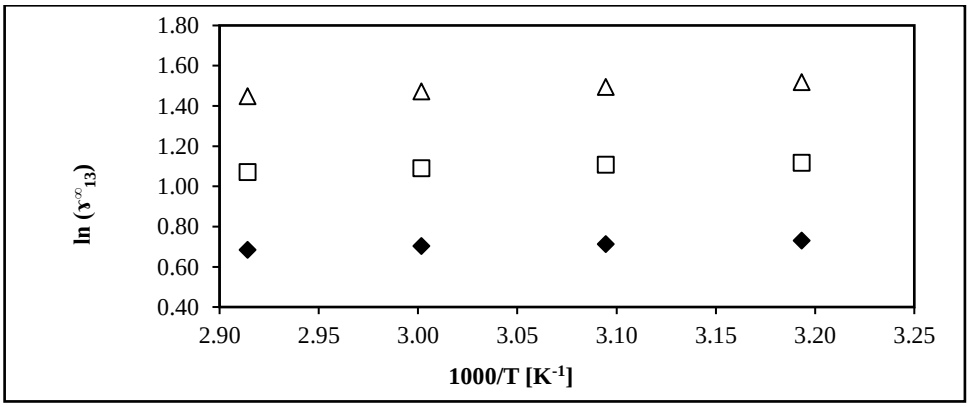

Figure 5-35: Plots of ln (γ_{13}^{∞}) against 1/T for alkylbenzenes; benzene (♦), toluene (□), and ethylbenzene (∆), (1) in DES4 (3).

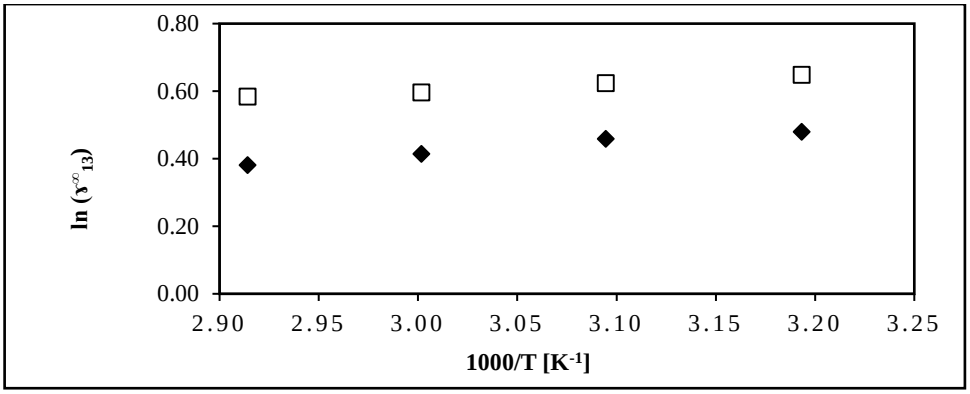

Figure 5-36: Plots of ln (γ_{13}^{∞}) against 1/T for ketones; acetone (♦) and butan-2-one (□), (1) in DES4 (3).

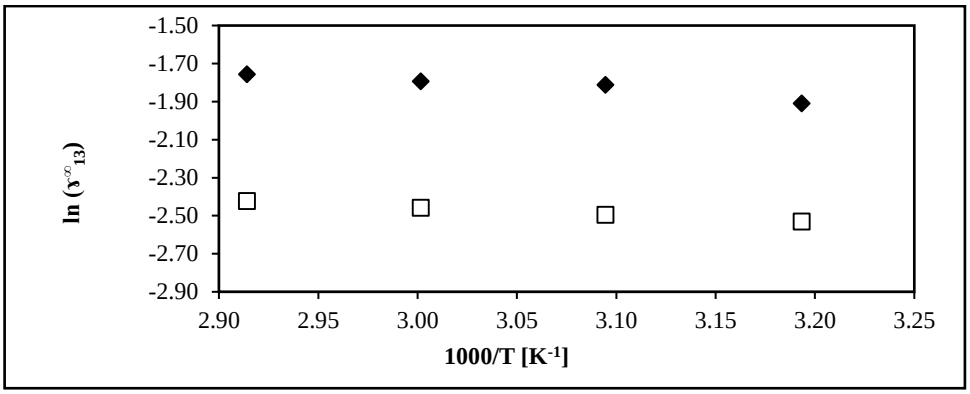

Figure 5-37: Plots of ln (γ_{13}^{∞}) against 1/T for heterocyclic; thiophene (♦) and pyridine (□), (1) in DES4 (3).

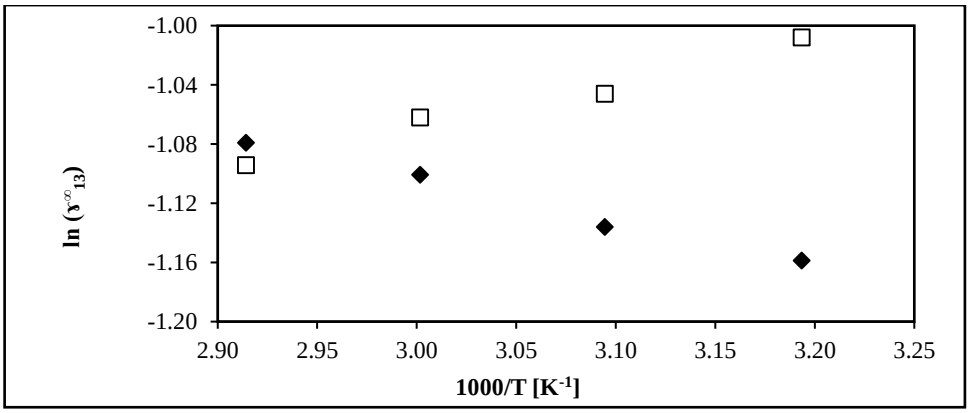

Figure 5-38: Plots of ln (γ_{13}^{∞}) against 1/T for ester; methyl acetate (♦) and ethyl acetate (□), (1) in DES4 (3).

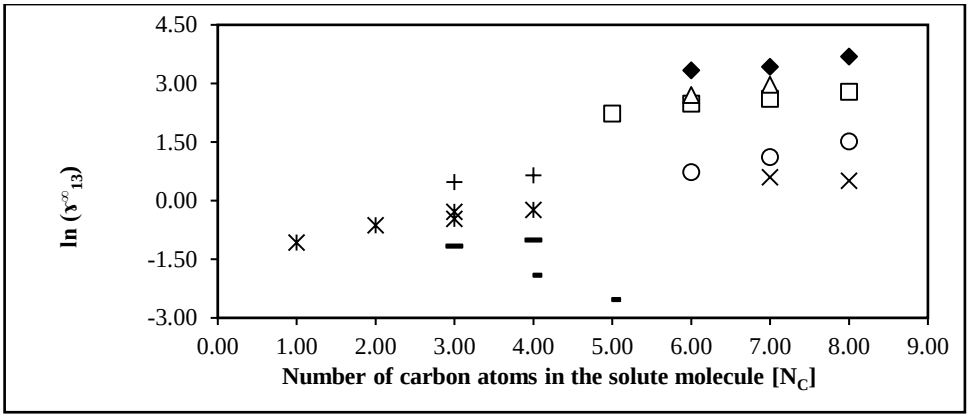

Figure 5-39: Plots of ln (γ_{13}^{∞}) against N_c for alkanes (♦), alk-1-enes (Δ), alk-1-ynes (x), cycloalkanes (□), alkanols (✶), alkyl benzenes (o), heterocyclic (-), ketones (+), and ester (–), (1) in DES4 (3).

CHAPTER SIX

DISCUSSION

Chapter Overview

This chapter discusses the experimental results obtained in this study and presented in Chapter Five. This chapter also highlights the purity of chemicals that were used. The relevance of DESs as separation agents was also assessed by benchmarking with commonly used ILs and industrial solvents for separating azeotropic and close-boiling mixtures. Thus, common industrial separation problems were selected to investigate the potential of DESs to separate such mixtures by determining selectivity and capacity at infinite dilution.

6.1. Chemicals used in this study

In this study, chemicals were sourced from different companies, local and international, as depicted in Appendix A (Tables A-1 & A-2). All the chemicals were found to contain purities within the acceptable limit and thus used without further refinement. The GLC technique utilised in this study is useful when expensive speciality chemicals or high purity chemicals are used, as the technique only requires a minuscule amount of chemical for analysis (i.e., $\leq 0.5\,\mu L$).

The properties of all chemicals used in this study were sourced from two textbooks: CRC Handbook of Chemistry and Physics, and the Handbook of Properties of Gas and Liquids (Poling *et al.*, 2001; Lide, 2004). These properties include critical volume, acentric factor, critical temperature and critical pressure. These properties describe the nature of the components and thus play an important role when computing IDACs. Activity coefficients at infinite dilution calculations also rely on pure component properties for determining the second virial coefficients. The second virial coefficients were evaluated using the correlations of McGlashan and Potter (1962) as discussed in section 3.3 (Equation 3-20). Moreover, the liquid molar volumes in this study were determined from the modified correlations of Rackett (1970) as discussed in section 3.3 (Equation 3-25).

For all DESs, it was necessary to measure at least two properties and compare results with available literature data. Hence, density and the refractive index of DESs were measured to assess their purity. Table 6-1 presents the properties of DESs in this study.

Table 6-1: Refractive indices and densities at T = 313.15 K for all DESs utilised in this study

Solvents	Refractive index	Density (g.cm^{-3})
	Experimental	Experimental
DES1	1.47183*	1.14522*
DES2	1.45599	1.07219
DES3	1.45424	1.05321
DES4	1.47923	1.04225

** Measured at T= 298.15 K*

The refractive indices and densities of DES2, DES3, and DES4 were measured at a temperature of 313.15 K due to their melting points above ambient temperature (298.15 K).

Refractive indices of the listed four DESs were measured using the Atago refractometer model RX-7000 α with an uncertainty of ± 0.0001. The equipment was calibrated by measuring the refractive index of ultra-pure water (1.33258 and 1.33052 at 298.15 K and 313.15 K) before measurements. For better accuracy, at least three different measurements were taken for each sample.

It can be observed that the DESs refractive index sequency was DES4 > DES3 ≅ DES2.

The densities of DESs were measured using the Anton Paar density and sound velocity meter, model DSA 500M with an uncertainty of ±0.0001 g/cm^3. The internal apparatus calibration was confirmed by measuring the density of ultra-pure water. The sample was syringed and injected (without any air-bubble) at least two times to measure the effectiveness of the technique.

The measured densities data for all DESs as a function of temperature followed this sequency; DES2 > DES3 > DES4.

For the four DESs that were subjected to refractive index and density measurements, no comparison with literature data was possible. However, DES1 density was found to strongly agree with literature data (1.155 g.cm^{-3}) leading to 0.85% relative deviation (Rodriguez *et al.*, 2016).

6.2. Measurements of activity coefficients at infinite dilution

As a test of the experimental technique, activity coefficients of selected solutes at infinite dilution were determined, as discussed in section 5.1, results presented in Table 5-1. The test system results

agreed strongly with literature values.

For new systems, the focus of this study was to assess the ability to separate binary mixtures that form azeotropes or have boiling points that are in proximity. Therefore, it was necessary to investigate the broad range of organic compounds as solutes. This helped to explain some of the trends for the measured data in terms of different functional groups. IDAC data are presented in Chapter Five. The real reflection of the effect of selected QASs and HBDs on IDACs is observed. However, since there has been no data provided for systems under investigation that involve DESs a comparison of IDAC data with literature data was not possible.

In this study, the prediction of IDACs using a model to correlate the data obtained was not attempted, as this moved beyond the study scope. For experimental data, two different solvents' mass fractions served as the consistency test and the check for possible adsorption effects, to determine whether or not the data would be reproducible. The solute mole fraction of 1×10^{-5} was maintained for these IDAC measurements for the purpose of representing infinite dilution conditions.

6.2.1. Analysis of IDAC for used DESs

Experimental data obtained from IDAC measurements in DES1, DES2, DES3 and DES4 are provided in Tables 5.4, 5.8, 5.12 and 5.16 and Figures 5.1 to 5.40. However, the better method of analysing these data is to plot IDACs by their functional groups as a function of the carbon chain length. The resultant plots generated in Figures 5.10, 5.20, 5-30 and 5-40 indicate the following hierarchy for IDAC values:

Alk-1-anes > alk-1-enes > cycloalkanes > alkylbenzenes > alk-1-ynes > ketones > alkanols > esters > heterocyclic compounds (i.e. pyridine and thiophene). While measuring the IDACs, it was observed that alkanols led to elongated retention times, indicating that alkanols interacted strongly with the investigated DESs.

From experimental the data, it was observed that alk-1-anes had the highest IDACs for DESs investigated in this study. Alk-1-anes IDACs increased with an increase in carbon chain length (Figures 5-30 & 5-40). This behaviour indicates that inter-molecular forces of attraction for mixtures of this type (DES3 and DES4) decreases as the carbon chain length increases. It was observed as well that alk-1-anes IDAC values decreased with an increase in carbon chain length (Figures 5-10 & 5-20) indicating that the inter-molecular force of attraction for mixtures of this type

(DES1 and DES2) increases as the carbon chain length increases.

Cycloalkanes had lower IDACs than the corresponding alk-1-anes. For cycloalkanes, the IDACs values obtained in DES2, DES3 and DES4 were increasing with an increase in carbon chain length (Figures 5-20, 5-30 & 5-40), whereas for DES1 there was a decrease with an increase in carbon chain length. Alk-1-enes exhibited higher values of IDACs than cycloalkanes but lower than those for corresponding alk-1-anes. It was also observed that for alk-1-ynes, IDACs in DES1, DES3 and DES4 were decreasing with an increase in carbon length.

The opposite trend was observed for IDAC values of alk-1-ynes in DES2: the IDACs for alkylbenzenes were reduced drastically as compared to alk-1-anes or alk-1-enes, or alk-1-ynes or cycloalkanes. This behaviour indicated that alkylbenzenes interact more with DESs than alk-1-anes or alk-1-enes, or alk-1-ynes or cycloalkanes. Overall, the behaviour of these functional groups in terms experimental IDAC values can be more accurately explained by examining the functional group molecular interactions with solvents.

Alkanols, esters, ketones and heterocyclics had very low IDACs, indicating that these solutes interacted more strongly with DESs than alk-1-anes or alk-enes or cycloalkanes or alk-1-ynes. These low IDACs also indicates that DESs were soluble in these mixtures. However, a more thorough interpretation of this behaviour is presented in section 6.2.3 which is devoted to molecular interactions.

6.2.2. Partial molar enthalpy

To evaluate the temperature dependence of IDACs, experimental activity coefficient measurements at infinite dilution were performed at temperatures of 313.15, 323.15, 333.15 and 343.15 K. Four, rather than three or fewer temperatures were convenient to effectively determine and improve the reliability of partial excess enthalpies of mixing at infinite dilution. These values, calculated from Equation 2-13, are reported in Chapter Five, in Tables 5-5, 5-9, 5-13, and 5-17.

For DES2, all molar excess enthalpy values except those for esters are positive; this implies that dissociation effects outweigh the association effects in mixtures that involve very low organic solute concentrations. This suggests that the IDACs of solutes are decreasing with an increase in temperature. However, for DES4, values for heterocyclics and one ester are negative, revealing that association effects outweigh dissociation effects in a mixture of very low concentration.

Furthermore, positive values signify that these solutes possess an endothermic heat of mixing, which also indicates limited solubility.

For DES1 and DES3, both effects were observed. In both solvents, excess molar enthalpies for all alcohols, alkylbenzenes and ketones are positive, whereas for all alk-1-anes, alk-1-enes, alk-1-ynes, cycloalkanes and esters, they are negative. These negative values signify the solubility of hydrocarbons in DESs, indicated by its exothermic heat of mixing.

For predicting IDACs, this data is crucial as it allows an extrapolation or interpolation of partial excess enthalpy at temperatures other than those measured experimentally. However, due to the dearth of data in literature, it was not possible to compare the reported values with literature data for other DESs.

6.2.3. Molecular interactions

The significance of IDAC values can be accurately explained by the molecular structure of solutes and the solvents.

Alk-1-anes are linear in molecular structure, and they contain only symmetrical carbon bonded chains to hydrogen atoms. They possess only a single bond, and they also have very little electronegativity between hydrogen and carbon, rendering them highly unreactive. Thus, the van der Waals forces that can operate in this functional group interactions are London dispersion forces.

For this study, the effect of molecular structure was observed as they interacted very little with all four DESs under investigation. This can be seen by the unusually high IDACs which also indicates that to all four DESs they are highly non-polar. This behaviour also insinuates that the mixtures were by far non-ideal, attributable to London forces that are too weak to overweigh the solute-solute bonds to facilitate solute-solvent interactions. Facilitating the breakdown of solute-solute bonds to allow the occurrence of solute-solvent bonding requires strong solvent London forces to provide more energy to the system. In general, these London forces dominate the non-polar interactions.

Alke-1-nes have a similar molecular structure as alk-1-anes; they also contain only symmetrical carbon bonded chains to hydrogen atoms. However, they do contain at least one double-bonded carbon atoms. Alk-enes are slightly more polar than alk-1-anes since they contain carbon and

hydrogen atoms which produce a pi and a sigma bond. Similar to alk-1-anes, the van der Waals forces that can operate in alke-1-enes are London dispersion forces.

In this study, alk-1-enes IDACs are slightly lower than corresponding alk-1-anes. The behaviour of alk-1-enes for all four DESs is attributable to the geometric shape and π electrons which tend to be more polarised than in alk-1-anes.

Alk-1-ynes have a similar molecular structure to the alk-1-anes and alk-1-enes where London dispersion forces dominate solute-solvent interactions, and a triple bond exists consisting of two pi bonds and a sigma bond which creates acidic protons. This occurs in the terminal hydrogen at the end of the molecule. This acidic proton significantly increases the interaction between DESs and alk-ynes mixtures, resulting in stronger interactions. Thus, reductions in values of IDACs in all DESs were observed.

Cycloalkanes have a cyclic/ring molecular structure and are similar to alk-anes. Consequently, the behaviour is similar to alk-1-anes.

Alkanols are highly polar due to the high electronegativity of the hydroxyl oxygen atoms. This influences the molecular interactions of alkanols with other substances. The London forces operate alkanols molecular interactions.

In this study, all four DESs were essentially polar, leading to an attainment of low activity coefficients at infinite dilution. This is due to strong London forces of attraction possessed by all four DESs. The low values of IDACs obtained in this study were associated with stronger interactions or readiness for solubilization.

Ketones are polar due to the high electronegativity of carbonyl group $C=O$ which defines the chemistry of ketones. The molecular structure contains the carbonyl groups on both sides, which does not possess a hydrogen atom attached to an electronegative oxygen molecule. For solute-solute interactions, ketones are characterised by London and dipole-dipole (Keesom) forces. However, solvent-solute interactions are dominated by London and Debye forces. Since DESs and ketones are polar in nature, there are, consequently large differences between the two.

Aromatics (alkylbenzenes and heterocyclic compounds) have a cyclic non-polar molecular

structure similar to cycloalkanes. However, the ring, consisting of six hydrogen atoms that are short of saturation, has delocalised π electrons which create an electron cloud possessing significant density above and below the aromatic ring. The behaviour that results from molecular interactions significantly affected and increased the polarizability of molecules. As a result, the IDAC values measured for alk-1-anes, alk-1enes, alk-1-ynes, and cycloalkanes in all four DESs were reduced significantly. The resulting activity coefficients produce the non-ideal mixtures shown by large values in three DESs (DES1, DES2 and DES3) for alkylbenzenes.

For heterocyclic compounds, the resulting activity coefficient produced non-ideal mixtures shown by low values in all four DESs. This behaviour can be attributed to London dispersion forces that increase the attraction, whereas the DESs molecular size was increasing.

Esters are polar in nature due to the exposed carbonyl group. Oxygen from a carbonyl group possesses high electronegativity. The molecular structure of esters contains strong Keesom solute-solute intermolecular forces which result in an occurrence of solute-solvent bonding. In this study, esters yielded lower IDAC values in all four DESs investigated, possibly attributed to the solute Debye forces which tend to polarise DESs molecular bonds.

6.2.4. Effects of hydrogen bond donor to experimental IDACs data

The role of HBD was revealed as critically important. This was one of the most important parameters aiding in validating a particular DES suitability for the separation of binary mixtures that exhibit azeotropes as well as those of close-boiling point. In this study, three HBDs were used (i.e. Glycerol, Ethylene glycol and 1,6 Hexanediol).

From what has been observed, the effect of varying the HBDs has significantly affected IDAC values. As a result, HBDs indicated the following hierarchy for IDAC values:

a) **Ethylene Glycol:** alk-1-anes > alk-1-enes > cycloalkanes > alkylbenzenes > cycloalkanes > alk-1-ynes > ketones > esters > alkanols > heterocyclics;
b) **Glycerol:** alk-1-enes > alk-1-anes > cycloalkanes > alkylbenzenes > alk-1-ynes > ketones > esters > alkanols > heterocyclics; and
c) **1,6 Hexanediol:** alk-1-anes > alk-1-enes > cycloalkanes > alkylbenzenes > ketones > alk-1-ynes > alkanols > esters > heterocyclics.

A possible explanation for this hierarchy could be attributed to the molecular structure exhibited by

each HBD. The polarity of molecules could better explain this due to hydroxyl groups and carbon chain lengths possessed by respective HBDs.

From observation, high carbon chains were associated with low polarity induced by the presence of hydroxyl groups. In glycerol, the IDAC was lower than in ethylene glycol due to oxygen-oxygen lone pair repulsion in the structure, reducing the hydrogen bonding capability. Also, low IDAC values for all functional groups in 1,6 hexanediol were observed due to the hydroxyl groups attached at the ends of this HBD.

In the molecular structure of glycerol, there are three hydroxyl groups attached, whereas for ethylene glycol and 1,6 hexanediol there are two hydroxyl groups enclosed to the molecular structure. From experimental data of IDACs, it was observed that the dissolution decreased with an increasing carbon chain length.

In this study, it was very clear that 1,6 hexanediol was able to wrap around the anion more tightly than glycerol and ethylene glycol to the chloride ion of tetramethylammonium salt. This was due to hydroxyl groups that were attached at the ends of 1,6 hexanediol. Also, 1,6 hexanediol had a large enough space between the HBD groups such that it envelopes the chloride anion present in the salt side of a DES so much that only one molecule can complex around it. However, the space between HBDs (i.e. Glycerol and Ethylene glycol) is not enough to completely wrap around the chloride anion. As a result, high IDAC values were obtained.

The fact that there are three HDB sites in glycerol as opposed to two in 1,6 hexanediol and ethylene glycol means there is a greater degree of hydrogen bonding to other molecules. So the addition of chloride interrupts this structure as some of the compounds exhibiting hydroxyl group no longer interact with each other, they now interact with chloride.

Moreover, HBDs indicated the following hierarchy for the selectivity and capacity values for the investigated common industrial separation problems:

a) **n-hexane (1) - hex-1-ene (2) separation problem**
   Selectivities: Ethylene Glycol > 1,6 Hexanediol > Glycerol
   Performance indices: Ethylene Glycol > 1,6 Hexanediol > Glycerol

b) **n-hexane (1) - benzene (2) separation problem**

Selectivities: Ethylene Glycol > 1,6 Hexanediol > Glycerol

Performance indices: 1,6 Hexanediol > Ethylene Glycol > Glycerol

c) **methanol (1) - benzene (2) separation problem**

Selectivities: 1,6 Hexanediol > Ethylene Glycol > Glycerol

Performance indices: 1,6 Hexanediol > Ethylene Glycol > Glycerol

d) **cyclohexane (1) - benzene (2) separation problem**

Selectivities: Ethylene Glycol > Glycerol > 1,6 Hexanediol

Performance indices: 1,6 Hexanediol > Ethylene Glycol > Glycerol

e) **cyclohexane (1) - ethanol (2) separation problem**

Selectivities: Ethylene Glycol > Glycerol > 1,6 Hexanediol

Performance indices: 1,6 Hexanediol > Ethylene Glycol > Glycerol

f) **acetone (1) - ethanol (2) separation problem**

Selectivities: Glycerol > 1,6 Hexanediol > Ethylene Glycol

Performance indices: 1,6 Hexanediol > Ethylene Glycol > Glycerol

g) **n-heptane (1) - toluene (2) separation problem**

Selectivities: Ethylene Glycol > 1,6 Hexanediol > Glycerol

Performance indices: 1,6 Hexanediol > Ethylene Glycol > Glycerol

From observation, ethylene glycol generally indicated high selectivity values followed by 1,6 hexanediol and glycerol. Also, 1,6 hexanediol indicated better performance index, followed by ethylene glycol and glycerol. This behaviour could be attributed to HBDs carbon chain length, hydroxyl groups and polarity, as explained for IDAC values.

6.3. Selectivities and capacities

A benefit of using a range of solutes was that the DES separation factors of the desired solute over other solutes could be determined. In this study, selectivity and capacity values were used for preliminary assessment of DESs as potential solvents to separate binary mixtures that form azeotropes or boiling mixtures that are close in proximity. Selectivity and capacity values were determined using Equations 2-3 and 2-4 at infinite dilution. As a result, data of some selected common combinations were obtained and presented in Tables 6-2 to 6-9 and finally compared at temperatures of 313.15, 323.15 and 333.15 K. Whenever possible, DES data were compared with

those of some ILs and solvents currently used in industry (Figure 6-1 to 6-8).

6.3.1. Selectivity and Limiting capacity of DESs for n-hexane (1) and hex-1-ene (2)

Table 6-2 and Figure 6-1 present selectivities of the four DESs and four ILs for n-hexane (1) over hex-1-ene (2) at temperatures of 313.15, 323.15 and 333.15 K. It also presents limiting capacities for listed solvents for hex-1-ene at the same temperatures.

Table 6-2: A comparison of the selectivity and limiting capacity of solvents for n-hexane (1) hex-1-ene (2) separation at different temperatures T [K]

Experimental selectivity and capacity at infinite dilution at T [K]						
	Selectivity, S_{12}^{∞}			**Limiting Capacity**, k_2^{∞}		
	n-hexane (1)/hex-1-ene (2)			**hex-1-ene (2)**		
Solvent	**313.15**	**323.15**	**333.15**	**313.15**	**323.15**	**333.15**
DES1[a]	0.78	0.72	0.75	0.004	0.003	0.003
DES2[a]	3.04	3.78	5.86	0.002	0.003	0.004
DES3[a]	1.34	1.80	1.36	0.019	0.019	0.019
DES4[a]	1.88	1.60	1.47	0.067	0.075	0.076
[HMIM][BTI][b]	1.70	1.67	1.64	0.217	0.223	0.225
[BMIM][SCN][c]	3.39[f]	3.26[f]	3.18[f]	0.019[f]	0.02[f]	0.023[f]
[OMIM][PF_6][d]	1.69	1.70	1.69	0.154	0.159	0.163
[NMP][e]	2.04	1.96	1.89	0.065	0.070	0.075

[a] This work; [b] Kato and Gmehling (2005); [c] Domańska and Laskowska (2009); [d] Olivier et al. (2010); [e] Krummen and Gmehling (2004); [f] interpolated value

The experimental data presented in Table 6-2 for n-hexane (1) - hex-1-ene (2) systems in Figure 6-1 were used to plot the selectivities of four DESs and four selected ILs at various temperatures.

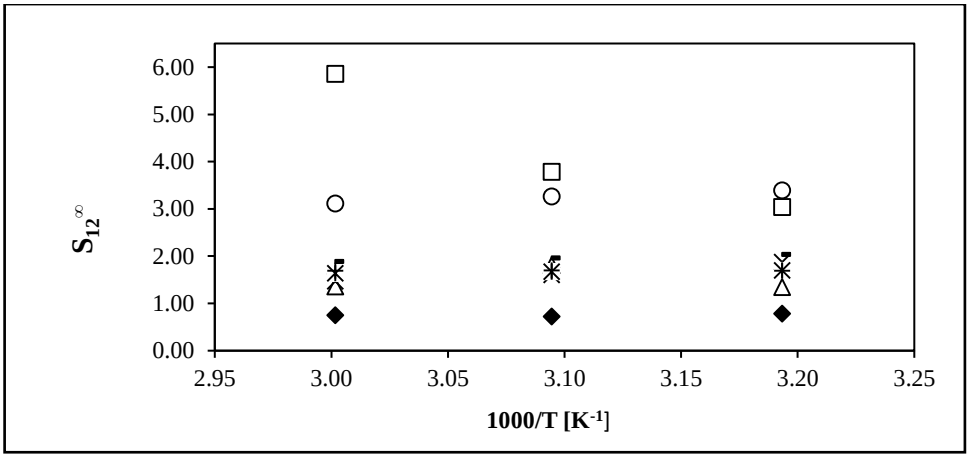

Figure 6-1: Selectivities of various solvents against 1/T for the combination of hex-1-ane (1)/ hex-1-ene (2), (♦), DES1 (□), DES2 (Δ), DES3 (x), DES4 (+), [OMIM][PF_6] (⋆), [HMIM][BTI] (-), [NMP] (o), [BMIM][SCN].

Figure 6-1 shows that the selectivities of DES1, DES3 and DES4 are very similar to this system, whereas DES2 is high when compared to the other three DESs. All selectivity values obtained in this study when comparing DESs and commercial, DESs were low, indicating that DES1, DES3 and DES4 would not improve the separation of the components of this system due to selectivities of less than 2. However, DES2 exhibited higher selectivity for n-hexane (1) over hex-1-ene (2) which indicates better performance than industrial molecular solvents.

Limiting capacity values decided the selection of the suitable solvent for this system at infinite dilution. All four DESs limiting capacity values were extremely low, signifying a poor performance for each of the four investigated DESs. As a result, the separation of this system using extractive distillation or liquid-liquid extraction column with lower limiting capacity values would require a significant amount of DESs. Moreover, this would results in an increased operation cost as more solvent will be added to the process which then needs to be recovered after each use.

6.3.2. Selectivity and Limiting capacity of DESs for n-hexane (1) and benzene (2)

Table 6-3 and Figure 6-2 present selectivities of the four DESs and four ILs for n-hexane (1) over benzene (2) at temperatures of 313.15, 323.15 and 333.15 K. It also presents limiting capacities for listed solvents for benzene at the same temperatures.

Table 6-3: A comparison of the selectivity and limiting capacity of solvents for n-hexane (1) /benzene (2) separation at different temperatures T [K]

Experimental selectivity and capacity at infinite dilution at T [K]						
	Selectivity, S_{12}^{∞}			Limiting Capacity, k_2^{∞}		
	n-hexane (1)/benzene (2)			benzene (2)		
Solvent	**313.15**	**323.15**	**333.15**	**313.15**	**323.15**	**333.15**
DES1[a]	4.04	5.05	5.98	0.018	0.020	0.021
DES2[a]	91.66	93.88	94.15	0.051	0.055	0.059
DES3[a]	7.00	7.33	7.63	0.102	0.104	0.105
DES4[a]	13.52	10.42	9.51	0.482	0.491	0.495
[HMIM][BTI][b]	10.29	9.59	9.20	1.316	1.282	1.266
[BMIM][SCN][c]	82.41[f]	71.26[f]	61.41[f]	0.463[f]	0.460[f]	0.457[f]
[OMIM][PF_6][d]	11.34	10.81	10.10	1.031	1.010	0.971
[NMP][e]	16.08	14.23	12.55	0.515	0.510	0.500

[a]This work; [b]Kato and Gmehling (2005); [c]Domańska and Laskowska (2009); [d]Olivier et al. (2010); [e]Krummen and Gmehling (2004); [f] interpolated value

The experimental data presented in Table 6-3 for n-hexane (1) - benzene (2) system in Figure 6-2 were used to plot the selectivities of four DESs and other selected solvents at different temperatures.

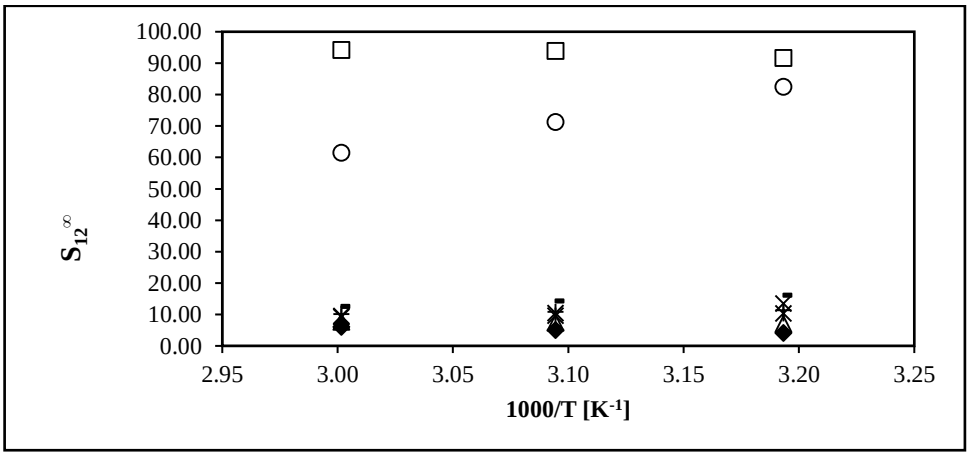

Figure 6-2: Selectivities of various solvents against 1/T for the combination of n-hexane (1)/benzene (2), (♦), DES1 (□), DES2 (∆), DES3 (x), DES4 (+), [OMIM][PF_6] (⋆), [HMIM][BTI] (-), [NMF] (o), [BMIM][SCN].

Figure 6-2 shows that DES2 had higher selectivities for n-hexane (1) over benzene (2) than did DES1, DES3 and DES4 at various temperatures. However, that could not improve the separation

of n-hexane and benzene, since other solvents possess high or similar selectivities to DES1, DES3 and DES4. DES2 indicated substantially high selectivity amongst all four DESs and all other solvents.

In this study, the limiting capacities presented in Table 6-3 for DES1, DES2 and DES3 were relatively low. The only solvent that provided reasonable limiting capacity was DES4 for the separation of n-hexane over benzene system. As a result, DES4 could be regarded as the best performing DES as it showed the best compromise between selectivity and capacity. However, all other solvents had the best separation potential over all four DESs in terms of selectivity-capacity combination. Amongst the DESs, DES4 would be regarded as a reasonable solvent to separate binary mixtures consisting of n-hexane (1) and benzene (2) due to high selectivity and good limiting capacity. Even so, the decision would be based on solvent costs and energy requirements to recover this solvent over other solvents (i.e. ILs are also viscous, if not more viscous than DESs).

6.3.3. Selectivity and Limiting capacity of DESs for methanol (1) and benzene (2)

Table 6-4 and Figure 6-3 present selectivities and limiting capacities of the four DESs and four ILs for methanol (1)/benzene (2) at 313.15, 323.15 and 333.15 K. It also presents limiting capacities for listed solvents for benzene at the same temperatures.

Table 6-4: A comparison of the selectivity and limiting capacity of solvents for methanol (1)/benzene (2) separation at different temperatures T [K]

Experimental selectivity and capacity at infinite dilution at T [K]						
	Selectivity, S_{12}^{∞} **methanol (1)/benzene (2)**			**Limiting Capacity**, k_2^{∞} **benzene (2)**		
Solvent	**313.15**	**323.15**	**333.15**	**313.15**	**323.15**	**333.15**
DES1[a]	0.02	0.02	0.03	0.018	0.020	0.021
DES2[a]	0.03	0.04	0.04	0.051	0.055	0.059
DES3[a]	0.13	0.13	0.13	0.102	0.104	0.105
DES4[a]	0.13	0.16	0.17	0.482	0.491	0.507
[HMIM][BTI][b]	1.57	1.41	1.29	1.316	1.282	1.266
[BMIM][SbF_6][c]	1.382	1.281	1.198	0.813	0.781	0.763
[OMIM][PF_6][d]	1.91	1.67	1.46	1.031	1.010	0.971
[$COC_2N_{1,1,2}$][FAP] [e]	-	2.484[f]	2.204[f]	-	0.793[f]	0.839[f]

[a]This work; [b]Kato and Gmehling (2005); [c]Olivier et al. (2011); [d]Olivier et al. (2010); [e]Marciniak and Wlazło (2015); [f]interpolated value

The experimental data presented in Table 6-4 for methanol (1) - benzene (2) system in Figure 6-3 were used to plot the selectivities of four DESs and four selected ILs at various temperatures.

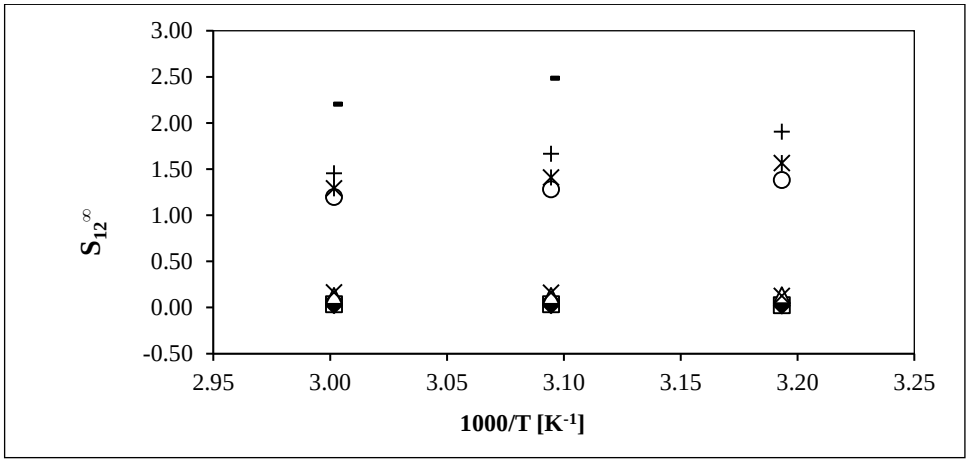

Figure 6-3: Selectivities of various solvents against 1/T for the combination of methanol (1)/benzene (2), (♦), DES1 (□), DES2 (Δ), DES3 (x), DES4 (+), [OMIM][PF_6] (⋆), [HMIM][BTI] (-), [$COC_2N_{1,1,2}$][FAP] (o), [BMIM][SbF_6].

Figure 6-3 shows that the selectivities of all DESs are generally lower than those of solvents, which were also relatively low. The low selectivities suggest that all four DESs would *not* improve the separation of methanol (1) - benzene (1) system.

The limiting capacity values for all DESs, except DES4, were low. The capacities of DESs as compared to other solvents were very low. Thus in this study, there is no suitable solvent for the separation of a binary mixture that consists of methanol (1) and benzene (2).

6.3.4. Selectivity and Limiting capacity of DESs for cyclohexane (1) and benzene (2)

Table 6-5 and Figure 6-4 provide selectivities of the four DESs and four ILs for cyclohexane (1) over benzene (2) at temperatures of 313.15, 323.15 and 333.15 K. It also presents limiting capacities for listed solvents for benzene at the same temperatures.

Table 6-5: A comparison of the selectivity and limiting capacity of solvents for cyclohexane (1) - benzene (2) separation at different temperatures T [K]

Experimental selectivity and capacity at infinite dilution at T [K]						
	Selectivity, S_{12}^{∞} cyclohexane (1)/benzene (2)			**Limiting Capacity, k_2^{∞} benzene (2)**		
Solvent	**313.15**	**323.15**	**333.15**	**313.15**	**323.15**	**333.15**
DES1[a]	3.50	4.45	5.15	0.018	0.020	0.021
DES2[a]	16.00	16.56	17.55	0.051	0.055	0.059
DES3[a]	3.51	3.71	3.92	0.101	0.104	0.105
DES4[a]	5.78	5.41	3.94	0.482	0.490	0.495
Sulfolane[b]	9.98[f]	8.34[f]	6.95[f]	0.424[f]	0.428[f]	0.432[f]
$[EMIM]^+[SCN]^-$[c]	28.425[f]	25.65[f]	23.34[f]	0.289[f]	0.287[f]	0.286[f]
$[OMIM][PF_6]$[d]	7.03	6.68	6.12	1.031	1.010	0.971
[NMP][e]	9.07	8.16	7.30	0.515	0.510	0.500

[a]This work; [b]Möllmann and Gmehling (1997); [c]Domańska and Marciniak (2008); [d]Olivier et al. (2010); [e]Krummen and Gmehling (2004); [f] interpolated value

The experimental data presented in Table 6-5 for cyclohexane (1) - benzene (2) system in Figure 6-4 were used to plot the selectivities of four DESs and other selected solvents at different temperatures.

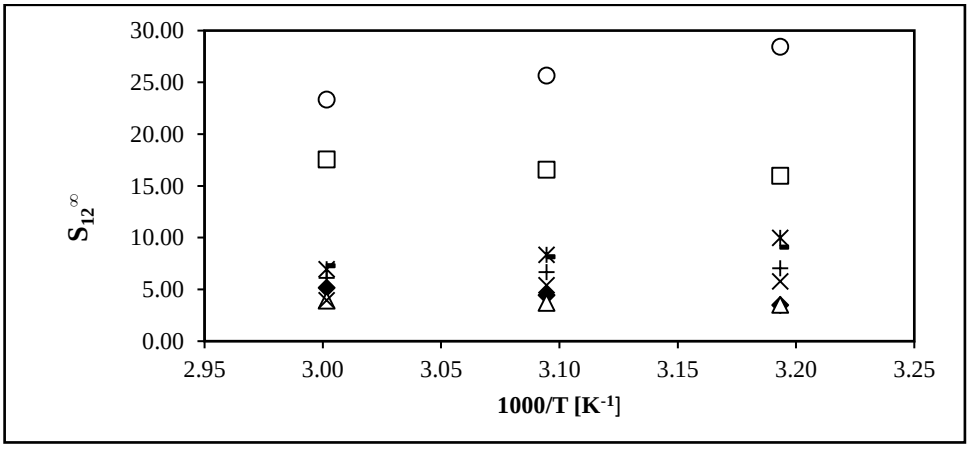

Figure 6-4: Selectivities of various solvents against 1/T for the combination of cyclohexane (1)/benzene (2), (♦), DES1 (□), DES2 (Δ), DES3 (x), DES4 (+), $[OMIM][PF_6]$ (⋆), [Sulfolane] (-), [NMP] (o), [BMIM][SCN].

In Figure 6-4, the selectivity values of cyclohexane (1) over benzene (2), for all four DESs, indicated

possible effective separation. However, DES2 shows considerably better performance than DES1, DES3 and DES4 regarding selectivity measured at infinite dilution. For other solvents, all four solvents performed better than all four DESs regarding selectivity.

From Table 6-5 it can be seen that DES4 has the highest capacity for benzene (2). However, to choose the best DES would require further investigation, since these solvents were possessing very low limiting capacities. Further, the choice would be based on the economics of the process. An ideal solvent would require that both selectivity and capacity at infinite dilution be reasonably high.

6.3.5. Selectivity and Limiting capacity of DESs for cyclohexane (1) and ethanol (2)

Table 6-6 and Figure 6-5 provide selectivities of the four DESs and four ILs for cyclohexane (1) over ethanol (2) at temperatures of 313.15, 323.15 and 333.15 K. It also presents limiting capacities for listed solvents for benzene at the same temperatures.

Table 6-6: A comparison of the selectivity and limiting capacity factors of solvent for cyclohexane (1) - ethanol (2) separation at different temperatures T [K]

Experimental selectivity and capacity at infinite dilution at T [K]						
	Selectivity, S_{12}^{∞}			**Limiting Capacity**, k_2^{∞}		
	cyclohexane (1)/ethanol (2)			**ethanol (2)**		
Solvent	**313.15**	**323.15**	**333.15**	**313.15**	**323.15**	**333.15**
DES1[a]	59.96	70.10	90.67	0.311	0.319	0.341
DES2[a]	140.00	137.19	144.60	0.444	0.456	0.487
DES3[a]	19.61	20.64	22.44	0.569	0.579	0.602
DES4[a]	22.59	21.32	21.76	1.884	1.933	2.983
[HMIM][BTI][b]	3.50	3.60	3.74	0.680	0.735	0.787
[EMIM][CH_3SO_3] [c]	162.04[f]	147.40[f]	133.79[f]	0.486[f]	0.481[f]	0.476[f]
[OMIM][PF_6][d]	2.94	3.22	3.46	0.431	0.488	0.549
$[EPY]^+[BTI]^-$[e]	10.00	10.53	10.80	0.581	0.658	0.730

[a]This work; [b]Kato and Gmehling (2005); [c]Domańska (2012); [d]Olivier et al. (2010); [e]Kato and Gmehling (2004); [f] interpolated value

The experimental data presented in Table 6-6 for cyclohexane (1) - ethanol (2) system in Figure 6-5 were used to plot the selectivities of four DESs and four selected ILs at various temperatures.

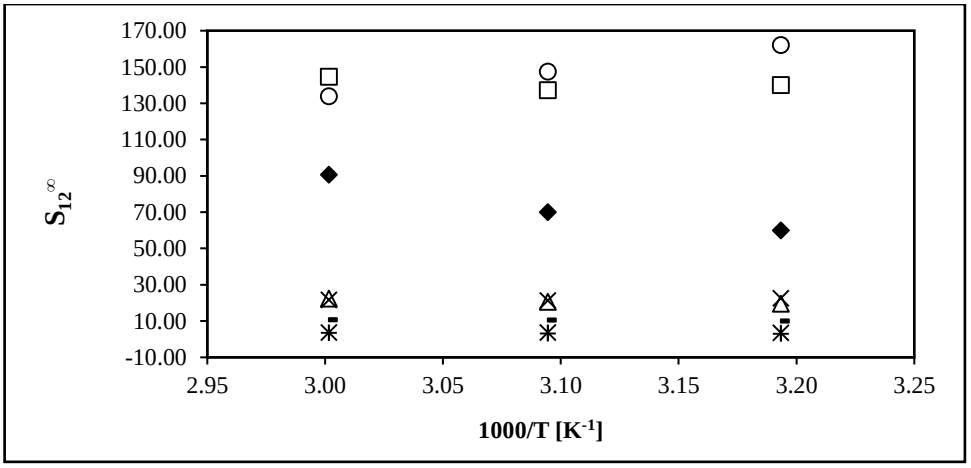

Figure 6-5: Selectivities of various solvents against 1/T for the combination of cyclohexane (1)/ethanol (2), (♦), DES1 (□), DES2 (Δ), DES3 (x), DES4 (+), [OMIM][PF_6] (✶), [HMIM][BTI] (-), $[EPY]^+[BTI]^-$ (o), [EMIM][CH3SO3].

Figure 6-5 presents data for a binary system that is interesting as it contains non-polar cyclohexane (1) and polar ethanol (2). The mixture forms an azeotrope which is hard to separate by conventional distillation processes. In this study, selectivities of the four DESs were extremely high. Figure 6-5 reveals that DES2 was the best solvent regarding selectivity for cyclohexane (1) - ethanol (2) separation obtained at infinite dilution. Furthermore, if the system temperature were to be increased further, DES2 would still exhibit the best selectivity.

The limiting capacities in this study were all high, but DES4 has far greater limiting capacity for ethanol (2), proving that DES4 had the greater potential to separate a binary mixture that consists of cyclohexane (1) and ethanol (2). Additionally, regarding the process economics, this would require a smaller quantity of DES4 for the separation.

6.3.6. Selectivity and Limiting capacity of DESs for acetone (1) and ethanol (2)

Table 6-7 and Figure 6-6 present selectivities of the four DESs and four ILs for acetone (1) over ethanol (2) at temperatures of 313.15, 323.15 and 333.15 K. It also presents limiting capacities for listed solvents for ethanol at the same temperatures.

Table 6-7: A comparison of the selectivity and limiting capacity of solvents for acetone (1) - ethanol (2) separation at different temperatures T [K]

Experimental selectivity and capacity at infinite dilution at T [K]						
	Selectivity, S_{12}^{∞} acetone (1)/ethanol (2)			**Limiting Capacity, k_2^{∞} ethanol (2)**		
Solvent	**313.15**	**323.15**	**333.15**	**313.15**	**323.15**	**333.15**
DES1[a]	3.32	3.31	3.39	0.311	0.319	0.341
DES2[a]	2.29	2.26	2.32	0.444	0.456	0.487
DES3[a]	2.99	2.85	2.86	0.569	0.579	0.602
DES4[a]	3.04	3.06	2.97	1.884	1.933	2.983
[HMIM][BTI][b]	0.22	0.25	0.27	0.680	0.735	0.787
[BMIM][SbF_6][c]	0.17	0.21	0.23	0.429	0.467	0.497
[OMIM][PF_6][d]	-	-	-	0.431	0.488	0.549
[EMIM][CH_3SO_3][e]	4.92	4.97	5.04	0.486	0.481	0.476

[a]This work; [b]Kato and Gmehling (2005); [c]Olivier et al. (2011); [d]Olivier et al. (2010); [e]Bahadur et al. (2014)

The experimental data presented in Table 6-7 for acetone (1) - ethanol (2) system in Figure 6-6 were used to plot the selectivities of four DESs and four selected ILs at various temperatures.

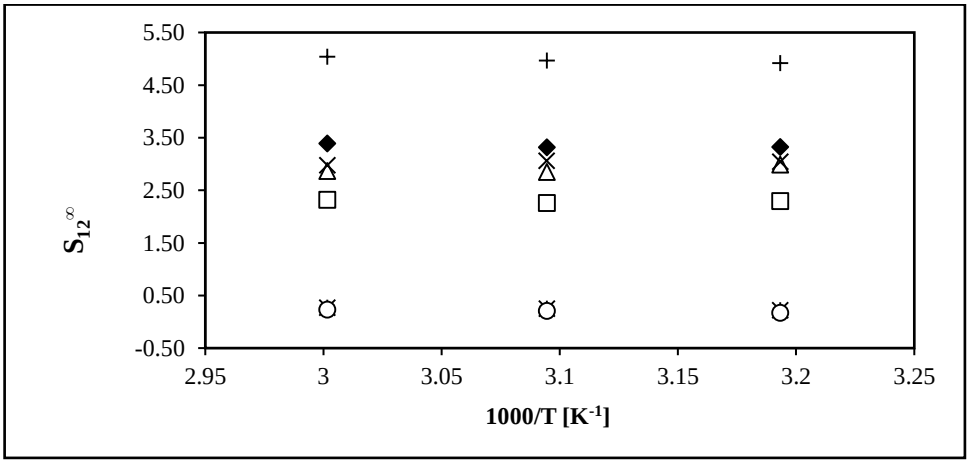

Figure 6-6 : Selectivities of various solvents against 1/T for the combination of acetone (1)/ethanol (2), (♦), DES1 (□), DES2 (Δ), DES3 (x), DES4 (⋆), $[HMIM]^+[BTI]^-$ (+), $[EMIM]^+[CH_3SO_3]^-$ (o), [BMIM][SbF_6].

Figure 6-6 indicates that the investigated DES performance regarding selectivity was independent of system temperature. This is evident by an increase in temperature which provides similar or

slightly different selectivity values of acetone (1) over ethanol (2). Regarding selectivity, all four DESs showed better performance, whereas other solvents exhibited poor ability to separate acetone (1) - ethanol (2) binary mixtures. However, DES1 indicated far better performance and thus would be a suitable solvent to separate this azeotropic mixture.

In this study, all four DESs had high limiting capacity for ethanol (2); likewise, for other solvents, a similar behaviour was observed. However, due to very low selectivity values possessed by industrial solvents, they are not suitable for the separation of this binary mixture. Thus, DES4 possesses a far better limiting capacity, as well as selectivity, and would be the best separation solvent for this azeotropic mixture.

6.3.7. Selectivity and Limiting capacity of DESs for n-heptane (1) and toluene (2)

Table 6-8 and Figure 6-7 provide selectivities of the four DESs and four ILs for n-heptane (1) over toluene (2) at temperatures of 313.15, 323.15 and 333.15 K. It also provides limiting capacities for listed solvents for cyclohexane at the same temperatures.

Table 6-8: A comparison of the selectivity and limiting capacity of solvents for n-heptane (1) - Toluene (2) separation at difference temperatures T [K].

Experimental selectivity and capacity at infinite dilution at T [K]						
	Selectivity, S_{12}^{∞} **heptane (1)/toluene (2)**			**Limiting Capacity**, k_2^{∞} **toluene (2)**		
Solvent	**313.15**	**323.15**	**333.15**	**313.15**	**323.15**	**333.15**
DES1[a]	2.22	2.71	3.10	0.010	0.011	0.012
DES2[a]	37.11	37.66	37.72	0.024	0.025	0.026
DES3[a]	7.11	6.99	6.32	0.073	0.074	0.073
DES4[a]	10.06	9.36	8.81	0.327	0.330	0.336
[HMIM][BTI][b]	10.29	9.52	8.95	0.971	0.952	0.926
[BMIM][SbF_6][c]	19.84	18.19	16.35	0.535	0.532	0.521
[OMIM][PF_6][d]	10.51	9.93	9.36	0.735	0.730	0.709
[BMIM][SCN^-][e]	65.43[f]	56.17[f]	42.56[f]	0.286[f]	0.284[f]	0.281[f]

[a]This work; [b]Kato and Gmehling (2005); [c]Olivier et al. (2011); [d]Olivier et al. (2010); [e]Domańska and Laskowska (2009); [f] interpolated value

The experimental data presented in Table 6-8 for n-heptane (1) - toluene (2) system in Figure 6-7 were used to plot the selectivities of four DESs and four selected ILs at various temperatures.

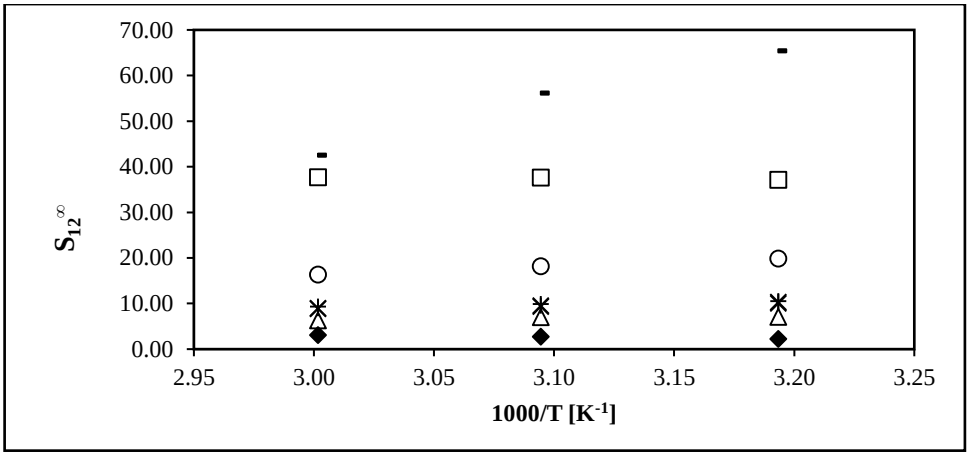

Figure 6-7: Selectivities of various solvents against 1/T for the combination of n-heptane (1)/toluene (2), (♦), DES1 (□), DES2 (Δ), DES3 (x), DES4 (+), [OMIM][PF_6] (*), [HMIM][BTI] (-), [BMIM][SCN] (o), [BMIM][SbF_6].

Figure 6-7 shows selectivity for the n-heptane (1) and toluene (2) combination. The provided data indicate that DES2 would perform better than any other DES since it had the highest selectivity for this binary mixture, even though all investigated DESs, as temperature increases, would still provide the similar selectivity or with a slight change. The same effect was observed for all other solvents. Regarding selectivity, that of ILs decreased by ± 2 units, whereas that of DES1 and DES2 increased by ± 0.30 units, and that of DES3 and DES4 decreased by ± 0.30 units.

According to data in Table 6-8, DES4 possesses the highest capacity for toluene. However, all ILs solvents presented in Table 6-8 showed greater limiting capacity than DESs. The best performing DESs was difficult to determine since all other solvents indicated far better performances. In addition to this, the choice would depend on solvent costs as well as process economics.

CHAPTER SEVEN

CONCLUSIONS AND RECOMMENDATIONS

In this study, the interactions of 24 organic solutes of various functional groups types – including alk-1-anes, cycloalkanes, alk-1-enes, alk-1-ynes, alkylbenzenes, alkanols, heterocyclic, ketones and esters – with Deep Eutectic Solvents (DESs) were examined at infinite dilution using gas-liquid chromatography (GLC). Measurements of IDACs were conducted over a wide temperature range in four different DESs:

- Tetramethylammonium chloride + Glycerol
- Tetramethylammonium chloride + Ethylene Glycol
- Tetramethylammonium chloride + 1,6 Hexanediol
- Tetrapropylammonium bromide + 1,6 Hexanediol

It was found that GLC was the suitable measurement technique to investigate DESs due to its availability and ease of use regarding manual computation of IDAC values from correlations. Furthermore, the GLC method requires neither calibration of the chromatographic detector nor any tedious preparation of the experimental device. The reliability of data produced by the GLC technique in this study was verified by the measurements for IDACs of the various solutes in hexadecane. As a result, test systems data strongly agreed with the IDAC measurements in literature. This verification was based on the deviation from literature data that was found to be within the expected deviation for all selected systems in hexadecane, proving that the GLC technique is capable of producing accurate and reliable IDAC data.

Regarding data related to the four DESs, all measured systems were new. The DESs studied were of very low volatility, making GLC applicable. This technique was advantageous since it utilised very low amounts of DESs (2.8675 – 21.5117 mmol) and produced relatively quick IDAC data due to the minute quantities of DES and organic solutes. It is worth noting that the study of DESs for obtaining IDAC data is in its infancy. Therefore, there was no substantial data available in the literature for comparison with all measured IDACs in this study.

This study resulted in the successful determination of selectivities and limiting capacities at infinite dilution of some challenging and common industrial separation problems. The determination of separation factors provided insights into the suitability of the DESs. This assessment would also

provide some information regarding the feasibility of the application of DESs to extractive distillation as well as solvent extraction. Experimental IDAC data were used to examine the potential of the investigated DESs to enhance the separation of some mixtures of close-boiling components as well as those forming azeotropes. The following observations were made:

- **n-hexane – hex-1-ene system:** Separation performance for the combination of n-hexane and hex-1-ene was difficult to decide. However, DES2 was found to be a reasonable solvent for the separation of n-hexane and hex-1-ene. Even though DES2 is not as highly selective as some other ILs and OCs, it has the advantage of being easily recovered. In conclusion, DES2 as a potential separation solvent would be based on process economics due to very low limiting capacity.

- **n-hexane – benzene system:** For this separation problem, the best selectivity was obtained for DES2. DES4 gave reasonable selectivity and limiting capacity at infinite dilution. Higher selectivities have been achieved in all four DESs. Thus, DES4 was potentially the most suitable DES for n-hexane and benzene separation.

- **methanol – benzene system:** The separation of methanol over benzene was not possible due to very low selectivities for all four DESs. In conclusion, the four investigated DESs cannot be the potential solvents for the separation of methanol and benzene as they had very low effectiveness.

- **cyclohexane – benzene system:** DES4 was identified as the best performing solvent for this separation problem. Distillation can be used to separate cyclohexane easily from benzene by introducing DES4 as an entrainer.

- **cyclohexane – ethanol system:** DES4 was determined to be the best DES for this separation problem on the basis of selectivity and performance index. Its performance increased with increasing temperature.

- **acetone – ethanol system:** The best selectivity, as well as performance index, were observed in the case of DES4 from amongst the other three DESs. However, it was observed that the separation performance for this separation process remained low in terms of selectivity.

- **n-heptane – toluene system:** For this combination, DES4 was determined to be the best separation solvent, taking into account both selectivity and performance index.

Based on the results, this study proved to make a significant contribution to initiatives that address the threat posed by OCs to the environment. DES4 was identified as an alternative solvent to successfully replace OCs and ILs on the basis of high selectivity and performance index exhibited by this solvent for several industrial separation problems. However, further investigation of DES4 through measurements of vapour-liquid equilibrium (VLE) and liquid-liquid equilibrium (LLE) data should be conducted. VLE and LLE data would provide valuable insight into the separation of such mixtures over the whole composition range using DES4. Thus, it would be easy to implement DES4 as an alternative green solvent to current harmful industrial solvents.

Experimental work was a vital component to assess DES potential for separating difficult industrial binary mixtures. The data generated in this study can extend the applicability range of predictive models such as UNIFAC, and modified UNIFAC models, which are already incorporated in some chemical engineering process simulators.

REFERENCES

Abbott, A. P., Al-Barzinjy, A. A., Abbott, P. D., Frisch, G., Harris, R. C., Hartley, J. and Ryder, K. S. 2014. Speciation, physical and electrolytic properties of eutectic mixtures based on $CrCl_3 \cdot 6H_2O$ and urea. *Physical Chemistry Chemical Physics*, 16 (19): 9047-9055.

Abbott, A. P., Barker, G. W., Walter, A. J. and Kočovský, P. 2003a. Electrochemical recognition of analytes using quaternary ammonium binaphthyl salts. *Analyst*, 128 (3): 245-248.

Abbott, A. P., Capper, G., Davies, D. L., Rasheed, R. K. and Tambyrajah, V. 2003b. Novel solvent properties of choline chloride/urea mixtures. *Chemical Communications*, (1): 70-71.

Abbott, A. P., Harris, R. C., Ryder, K. S., D'Agostino, C., Gladden, L. F. and Mantle, M. D. 2011. Glycerol eutectics as sustainable solvent systems. *Green Chemistry*, 13 (1): 82-90.

Abbott, M. M. 1986. Low-pressure phase equilibria: Measurement of VLE. *Fluid Phase Equilibria*, 29: 193-207.

Alessi, P., Fermeglia, M. and Kikic, I. 1991. Significance of dilute regions. *Fluid Phase Equilibria*, 70 (2-3): 239-250.

Anastas, P. T. and Kirchhoff, M. M. 2002. Origins, current status, and future challenges of green chemistry. *Accounts of chemical research*, 35 (9): 686-694.

Aparicio, S., Alcalde, R., Garcia, B. and Leal, J. M. 2009. High-pressure study of the methylsulfate and tosylate imidazolium ionic liquids. *Journal of Physical Chemistry B*, 113 (16): 5593-5606.

Atik, Z., Gruber, D., Krummen, M. and Gmehling, J. 2004. Measurement of activity coefficients at infinite dilution of benzene, toluene, ethanol, esters, ketones, and ethers at various temperatures in water using the dilutor technique. *Journal of Chemical & Engineering Data*, 49 (5): 1429-1432.

Bahadur, I., Govender, B. B., Osman, K., Williams-Wynn, M. D., Nelson, W. M., Naidoo, P. and Ramjugernath, D. 2014. Measurement of activity coefficients at infinite dilution of organic solutes in the ionic liquid 1-ethyl-3-methylimidazolium 2-(2-methoxyethoxy) ethylsulfate at T=(308.15, 313.15, 323.15 and 333.15)K using gas+liquid chromatography. *Journal of Chemical Thermodynamics*, 70: 245-252.

Bastos, J. C., Medina, A. and Soares, M. 1984. Selection of solvents for extractive distillation: A data bank for activity coefficients at infinite dilution. *Ind. Eng. Chem. Process Des. Dev.;(United States)*, 24 (2)

Castells, C. B., Carr, P. W., Eikens, D. I., Bush, D. and Eckert, C. A. 1999. Comparative study of semitheoretical models for predicting infinite dilution activity coefficients of alkanes in organic solvents. *Industrial & Engineering Chemistry Research*, 38 (10): 4104-4109.

Chien, C., Kopecni, M., Laub, R. and Smith, C. 1981. Solute liquid-gas activity and partition coefficients with mixtures of n-hexadecane and n-octadecane with N, N-dibutyl-2-ethylhexylamide solvents. *Journal of Physical Chemistry*, 85 (13): 1864-1871.

Clark, J. H. and Tavener, S. J. 2007. Alternative solvents: shades of green. *Organic process research & development*, 11 (1): 149-155.

Conder, J. R. and Young, C. L. 1979. *Physicochemical measurement by gas chromatography*. John Wiley & Sons.

Coquelet, C. and Richon, D. 2005. Measurement of Henry's law constants and infinite dilution activity coefficients of propyl mercaptan, butyl mercaptan, and dimethyl sulfide in methyldiethanolamine (1) + water (2) with $w_1 = 0.50$ using a gas stripping technique. *Journal of Chemical & Engineering Data*, 50 (6): 2053-2057.

Cruickshank, A., Windsor, M. and Young, C. 1966. The use of gas-liquid chromatography to determine activity coefficients and second virial coefficients of mixtures. I. Theory and verification of method of data analysis. In: Proceedings of *Proceedings of the Royal Society of London A: Mathematical, Physical and Engineering Sciences*. Royal Society, 259-270.

Dávila, M. J., Aparicio, S., Alcalde, R., García, B. and Leal, J. M. 2007. On the properties of 1-butyl-3-methylimidazolium octylsulfate ionic liquid. *Green Chemistry*, 9 (3): 221-232.

De Santi, V., Cardellini, F., Brinchi, L. and Germani, R. 2012. Novel Brønsted acidic deep eutectic solvent as reaction media for esterification of carboxylic acid with alcohols. *Tetrahedron Letters*, 53 (38): 5151-5155.

Dohnal, V. and Horáková, I. 1991. A new variant of the Rayleigh distillation method for the determination of limiting activity coefficients. *Fluid Phase Equilibria*, 68: 173-185.

Domańska, U., Królikowski, Marek. 2012. Measurements of activity coefficients at infinite dilution for organic solutes and water in the ionic liquid 1-ethyl-3-methylimidazolium methanesulfonate. *Journal of Chemical Thermodynamics*, 54: 20-27.

Domańska, U. and Laskowska, M. 2009. Measurements of activity coefficients at infinite dilution of aliphatic and aromatic hydrocarbons, alcohols, thiophene, tetrahydrofuran, MTBE, and water in ionic liquid [BMIM][SCN] using GLC. *Journal of Chemical Thermodynamics*, 41 (5): 645-650.

Domańska, U. and Marciniak, A. 2008. Measurements of activity coefficients at infinite dilution of aromatic and aliphatic hydrocarbons, alcohols, and water in the new ionic liquid [EMIM][SCN] using GLC. *Journal of Chemical Thermodynamics*, 40 (5): 860-866.

Everett, D. 1965. Effect of gas imperfection on GLC measurements: a refined method for determining activity coefficients and second virial coefficients. *Transactions of the Faraday Society*, 61: 1637-1645.

Everett, D. H. and Powl, J. C. 1976. Adsorption in slit-like and cylindrical micropores in the henry's law region. A model for the microporosity of carbons. *Journal of the Chemical Society, Faraday Transactions 1: Physical Chemistry in Condensed Phases*, 72: 619-636.

Fowlis, I. and Scott, R. P. W. 1963. A vapour dilution system for detector calibration. *Journal of Chromatography A*, 11: 1-10.

Francisco, M., van den Bruinhorst, A. and Kroon, M. C. 2013. Low-transition-temperature mixtures (LTTMs): A new generation of designer solvents. *Angewandte Chemie international edition*, 52 (11): 3074-3085.

Fredenslund, A., Gmehling, J. and Rasmussen, P. 1977. *Vapor-liquid equilibria using UNIFAC: a group contribution method*. Elsevier Scientific Pub. Co.

Fredenslund, A., Jones, R. L. and Prausnitz, J. M. 1975. Group-contribution estimation of activity coefficients in nonideal liquid mixtures. *AIChE Journal*, 21 (6): 1086-1099.

García, G., Aparicio, S., Ullah, R. and Atilhan, M. 2015. Deep Eutectic Solvents: Physicochemical Properties and Gas Separation Applications. *Energy & Fuels*, 29 (4): 2616-2644.

Gautreaux, M. and Coates, J. 1955. Activity coefficients at infinite dilution. *AIChE Journal*, 1 (4): 496-500.

Ghareh Bagh, F. S., Shahbaz, K., Mjalli, F. S., Hashim, M. A. and AlNashef, I. M. 2015. Zinc (II) chloride-based deep eutectic solvents for application as electrolytes: Preparation and characterization. *Journal of Molecular Liquids*, 204: 76-83.

Goodman, N. 1963. Statistical analysis based on a certain multivariate complex Gaussian distribution (an introduction). *Annals of mathematical statistics*, 34 (1): 152-177.

Gu, L., Huang, W., Tang, S., Tian, S. and Zhang, X. 2015. A novel deep eutectic solvent for biodiesel preparation using a homogeneous base catalyst. *Chemical Engineering Journal*, 259: 647-652.

Guiochon, G. and Guillemin, C. L. 1988. *Quantitative gas chromatography for laboratory analyses and on-line process control*. Elsevier.

Gutiérrez, M. C., Carriazo, D., Tamayo, A., Jiménez, R., Picó, F., Rojo, J. M., Ferrer, M. L. and del Monte, F. 2011. Deep-Eutectic-Solvent-Assisted Synthesis of Hierarchical Carbon Electrodes Exhibiting Capacitance Retention at High Current Densities. *Chemistry-A European Journal*, 17 (38): 10533-10537.

Hayyan, A., Mjalli, F. S., AlNashef, I. M., Al-Wahaibi, Y. M., Al-Wahaibi, T. and Hashim, M. A. 2013. Glucose-based deep eutectic solvents: Physical properties. *Journal of Molecular Liquids*, 178: 137-141.

Heintz, A., Kulikov, D. V. and Verevkin, S. P. 2001. Thermodynamic properties of mixtures containing ionic liquids. 1. Activity coefficients at infinite dilution of alkanes, alkenes, and alkylbenzenes in 4-methyl-n-butylpyridinium tetrafluoroborate using gas− liquid chromatography. *Journal of Chemical & Engineering Data*, 46 (6): 1526-1529.

Hua Zhao, C. Z., Tanisha D. Crittle. 2013. Choline-based deep eutectic solvents for enzymatic preparation of biodiesel from soybean oil. *Journal of Molecular Catalysis B: Enzymatic*, 85-86: 243-247.

Hudson, G. and McCoubrey, J. 1960. Intermolecular forces between unlike molecules. A more complete form of the combining rules. *Transactions of the Faraday Society*, 56: 761-766.

Hussam, A. and Carr, P. W. 1985. Rapid and precise method for the measurement of vapor/liquid equilibria by headspace gas chromatography. *Analytical Chemistry*, 57 (4): 793-801.

James, A. and Martin, A. 1952. Gas-liquid partition chromatography: the separation and micro-estimation of volatile fatty acids from formic acid to dodecanoic acid. *Biochemical Journal*, 50 (5): 679.

Jhong, H.-R., Wong, D. S.-H., Wan, C.-C., Wang, Y.-Y. and Wei, T.-C. 2009. A novel deep eutectic solvent-based ionic liquid used as electrolyte for dye-sensitized solar cells. *Electrochemistry Communications*, 11 (1): 209-211.

Jibril, B., Mjalli, F., Naser, J. and Gano, Z. 2014. New tetrapropylammonium bromide-based deep eutectic solvents: Synthesis and characterizations. *Journal of Molecular Liquids*, 199: 462-469.

Kato, R. and Gmehling, J. 2004. Activity coefficients at infinite dilution of various solutes in the ionic liquids $[MMIM]^+[CH_3SO_4]^-$, $[MMIM]^+[CH_3OC_2H_4SO_4]^-$, $[MMIM]^+[(CH_3)_2PO_4]^-$, $[C_5H_5NC_2H_5]^+[(CF_3SO_2)_2N]^-$ and $[C_5H_5NH]^+[C_2H_5OC_2H_4OSO_3]^-$. *Fluid Phase Equilibria*, 226: 37-44.

Kato, R. and Gmehling, J. 2005. Systems with ionic liquids: Measurement of VLE and γ^∞ data and prediction of their thermodynamic behavior using original UNIFAC, mod. UNIFAC (Do) and COSMO-RS (Ol). *Journal of Chemical Thermodynamics*, 37 (6): 603-619.

Klamt, A. 1995. Conductor-like Screening Model for Real Solvents: A New Approach to the Quantitative Calculation of Solvation Phenomena. *Journal of Physical Chemistry*, 99 (7): 2224-2235.

Kojima, K. and Tochigi, K. 1979. *Prediction of vapor-liquid equilibria by the ASOG method*. Tokyo; Amsterdam; New York: Kodansha ; Elsevier Scientific Pub. Co.

Krummen, M. and Gmehling, J. 2004. Measurement of activity coefficients at infinite dilution in N-methyl-2-pyrrolidone and N-formylmorpholine and their mixtures with water using the dilutor technique. *Fluid Phase Equilibria*, 215 (2): 283-294.

Krummen, M., Gruber, D. and Gmehling, J. 2000. Measurement of activity coefficients at infinite dilution in solvent mixtures using the dilutor technique. *Industrial & Engineering Chemistry Research*, 39 (6): 2114-2123.

Laub, R. J. and Pecsok, R. L. 1978. *Physicochemical applications of gas chromatography*. Wiley.

Lawes, S., Hainsworth, S. V., Blake, P., Ryder, K. and Abbott, A. 2010. Lubrication of steel/steel contacts by choline chloride ionic liquids. *Tribology letters*, 37 (2): 103-110.

Leroi, J.-C., Masson, J.-C., Renon, H., Fabries, J.-F. and Sannier, H. 1977. Accurate measurement of activity coefficient at infinite dilution by inert gas stripping and gas chromatography. *Industrial & Engineering Chemistry Process Design and Development*, 16 (1): 139-144.

Leron, R. B., Wong, D. S. H. and Li, M.-H. 2012. Densities of a deep eutectic solvent based on choline chloride and glycerol and its aqueous mixtures at elevated pressures. *Fluid Phase Equilibria*, 335: 32-38.

Letcher, T. and Whitehead, P. 1997. The determination of activity coefficients of alkanes, alkenes, cycloalkanes, and alkynes at infinite dilution with the polar solvents dimethyl sulphoxide (DMSO), or N, N-dimethylformamide (DMF), or N-methyl-2-pyrrolidinone (NMP) using a glc technique at the temperatures 283.15 K and 298.15 K. *Journal of Chemical Thermodynamics*, 29 (11): 1261-1268.

Letcher, T. M. 1978. Activity coefficients at infinite dilution from gas-liquid chromatography. In: McGlashan, M. L. ed. *Chemical Thermodynamics: Volume 2*. Royal Society of Chemistry, 46-70.

Letcher, T. M. 1980. Activity coefficients at infinite dilution from gas-liquid chromatography. *Faraday Symposia of the Chemical Society*, 15 (0): 103-112.

Lide, D. R. 2004. *CRC handbook of chemistry and physics*. CRC press.

Liu, Y.-T., Chen, Y.-A. and Xing, Y.-J. 2014. Synthesis and characterization of novel ternary deep eutectic solvents. *Chinese Chemical Letters*, 25 (1): 104-106.

Marciniak, A. and Wlazło, M. 2015. Activity coefficients at infinite dilution, physicochemical and thermodynamic properties for organic solutes and water in the ionic liquid ethyl-dimethyl-(2-methoxyethyl)ammonium trifluorotris-(perfluoroethyl)phosphate. *Journal of Chemical Thermodynamics*, 89: 245-250.

McGlashan, M. and Potter, D. 1962. An apparatus for the measurement of the second virial coefficients of vapours; the second viral coefficients of some n-alkanes and of some mixtures of n-

alkanes. In: Proceedings of *Proceedings of the Royal Society of London A: Mathematical, Physical and Engineering Sciences*. Royal Society, 478-500.

Mohsenzadeh, A., Al-Wahaibi, Y., Jibril, A., Al-Hajri, R. and Shuwa, S. 2015. The novel use of Deep Eutectic Solvents for enhancing heavy oil recovery. *Journal of Petroleum Science and Engineering*, 130: 6-15.

Möllmann, C. and Gmehling, J. 1997. Measurement of Activity Coefficients at Infinite Dilution Using Gas−Liquid Chromatography. 5. Results for N-Methylacetamide, N,N-Dimethylacetamide, N,N-Dibutylformamide, and Sulfolane as Stationary Phases. *Journal of Chemical & Engineering Data*, 42 (1): 35-40.

Morrison, H. G., Sun, C. C. and Neervannan, S. 2009. Characterization of thermal behavior of deep eutectic solvents and their potential as drug solubilization vehicles. *International journal of pharmaceutics*, 378 (1): 136-139.

Muhlbauer, A. 1997. *Phase Equilibria: Measurement & Computation*. CRC press.

Olivier, E., Letcher, T. M., Naidoo, P. and Ramjugernath, D. 2010. Activity coefficients at infinite dilution of organic solutes in the ionic liquid 1-octyl-3-methylimidazolium hexafluorophosphate using gas–liquid chromatography at T=(313.15, 323.15, and 333.15)K. *Journal of Chemical Thermodynamics*, 42 (5): 646-650.

Olivier, E., Letcher, T. M., Naidoo, P. and Ramjugernath, D. 2011. Activity coefficients at infinite dilution of organic solutes in the ionic liquid 1-butyl-3-methylimidazolium hexafluoroantimonate using gas–liquid chromatography at T=(313.15, 323.15, and 333.15)K. *Journal of Chemical Thermodynamics*, 43 (6): 829-833.

Palmer, D. A. 1987. CRC handbook of applied thermodynamics.

Parcher, J. and Hussey, C. 1973. Thermodynamic measurements by frontal chromatography. Liquid surface adsorption effects. *Analytical Chemistry*, 45 (1): 188-191.

Pividal, K. A., Birtigh, A. and Sandler, S. I. 1992. Infinite dilution activity coefficients for oxygenate systems determined using a differential static cell. *Journal of Chemical and Engineering Data*, 37 (4): 484-487.

Plechkova, N. V. and Seddon, K. R. 2008. Applications of ionic liquids in the chemical industry. *Chemical Society Reviews*, 37 (1): 123-150.

Poling, B. E., Prausnitz, J. M. and O'Connell, J. P. 2001. *The properties of gases and liquids*. McGraw-Hill.

Porter, P., Deal, C. and Stross, F. 1956. The determination of partition coefficients from gas-liquid partition chromatography. *Journal of the American Chemical Society*, 78 (13): 2999-3006.

Prausnitz, J. M. 1980. *Computer calculations for multicomponent vapor-liquid and liquid-liquid equilibria*. Prentice-Hall.

Rackett, H. G. 1970. Equation of state for saturated liquids. *Journal of Chemical and Engineering Data*, 15 (4): 514-517.

Radosevic, K., Bubalo, M. C., Srcek, V. G., Grgas, D., Dragicevic, T. L. and Redovnikovic, I. R. 2015. Evaluation of toxicity and biodegradability of choline chloride based deep eutectic solvents. *Ecotoxicol Environ Saf*, 112: 46-53.

Richon, D. 2011. New equipment and new technique for measuring activity coefficients and Henry's constants at infinite dilution. *Review of Scientific Instruments*, 82 (2): 025108.

Rodriguez, N. R., Ferre Guell, J. and Kroon, M. C. 2016. Glycerol-Based Deep Eutectic Solvents as Extractants for the Separation of MEK and Ethanol via Liquid–Liquid Extraction. *Journal of Chemical & Engineering Data*, 61 (2): 865-872.

Sarwono M.M., M. K. O. H.-K., LM. Alnashef. 2013. Application of Deep Eutectic Solvents for the Separation of Aliphatics and Aromatics. Paper presented at the *2013 International Conference on Technology, Informatics, Management, Engineering & Environment (TIME-E 2013)*. Bandung, Indonesia, June 23-26. IEEE, 48-53.

Schult, C. J., Neely, B. J., Robinson, R., Gasem, K. and Todd, B. A. 2001. Infinite-dilution activity coefficients for several solutes in hexadecane and in n-methyl-2-pyrrolidone (NMP): experimental measurements and UNIFAC predictions. *Fluid Phase Equilibria*, 179 (1): 117-129.

Seader, J. D., Henley, E. J. and Roper, D. K. 2011. *Separation process principles* 3rd ed. United States of America: John Wiley & Sons, Inc.

Serrano, M. C., Gutiérrez, M. C., Jiménez, R., Ferrer, M. L. and del Monte, F. 2012. Synthesis of novel lidocaine-releasing poly (diol-co-citrate) elastomers by using deep eutectic solvents. *Chemical Communications*, 48 (4): 579-581.

Shahbaz, F. S., Ghareh Bagh, F.S. Mjalli, I.M. AlNashef, M.A. Hashim. 2013. Prediction of refractive index and density of deep eutectic solventsusing atomic contributions. *Fluid Phase Equilibria*, 354: 304–311.

Shahbaz, K., Mjalli, F. S., Hashim, M. A. and AlNashef, I. M. 2011a. Eutectic solvents for the removal of residual palm oil-based biodiesel catalyst. *Separation and Purification Technology*, 81 (2): 216-222.

Shahbaz, K., Mjalli, F. S., Hashim, M. A. and AlNashef, I. M. 2011b. Prediction of deep eutectic solvents densities at different temperatures. *Thermochimica Acta*, 515 (1-2): 67-72.

Skopek, M. A., Mohamoud, M. A., Ryder, K. S. and Hillman, A. R. 2009. Nanogravimetric observation of unexpected ion exchange characteristics for polypyrrole film p-doping in a deep eutectic ionic liquid. *Chemical Communications*, (8): 935-937.

Smith, E. L., Abbott, A. P. and Ryder, K. S. 2014. Deep eutectic solvents (DESs) and their applications. *Chemical reviews*, 114 (21): 11060-11082.

Smith, J. M., Van Ness, H. C. and Abbott, M. M. 2001. *Introduction to Chemical Engineering Thermodynamics*. McGraw-Hill.

Spencer, C. F. and Danner, R. P. 1972. Improved equation for prediction of saturated liquid density. *Journal of Chemical and Engineering Data*, 17 (2): 236-241.

Suleiman, D. and Eckert, C. A. 1994. Limiting activity coefficients of diols in water by a dew point technique. *Journal of Chemical and Engineering Data*, 39 (4): 692-696.

Tarakad, R. R. and Danner, R. P. 1977. An improved corresponding states method for polar fluids: correlation of second virial coefficients. *AIChE Journal*, 23 (5): 685-695.

Taylor, B., Mohr, P. and Douma, M. 2007. The NIST Reference on Constants. *Units, and Uncertainty (NIST Special Publication, 1995)*: 811.

Thomas, E. R., Newman, B. A., Long, T. C., Wood, D. A. and Eckert, C. A. 1982. Limiting activity coefficients of nonpolar and polar solutes in both volatile and nonvolatile solvents by gas chromatography. *Journal of Chemical and Engineering Data*, 27 (4): 399-405.

Tsonopoulos, C., Dymond, J. H. and Szafranski, A. 1989. Second virial coefficients of normal alkanes, linear 1-alkanols and their binaries. *Pure and Applied Chemistry*, 61 (8): 1387-1394.

Tumba, K., Letcher, T. M., Naidoo, P. and Ramjugernath, D. 2013. Activity coefficients at infinite dilution of organic solutes in the ionic liquid trihexyltetradecylphosphonium bis (trifluoromethylsulfonyl) imide using gas–liquid chromatography at T = (313.15, 333.15, 353.15 and 373.15)K. *Journal of Chemical Thermodynamics*, 65 (0): 159-167.

Tumba, K. A. 2010. Infinite dilution activity coefficient measurements of organic solutes in fluorinated ionic liquids by gas-liquid chromatography and the inert gas stripping method. Faculty of Engineering, School of Chemical Engineering, University of KwaZulu-Natal.

Ventura, S. P., e Silva, F. A., Gonçalves, A. M., Pereira, J. L., Gonçalves, F. and Coutinho, J. A. 2014. Ecotoxicity analysis of cholinium-based ionic liquids to Vibrio fischeri marine bacteria. *Ecotoxicology and environmental safety*, 102: 48-54.

Verevkin, S. P., Sazonova, A. Y., Frolkova, A. K., Zaitsau, D. H., Prikhodko, I. V. and Held, C. 2015. Separation Performance of BioRenewable Deep Eutectic Solvents. *Industrial & Engineering Chemistry Research*, 54 (13): 3498-3504.

Walas, S. 1985. *Phase Equilibria in Chemical Technology*: Butterworth-Heinemann, Boston, London, Oxford, UK.

Weir, R. D. D. and de Loos, T. W. W. 2005. *Measurement of the Thermodynamic Properties of Multiple Phases*. Elsevier Science.

Wen, Q., Chen, J.-X., Tang, Y.-L., Wang, J. and Yang, Z. 2015. Assessing the toxicity and biodegradability of deep eutectic solvents. *Chemosphere*, 132: 63-69.

Wilson, G. M. and Deal, C. H. 1962. Activity Coefficients and Molecular Structure. Activity Coefficients in Changing Environments-Solutions of Groups. *Industrial & Engineering Chemistry Fundamentals*, 1 (1): 20-23.

Xu, K., Wang, Y., Huang, Y., Li, N. and Wen, Q. 2015. A green deep eutectic solvent-based aqueous two-phase system for protein extracting. *Anal Chim Acta*, 864: 9-20.

APPENDIX A

ORIGIN, PURITY AND PROPERTIES OF CHEMICALS

A.1. Chemical Purity

Table A-1: Suppliers and quoted purity of all Organic salts and HBDs used in this study.

Compounds	Supplier	Quoted purity (%)
Tetramethylammonium chloride	Sigma-Aldrich	≥ 99.0
Tetrapropylammonium bromide	Sigma-Aldrich	≥ 99.9
Ethylene glycol	Sigma-Aldrich	≥ 99.9
Glycerol	Sigma-Aldrich	≥ 98.5
1,6 Hexanediol	Sigma-Aldrich	≥ 99.0

Table A-2: Suppliers and quoted purity of all solutes used in this study.

Solute	Supplier	Quoted purity (%)
n-hexane	Merck	≥ 99.0
n-heptane	Sigma-Aldrich	≥ 99.9
n-octane	Sigma-Aldrich	≥ 99.9
cyclopentane	Flucka	≥ 98.5
cyclohexane	ACE	≥ 99.0
cycloheptane	ACE	≥ 99.9
cyclooctane	Sigma-Aldrich	≥ 99.5
hex-1-ene	Sigma-Aldrich	≥ 98.0
hept-1-ene	Flucka	≥ 98.0
hept-1-yne	Sigma-Aldrich	≥ 99.9
oct-1-yne	Sigma-Aldrich	≥ 99.9
ethanol	Sigma-Aldrich	≥ 99.9
methanol	Macron	≥ 99.9
propan-1-ol	Lab scan	≥ 99.5
propan-2-ol	Lab scan	≥ 99.5
benzene	Sigma-Aldrich	≥ 99.9
toluene	Sigma-Aldrich	≥ 99.9
ethylbenzene	Sigma-Aldrich	≥ 99.9
acetone	Sigma-Aldrich	≥ 99.9
butan-2-one	Sigma-Aldrich	≥ 99.7
thiophene	Sigma-Aldrich	≥ 99.9
pyridine	Sigma-Aldrich	≥ 99.9
Methyl acetate	Capital lab	≥ 98.0
ethyl acetate	ACE	≥ 99.5
dichloromethane	Sigma-Aldrich	≥ 99.9
helium	Afrox-SA	≥ 99.99

A.2. Antoine Equation Constants

Table A-3: Antoine constants for all solutes'saturated vapour pressures used in this study.

Antoine constants				
Solute	**A**	**B**	**C**	**Ref**
n-hexane	4.00139	1170.875	224.317	a
n-heptane	4.02023	1263.909	216.432	a
n-octane	4.05075	1356.36	209.635	a
cyclopentane	4.06783	1152.574	234.51	a
cyclohexane	3.93002	1182.774	220.618	a
cycloheptane	3.9633	1322.21997	215.297	a
cyclooctane	3.98125	1434.67	209.712	a
hex-1-ene	3.9826	1148.62	225.34	a
hept-1-ene	4.02677	1258.34	219.3	a
hept-1-yne	6.24468	918.34	173.473	a
oct-1-yne	6.93838	1352.05	206.916	a
ethanol	5.33675	1648.22	230.918	a
methanol	5.2027	1580.08	239.5	a
propan-1-ol	4.99991	1512.94	205.807	a
propan-2-ol	5.24268	1580.92	219.61	a
isobutyl alcohol	4.34504	1190.38	166.67	a
benzene	3.98523	1184.24	217.572	a
toluene	4.05043	1327.62	217.625	a
ethylbenzene	4.06861	1415.77	212.3	a
acetone	4.2184	1197.01	228.06	a
butan-2-one	4.1386	1232.63	218.69	a
thiophene	4.08416	1246.02	221.35	a
pyridine	4.16749	1373.026	214.69	a
Methyl acetate	4.18621	1156.43	219.69	b
ethyl acetate	4.13361	1195.13	212.47	b
water	8.10765	1750.286	235	a
helium	1.6836	8.1548	273.71	a

[a]*Poling et al. (2001);* [b]*Lide (2004)*

The Antoine constants were calculated by Equation (A-1) given by (Poling *et al.*, 2001):

$$\log_{10} P = A - \frac{B}{t + C} \qquad \text{(A-1)}$$

where, P is in bar and t is in $^{\circ}\mathrm{C}$.

A.3. Physical and Critical Properties

The critical properties of the carrier gas and the solutes used in the calculations of the virial coefficients were sourced from CRC Handbook of Chemistry and Physics, and the Handbook of Properties of Gas and Liquids.

Table A-4: Critical temperature, T_c [a,b] Ionisation potential, E_i [b] critical volume, V_c [a] critical pressure, P_c [a] compressibility factor, Z_c [a] and the acentric factor, ω [a] for carrier gas and all the solutes used in this study.

Chemical	E_i /kJ.mol^{-1}	T_c /K	V_c /cm^3.mol^{-1}	P_c /bar	Z_c	ω
helium	2372.6	5.19	57.30	2.27	0.301	-0.390
n-hexane	977.4	507.9	368	30.25	0.264	0.299
n-heptane	957.1	540.2	428	27.40	0.261	0.350
n-octane	947.5	568.7	492	24.90	0.259	0.399
cyclopentane	1014.1	511.6	260	45.08	0.276	0.192
cyclohexane	951.3	553.5	308	40.73	0.273	0.211
cycloheptane	962.0	604.3	359	38.40	0.274	0.242
cyclooctane	941.7	647.2	410	35.70	0.271	0.254
hex-1-ene	910.8	504.0	355.1	31.43	0.266	0.281
hept-1-ene	910.8	537.3	409	29.20	0.267	0.343
hept-1-yne	960.0	551.6	376.5	33.40	0.274	0.389
oct-1-yne	960.0	598.5	441	31.01	0.275	0.262
methanol	1046.9	512.6	118	80.97	0.224	0.565
ethanol	1010.2	513.9	167	61.48	0.240	0.649
propan-1-ol	982.2	536.8	219	51.75	0.254	0.629
propan-2-ol	981.3	508.3	220	47.62	0.248	0.665
Isobutyl alcohol	999.668	547	273	43	0.258	0.590
benzene	892.1	562.2	256	48.95	0.268	0.210
toluene	851.0	591.8	316	41.08	0.264	0.264
ethylbenzene	846.2	617.2	374	36.09	0.263	0.304
acetone	935.9	508.1	209.0	47.0	0.233	0.307
butan-2-one	918.54	536.8	267.0	24.10	0.252	0.322
thiophene	871.592	580	219	56.6	0.252	0.196
pyridine	915.9105	620	254	56.7	0.267	0.242
Methylacetate	1009.412	506.8	228	46.94	0.255	0.366
ethyl acetate	985.835	402.4	163.5	56.3	0.275	0.362

[a]*Poling et al. (2001);* [b]*Lide (2004)*

APPENDIX B

ORGANIC MOLECULAR STRUCTURE

B.1. Structure of HBDs and halide salts

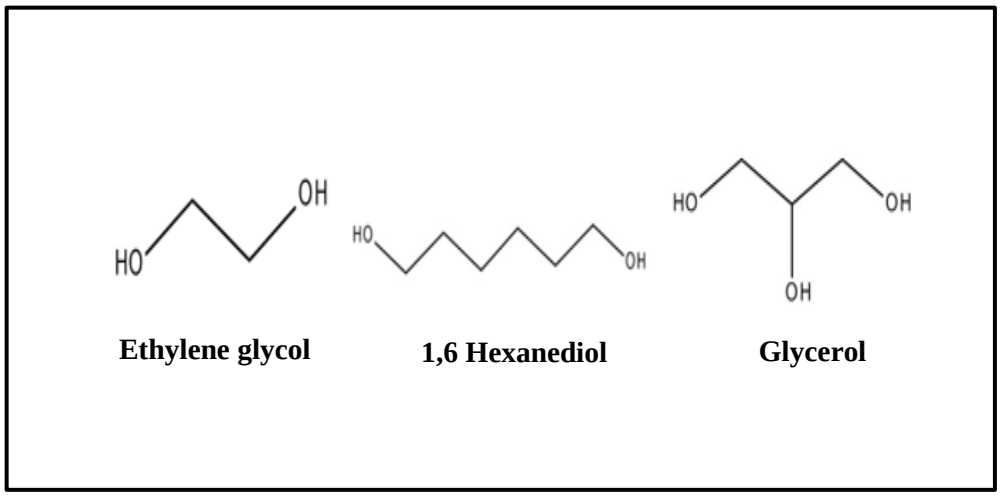

Figure B-1: The molecular structure of hydrogen bond donors used in this study.

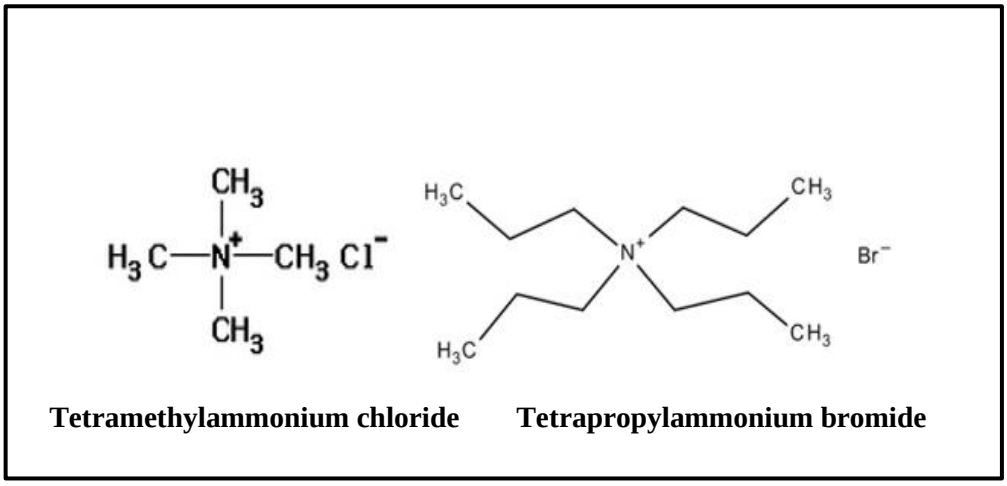

Figure B-2: The molecular structure of halide salts used in this study.

APPENDIX C

SAMPLE OF CALCULATIONS

C.1. Calculations of activity coefficients at infinite dilution

This appendix illustrates the procedure to calculate the experimental IDAC values using n-hexane at T = 313.15 K in DES1. Table C-1 below presents n-hexane experimental parameters as well as calculated properties used to obtain the activity coefficient data at infinite dilution.

Table C-1: Experimental parameters and component properties for n-hexane in DES1 at T = 313.15 K

Parameter/ Property	Units	Values	Equations
n_3	[mmol]	0.0213	-
T	[K]	313.15	-
P_1^*	[Pa]	37288.6411	A-1
B_{11}	[$m^3.mol^{-1}$]	-0.0017	3-20
V_N	[$m^3.mol^{-1}$]	6.8071×10^{-6}	3-17
B_{12}	[$m^3.mol^{-1}$]	-5.3854×10^{-5}	3-20
T_f	[K]	295.2500	-
P_i	[Pa]	137700.0	4-1
P_o	[Pa]	100700.0	-
V_1^*	[$m^3.mol^{-1}$]	0.0013	3-25
t	[s]	0.2680	-
U	[$m^3.s^{-1}$]	0.4892	-
V_1^∞	[$m^3.mol^{-1}$]	0.0013	3-25
J_2^3	-	1.1932	3-18

From Table C-1, t is the time difference between the retention time of the carrier gas (t_r) and the retention of the unretained carrier gas (t_g).

For the determination of the second virial coefficient and mixed virial coefficient (B_{11} and B_{12}), the critical data and ionistion energy utilised are given in Table A-4.

The corrected column outlet flow rate U_o was determined from the bubble flow rate measured at the column outlet U. The vapour pressure of water and n-hexane (Table A-3) were determined using

the Antione Equation (A-1). The corrected outlet flow rate value was found to be 5.051×10^{-07} m^3/s. Therefore, using Equation 3-16, activity coefficient of n-hexane at infinite dilution was found to be 223.924 (see Table 5-2).

C.2. Estimation of the experimental uncertainties

Quantifying the uncertainty in experimental measurements of IDACs is important. The uncertainty in the mass of solvent coated around the chromosorb in a column would result in the significant uncertainty in the IDAC data. The slight fluctuation of experimental IDAC measurements is predominantly based on repeatability uncertainty. This behaviour due to the repeatability of measurements is known as a Gaussian type of distribution (Goodman, 1963). This is due to the assumption that the measurements are anticipated to fall close to the mean and statistical sciences are utilised to analyse the data set. As such, this is referred to as a systematic uncertainty. Taylor *et al.* (2007), describe in details how to estimate and express uncertainty.

In this study, the following equation was used to estimate the experimental uncertainty for IDAC due to repeatability (multiple solute injections and column loadings):

$$u_{rep}\left(\gamma^{\infty}\right)=\sqrt{\frac{1}{n(n-1)}\sum_{i=1}^{n}\left(\gamma_i^{\infty}-\overline{\gamma^{\infty}}\right)^2} \tag{C-1}$$

where u_{rep} is an IDAC experimental standard uncertainty (known as the standard deviation) on repeatability; and n is the number of duplicated measurements; *'i'* represent component *i*.

Equation (3-16) that was developed by (Everett, 1965) and (Cruickshank *et al.*, 1966) is a function of multiple variables. These variables significantly affected the measurement of IDAC data. Bahadur *et al.* (2014) provided details on how to account for the standard uncertainty due to the fluctuations of these independent variables. In this work, the same method was used and the contribution of uncertainty on experimental parameters are presented in Table C-1 and C-2. The following Equations (C-2, C-3 and C-4) were used for uncertainty due to independent variables:

$$u_{eve}\left(\gamma_{13}^{\infty}\right)=\left(\begin{array}{l}\left[\left(\frac{\partial\gamma_i^{\infty}}{\partial n_3}\right)u\left(n_3\right)\right]^2+\left[\left(\frac{\partial\gamma_i^{\infty}}{\partial T}\right)u\left(T\right)\right]^2\\+\left[\left(\frac{\partial\gamma_i^{\infty}}{\partial V_N}\right)u\left(V_N\right)\right]^2+\left[\left(\frac{\partial\gamma_i^{\infty}}{\partial J_2^3}\right)u\left(J_2^3\right)\right]^2\\+\left[\left(\frac{\partial\gamma_i^{\infty}}{\partial P_1^*}\right)u\left(P_1^*\right)\right]^2+\left[\left(\frac{\partial\gamma_i^{\infty}}{\partial B_{11}}\right)u\left(B_{11}\right)\right]^2\\+\left[\left(\frac{\partial\gamma_i^{\infty}}{\partial B_{12}}\right)u\left(B_{12}\right)\right]^2+\left[\left(\frac{\partial\gamma_i^{\infty}}{\partial P_o}\right)u\left(P_o\right)\right]^2\\+\left[\left(\frac{\partial\gamma_i^{\infty}}{\partial V_1^*}\right)u\left(V_1^*\right)\right]^2+\left[\left(\frac{\partial\gamma_i^{\infty}}{\partial V_1^{\infty}}\right)u\left(V_1^{\infty}\right)\right]^2\end{array}\right)^{\frac{1}{2}} \quad \text{(C-2)}$$

and

$$u\left(V_N\right)=\left(\begin{array}{l}\left[\left(\frac{\partial V_N}{\partial J_2^3}\right)u\left(J_2^3\right)\right]^2+\left[\left(\frac{\partial V_N}{\partial t}\right)u\left(t\right)\right]^2+\left[\left(\frac{\partial V_N}{\partial T}\right)u\left(T\right)\right]^2\\+\left[\left(\frac{\partial V_N}{\partial T_f}\right)u\left(T_f\right)\right]^2+\left[\left(\frac{\partial V_N}{\partial P_o}\right)u\left(P_o\right)\right]^2+\left[\left(\frac{\partial V_N}{\partial P_w^*}\right)u\left(P_w^*\right)\right]^2\end{array}\right)^{\frac{1}{2}} \quad \text{(C-3)}$$

and

$$u\left(J_2^3\right)=\left(\left[\left(\frac{\partial J_2^3}{\partial P_i}\right)u\left(P_i\right)\right]^2+\left[\left(\frac{\partial J_2^3}{\partial P_o}\right)u\left(P_o\right)\right]^2\right)^{\frac{1}{2}} \quad \text{(C-4)}$$

Combined uncertainty can be obtained by adding the squares of the uncertainties due to the experimental parameters and the repeatability, and getting the square root of the obtained value. Equation C-5 is the expression of the combined uncertainty.

$$u\left(\gamma_{13}^{\infty}\right)=\sqrt{\left[u_{rep}\left(\gamma_{13}^{\infty}\right)\right]^2+\left[u_{eve}\left(\gamma_{13}^{\infty}\right)\right]^2} \quad \text{(C-5)}$$

Tables C-6 to C-13 present the combined uncertainty on the IDAC measurements.

Table C-2: The estimated uncertainty on experimental parameters.

Variables	Measurement units	Estimate
u(n_3)	[mmol]	±1.50 %
u(T)	[K]	±0.50 %
u(P_1^*)	[Pa]	±0.05 %
u(B_{11})	[$m^3.mol^{-1}$]	±2.00 %
u(V_N)	[$m^3.mol^{-1}$]	±2.93 %
u(B_{12})	[$m^3.mol^{-1}$]	±3.21 %
u(P_i)	[Pa]	±2.50 %
u(P_o)	[Pa]	±5.00 %
u(V_1^*)	[$m^3.mol^{-1}$]	±1.30 %
u(V_1^∞)	[$m^3.mol^{-1}$]	±1.30 %
u(J_2^3)	-	±1.50 %

Table C-3: The estimated uncertainty of variables that affect net retention volume.

Variables	Measurement units	Estimate
u(T)	[K]	±0.50 %
u(t)	[s]	±1.30 %
u(P_i)	[Pa]	±2.50%
u(P_w)	[Pa]	±1.30 %
u(P_o)	[Pa]	±5.00 %
u(q_{ov})	[$m^3.s^{-1}$]	±1.70 %
u(T_f)	[K]	±1.50 %

C.2.1. Calculations of experimental uncertainty

To illustrate the method used for uncertainty calculation, IDAC for n-hexane in DES1 is considered at T = 313.15 K (Tables 5-2 and 5-3). Table C-1 presented n-hexane experimental parameters used to obtain the activity coefficient data at infinite dilution.

From the experimental data provided in Table C-1, the experimental uncertainty for each variable can be easily obtained. Thus, Table C-4 and C-5 presents uncertainty for both dependent and independed variables in DES1 at T = 313.15 K for n-hexane.

Table C-4: The estimated uncertainty (i.e. n-hexane) on experimental parameters at T = 313.15 K in DES1.

Variables	Measurement units	Estimate
u(n_3)	[mmol]	±0.90 %
u(T)	[K]	±0.50 %
u(P_1^*)	[Pa]	±0.05 %
u(B_{11})	[$m^3.mol^{-1}$]	±1.30 %
u(V_N)	[$m^3.mol^{-1}$]	±1.54 %
u(B_{12})	[$m^3.mol^{-1}$]	±1.91 %
u(P_i)	[Pa]	±1.60 %
u(P_o)	[Pa]	±3.00 %
u(V_1^*)	[$m^3.mol^{-1}$]	±1.10 %
u(V_1^∞)	[$m^3.mol^{-1}$]	±1.10 %
u(J_2^3)	-	±1.00 %

Table C-5: The estimated uncertainty (i.e n-hexane) of variables that affect net retention volume at T = 313.15 K in DES1.

Variables	Measurement units	Estimate
u(T)	[K]	±0.50 %
u(t)	[s]	±1.12 %
u(P_i)	[Pa]	±2.10 %
u(P_w)	[Pa]	±1.20 %
u(P_o)	[Pa]	±3.00 %
u(q_{ov})	[$m^3.s^{-1}$]	±1.20 %
u(T_f)	[K]	±1.10 %

Considering all the data points in this study, the highest combined value of uncertainty on IDAC values was 9.53 %.

Table C-6: Combined uncertainty on IDAC values in DES1 at T = 313.15, 323.15, 333.15 and 343.15 K.

Experimental uncertainties at T [K]				
Solute	**T=313.15**	**T=323.15**	**T=333.15**	**T=343.15**
n-hexane	0.914	0.724	0.934	0.275
n-heptane	0.567	0.792	0.500	0.820
n-octane	1.205	0.109	0.365	0.681
cyclopentane	2.319	1.512	5.175	2.650
cyclohexane	1.965	3.874	1.643	1.928
cycloheptane	0.441	7.447	0.622	1.941
cyclooctane	0.462	1.371	3.438	3.992
hex-1-ene	1.154	0.582	7.206	2.808
hept-1-ene	1.712	0.263	0.171	0.057
hept-1-yne	0.407	0.422	0.067	0.017
oct-1-yne	1.277	0.946	0.233	0.182
ethanol	0.021	0.017	0.031	0.025
methanol	0.011	0.019	0.009	0.009
propan-1-ol	0.089	0.016	0.042	0.006
propan-2-ol	0.007	0.015	0.003	0.009
isobutyl alcohol	0.259	0.868	0.495	0.122
benzene	0.141	1.297	1.344	0.565
toluene	0.173	0.448	0.045	0.055
ethylbenzene	0.864	0.109	0.373	0.742
acetone	0.000	0.035	0.110	0.085
butan-2-one	0.188	0.100	0.173	0.119
thiophene	0.069	0.042	0.044	0.054
pyridine	0.011	0.006	0.004	0.002
methyl acetate	0.002	0.002	0.059	0.007
ethyl acetate	0.002	0.043	0.230	0.189

Table C-7: Combined uncertainty (in percent) on IDAC values in DES1 at T = 313.15, 323.15, 333.15 and 343.15 K.

Experimental uncertainties at T [K]				
Solutes	**T=313.15**	**T=323.15**	**T=333.15**	**T=343.15**
n-hexane	0.41	0.29	0.34	0.09
n-heptane	0.17	0.16	0.19	0.18
n-octane	0.57	0.05	0.14	0.23
cyclopentane	1.19	0.64	1.95	0.88
cyclohexane	1.02	1.76	0.69	0.74
cycloheptane	0.23	3.52	0.28	0.79
cyclooctane	0.25	0.68	1.60	1.70
hex-1-ene	0.40	0.17	1.94	0.65
hept-1-ene	0.82	0.11	0.07	0.02
hept-1-yne	0.59	0.59	0.09	0.02
oct-1-yne	2.44	1.69	0.40	0.29
ethanol	0.12	0.20	0.11	0.07
methanol	0.92	1.54	0.74	0.78
propan-1-ol	1.37	0.25	0.73	0.10
propan-2-ol	0.10	0.23	0.05	0.14
isobutyl alcohol	0.90	3.83	2.58	0.71
benzene	0.25	2.63	2.90	1.33
toluene	0.18	0.50	0.05	0.07
ethylbenzene	0.59	0.08	0.27	0.56
acetone	0.00	0.33	1.11	0.88
butan-2-one	0.79	0.44	0.81	0.58
thiophene	2.67	1.62	1.69	2.01
pyridine	1.83	1.01	0.62	0.21
methyl acetate	0.04	0.09	2.06	0.24
ethyl acetate	0.42	0.81	4.67	3.89

Table C-8: Combined uncertainty on IDAC values in DES2 at T = 313.15, 323.15, 333.15 and 343.15 K.

Experimental uncertainties at T [K]				
Solute	**T=313.15**	**T=323.15**	**T=333.15**	**T=343.15**
n-hexane	28.690	35.847	37.012	13.396
n-heptane	4.267	5.367	4.768	5.000
n-octane	10.380	13.685	12.051	5.125
cyclopentane	0.329	0.209	0.592	0.460
cyclohexane	2.071	5.492	1.509	0.775
cycloheptane	0.793	0.238	2.177	2.327
cyclooctane	20.319	19.796	6.909	10.773
hex-1-ene	2.064	10.136	0.248	1.302
hept-1-ene	9.951	26.404	3.883	11.583
hept-1-yne	0.124	0.763	0.365	0.592
oct-1-yne	0.075	0.763	0.114	0.058
ethanol	0.008	0.007	0.004	0.002
methanol	0.006	0.005	0.002	0.005
propan-1-ol	0.006	0.002	0.007	0.009
propan-2-ol	0.007	0.013	0.012	0.011
isobutyl alcohol	0.588	0.449	0.386	0.251
benzene	0.755	0.197	0.115	0.411
toluene	0.814	0.942	0.300	0.241
ethylbenzene	1.529	0.258	0.553	0.729
acetone	0.111	0.000	0.052	0.057
butan-2-one	0.088	0.045	0.109	0.156
thiophene	0.016	0.014	0.016	0.001
pyridine	0.010	0.007	0.008	0.006
methyl acetate	0.001	0.001	0.000	0.006
ethyl acetate	0.025	0.036	0.010	0.000

Table C-9: Combined uncertainty (in percent) on IDAC values in DES2 at T = 313.15, 323.15, 333.15 and 343.15 K.

Experimental uncertainties at T [K]				
Solutes	**T=313.15**	**T=323.15**	**T=333.15**	**T=343.15**
n-hexane	1.59	2.10	2.33	0.92
n-heptane	0.94	0.98	1.23	0.87
n-octane	0.85	1.16	1.06	0.47
cyclopentane	0.16	0.10	0.32	0.28
cyclohexane	0.66	1.82	0.51	0.28
cycloheptane	0.17	0.06	0.58	0.72
cyclooctane	3.21	3.46	1.31	2.16
hex-1-ene	0.35	2.57	0.09	0.65
hept-1-ene	0.92	3.95	1.00	4.37
hept-1-yne	0.30	1.91	0.98	1.68
oct-1-yne	0.14	1.53	0.25	0.14
ethanol	0.62	0.57	0.66	0.60
methanol	0.77	0.81	0.38	0.87
propan-1-ol	0.21	0.06	0.29	0.41
propan-2-ol	0.24	0.48	0.47	0.44
isobutyl alcohol	5.40	4.99	5.07	3.76
benzene	3.83	1.08	0.68	2.61
toluene	1.93	2.38	0.79	0.67
ethylbenzene	1.81	0.34	0.79	1.13
acetone	2.15	0.01	1.09	1.24
butan-2-one	0.89	0.47	1.21	1.80
thiophene	1.46	1.30	1.51	0.13
pyridine	2.42	1.80	2.11	1.44
methyl acetate	0.13	0.12	0.04	0.53
ethyl acetate	1.22	1.73	0.47	0.00

Table C-10: Combined uncertainty on IDAC values in DES3 at T = 313.15, 323.15, 333.15 and 343.15 K.

Experimental uncertainties at T [K]				
Solutes	**T=313.15**	**T=323.15**	**T=333.15**	**T=343.15**
n-hexane	0.369	0.105	0.163	0.488
n-heptane	1.281	0.068	7.715	8.803
n-octane	1.675	0.953	0.479	1.041
cyclopentane	1.309	0.625	0.767	0.520
cyclohexane	2.162	0.861	0.118	0.174
cycloheptane	1.698	2.187	2.476	3.049
cyclooctane	0.527	0.366	0.443	0.302
hex-1-ene	0.093	0.076	0.170	0.313
hept-1-ene	0.270	0.316	0.084	0.057
hept-1-yne	0.103	0.008	0.016	0.068
oct-1-yne	0.221	0.042	0.037	0.165
ethanol	0.011	0.001	0.008	0.017
methanol	0.005	0.003	0.008	0.016
propan-1-ol	0.050	0.005	0.002	0.020
propan-2-ol	0.002	0.008	0.005	0.005
isobutyl alcohol	0.020	0.045	0.021	0.055
benzene	0.037	0.110	0.089	0.047
toluene	0.240	0.332	0.264	0.348
ethylbenzene	0.479	0.630	0.628	1.072
acetone	0.066	0.016	0.054	0.032
butan-2-one	0.020	0.025	0.004	0.015
thiophene	0.001	0.007	0.009	0.022
pyridine	0.000	0.002	0.002	0.004
methyl acetate	0.002	0.001	0.000	0.002
ethyl acetate	0.002	0.002	0.001	0.001

Table C-11: Combined uncertainty (in percent) on IDAC values in DES3 at T = 313.15, 323.15, 333.15 and 343.15 K.

Experimental uncertainties at T [K]				
Solutes	**T=313.15**	**T=323.15**	**T=333.15**	**T=343.15**
n-hexane	0.54	0.15	0.23	0.65
n-heptane	1.32	0.07	8.98	10.09
n-octane	1.42	0.78	0.39	0.81
cyclopentane	4.73	2.30	2.87	1.86
cyclohexane	6.28	2.42	0.32	0.45
cycloheptane	4.15	5.38	6.11	7.46
cyclooctane	1.03	0.70	0.84	0.57
hex-1-ene	0.18	0.15	0.32	0.58
hept-1-ene	0.45	0.51	0.13	0.10
hept-1-yne	1.30	0.09	0.20	0.81
oct-1-yne	3.09	0.57	0.49	2.15
ethanol	0.64	0.04	0.48	1.05
methanol	0.38	0.21	0.66	1.38
propan-1-ol	2.30	0.23	0.12	1.02
propan-2-ol	0.10	0.38	0.21	0.23
isobutyl alcohol	0.82	2.13	1.07	3.11
benzene	0.38	1.15	0.94	0.50
toluene	1.76	2.45	1.94	2.59
ethylbenzene	2.47	3.27	3.26	5.51
acetone	1.26	0.33	1.14	0.70
butan-2-one	0.32	0.41	0.07	0.27
thiophene	0.15	0.95	1.08	2.63
pyridine	0.04	0.81	1.00	1.48
methyl acetate	0.15	0.09	0.03	0.20
ethyl acetate	0.22	0.15	0.11	0.07

Table C-12: Combined uncertainty on IDAC values in DES4 at T = 313.15, 323.15, 333.15 and 343.15 K.

Experimental uncertainties at T [K]				
Solutes	**T=313.15**	**T=323.15**	**T=333.15**	**T=343.15**
n-hexane	0.197	0.199	0.617	0.295
n-heptane	0.340	0.062	0.630	0.920
n-octane	1.045	0.897	0.444	0.203
cyclopentane	0.447	0.332	0.296	0.421
cyclohexane	0.388	0.017	0.433	0.295
cycloheptane	0.390	0.307	0.139	0.086
cyclooctane	0.488	0.409	0.233	0.022
hex-1-ene	0.387	0.309	1.157	1.235
hept-1-ene	0.304	0.068	0.242	0.034
hept-1-yne	0.086	0.093	0.029	0.014
oct-1-yne	0.086	0.071	0.035	0.000
ethanol	0.021	0.013	0.012	0.001
methanol	0.015	0.003	0.010	0.000
propan-1-ol	0.042	0.025	0.016	0.000
propan-2-ol	0.037	0.027	0.027	0.031
isobutyl alcohol	0.024	0.019	0.008	0.000
benzene	0.102	0.081	0.013	0.029
toluene	0.137	0.128	0.068	0.015
ethylbenzene	0.210	0.147	0.101	0.009
acetone	0.052	0.059	0.006	0.024
butan-2-one	0.068	0.037	0.020	0.010
thiophene	0.008	0.007	0.003	0.001
pyridine	0.002	0.001	0.001	0.000
methyl acetate	0.010	0.012	0.010	0.010
ethyl acetate	0.007	0.008	0.001	0.004

Table C-13: Combined uncertainty (in percent) on IDAC values in DES4 at T = 313.15, 323.15, 333.15 and 343.15 K.

Experimental uncertainties at T [K]				
Solutes	**T=313.15**	**T=323.15**	**T=333.15**	**T=343.15**
n-hexane	0.70	0.94	3.21	1.61
n-heptane	1.10	0.22	2.41	3.80
n-octane	2.61	2.38	1.24	0.62
cyclopentane	4.79	3.96	3.72	4.97
cyclohexane	3.24	0.16	3.91	3.04
cycloheptane	2.87	2.42	1.16	0.76
cyclooctane	3.01	2.68	1.61	0.16
hex-1-ene	2.59	2.33	8.83	9.53
hept-1-ene	1.56	0.38	1.45	0.20
hept-1-yne	4.73	5.10	1.59	0.81
oct-1-yne	5.18	4.27	2.14	0.02
ethanol	3.92	2.53	2.45	0.24
methanol	4.40	0.80	3.02	0.11
propan-1-ol	6.62	4.01	2.77	0.07
propan-2-ol	4.94	3.70	3.78	4.60
isobutyl alcohol	3.00	2.82	1.39	0.04
benzene	4.93	3.97	0.66	1.47
toluene	4.47	4.22	2.30	0.51
ethylbenzene	4.60	3.30	2.31	0.21
acetone	3.24	3.72	0.40	1.61
butan-2-one	3.56	1.98	1.04	0.56
thiophene	5.12	4.22	2.05	0.44
pyridine	2.23	1.38	1.09	0.40
methyl acetate	3.17	3.65	2.86	2.04
ethyl acetate	1.91	2.20	0.28	1.14

APPENDIX D

COMPUTER PROGRAM

This appendix presents the programs coded in Matlab used for the evaluation of activity coefficient at infinite dilution and the experimental uncertainty.

D.1. Coded program for IDAC calculation in Matlab

```
%Mr Nkululeko Nkosi (3 September 2016)**** nkullenkosi@gmail.com
%Main file for infinite dilution activity coefficient computation%
```

Variables

```
%t     Column temperature.
%R     Ideal gas constant.
%n3    Number of moles of the solvent.
%g     infinite dilution activity coefficient.
%Vn    Net retention volume.
%P1    Saturated vapour pressure at temperature for the solute at t
(column).
%B11   Second virial coefficient of the solute.
%V1s   Molar volume of the solute.
%V1inf Partial molar volume of the solute at infinite dilution (=V1*)
%B12   Cross second virial coefficient of the solute and carrier gas.
%P0    Outlet pressure (same as atmospheric pressure).
%J23   Pressure correction term.
%Vc    Critical molar volume of pure solute.
%Tc    Critical temperature of the pure solute.
%w     Acentric factor of the pure solute.
%U0    Corrected carrier gas outlet flowrate from the column.
%n     Number of carbon atoms in the solute.
%tr    Solute retention time.
%tg    Unretained gas retention time.
%Tc12  Mixed Critical temperature.
%Tc22  Carrier gas critical temperature.
%Tc11  Solute critical temperature.
%Vc11  Solute critical molar volume.
%Vc22  Carrier gas critical molar volume.
%Vc12  Mixed critical molar volume.
%Ic11  Solute critical ionisation potential.
```

```
%Ic22  Carrier gas critical ionisation potential.
%Ic12  Mixed critical ionisation potential.
%Tf    Flow meter outlet temperature.
%Pw    Vapour pressure of water at Tf.
%U     Measured carrier gas flowrate from flowmeter.
%mp    Packing total mass in the column.
%wtper Solvent mass percent.
%Mm    Solvent molecular mass.
%.....................................................................%
```

Experiment data

```
close all
clc
workspace


t=40                    % column temperature in oC
trair=0.604;            % tr of the unretained component in min
trsolute=0.872;         % tr solute in min
P_outlet=100.7;         % kPa
P_inlet=137.7;          % in kPa
U_flowmeter= 12.5;      % in ml/min
temp_flowmeter=22.1; % oC
```

Column Loading

```
Mm=92;                  % Molar mass of the solvent (3)
mp=2.5586;              % mass of the packing
wtper=30.16;            % Mass percent of the solvent in the packing
```

Components

```
component='n-hexane'
carrier_gas='helium'
flowmeter_liquid='water'
%---------------------------------------------------------------------%
```

Calculations

```
T=t+273.15;
P0=P_outlet*1e3;        % Pa
Pin=P_inlet*1e3;        % in Pa
U0=U_flowmeter/60/1e6   % in ml/min
Tf=temp_flowmeter+273.15;
tr=trsolute*60;         % retention time of solute in seconds
tg=trair*60;            % retention time of the unretained component in
                       seconds
```

```
R=8.314 ;                %ideal gas constant
```

Properties of n-hexane

```
prop1=function_switch_properties(component)
prop2=function_switch_properties(carrier_gas)
propw=function_switch_properties(flowmeter_liquid)


A1=prop1(1)
B1=prop1(2)
C1=prop1(3)
tmin=prop1(4);tmax=prop1(5);
Tc11=prop1(6)
Pc11=prop1(7)*1e3
Vc11=prop1(8)*1e-6
w11=prop1(9)
n1=prop1(10)
Ic11=prop1(11)
```

Properties of water vapour

```
Aw=propw(1); Bw=propw(2); Cw=propw(3);tminw=propw(4);
tmaxw=propw(5);Tcw=propw(6); Pcw=propw(7)*1e3;
Vcw=propw(8)*1e-6; ww=propw(9);nw=propw(10);Icw=propw(11);


A2=prop2(1)
B2=prop2(2)
C2=prop2(3)
tmin2=prop2(4); tmax2=prop2(5);
Tc22=prop2(6)
Pc22=prop2(7)*1e3
Vc22=prop2(8)*1e-6
w22=prop2(9)
n2=prop2(10)
Ic22=prop2(11)


P1=5.46518e4             %P1=(10^(A1-(B1/(t+C1))))/760*101325
Pw=(10^(Aw-(Bw/(temp_flowmeter+Cw))))/760*101325
%-----------------------------------------------------------------------%

n3=(mp*wtper)/Mm/100


%The mixed critical volume, %(i.e Helium and solute(m^3/mol)
Vc12=(1/8)*(Vc11^(1/3)+Vc22^(1/3))^3


Ic12=(Ic11+Ic22)*((Vc11^(1/3)+Vc22^(1/3))^6)/(Vc12^2)  %The ionisation
potential of the mixture
Tc12=128*((Tc11+Tc22)^0.5)*((Ic11*Ic22)^0.5)*(Vc11*Vc22)/((Ic11+Ic22)^0.
5)/((Vc11^(1/3)+Vc22^(1/3))^6)  % The critical properties of the mixture
```

```
%Tc12=sqrt(Tc11*Tc22)*(2*sqrt(Ic11*Ic22)/(Ic11+Ic22))*(sqrt(Vc11*Vc22)/V
c12)^2


n12=0.5*(n1+n2)  %The number of carbon atoms of the mixture (n2=1 for
helium);(i.e Helium and solute)


A function to calculate the virial coefficients
B11=Vc11*(0.43-0.886*(Tc11/T)-0.694*(Tc11/T)^2-0.0375*(n1-
1)*(Tc11/T)^(4.5))


B12=Vc12*(0.43-0.886*(Tc12/T)-0.694*(Tc12/T)^2-0.0375*(n12-
1)*(Tc12/T)^(4.5))


J23=(2/3)*(((Pin/P0)^3)-1)/(((Pin/P0)^2)-1)


V1s=(Vc11)*(0.29056-0.08775*w11)^((1-(T/Tc11))^(2/7)) % The molar volume
of the solute, is given by:
V1inf=V1s;
%.....................................................................%

Ufcorr=U0*(1-(Pw/P0))*(T/Tf) % The corrected outlet volumetric flowrate,
%(i.e n-hexane (m^3/s)and(K))


%Vn=(J23^(3))*Ufcorr*(tr-tg)


Vn=(J23^-1)*Ufcorr*(tr-tg)
%.....................................................................%


%Determination of gamma infinity:

log_g=log((n3*R*T)/(Vn*P1))-((B11-V1s)*P1/(R*T))+((2*B12-
V1inf)*(J23)*P0/(R*T))


temperature=t
component
gamma_infinity=exp(log_g)
```

D.2. Coded program for combined uncertainty calculation in Matlab

Gamma infinite uncertainty calculations

```
%Variables considered%
sysm n3 T Vn P1sat B11 B12 Pout V1sat V1gama J23 R
```

```
% Gamma infinite equation
gamma_infinity =((n3*R*T)/(Vn-P1sat))*exp((Po*J23*(2*B12-V1sat)-
(P1sat)*(B11-V1sat))/(R*T))
%-----------------------------------------------------------------%
```

Variables worked out differential equations

Number of moles of solvent

```
% ans = -(R*T*exp(-(P1sat*V1gamma + B11*P1sat - 2*B12*J23*Pout +
J23*Pout*V1sat)/(R*T)))/(P1sat - Vn)

% diff(g,n3)
%.................................................................%
```

System temperature

```
% ans = - (R*n3*exp(-(P1sat*V1gamma + B11*P1sat - 2*B12*J23*Pout +
J23*Pout*V1sat)/(R*T)))/(P1sat - Vn) - (n3*exp(-(P1sat*V1gamma +
B11*P1sat - 2*B12*J23*Pout + J23*Pout*V1sat)/(R*T))*(P1sat*V1gamma +
B11*P1sat - 2*B12*J23*Pout + J23*Pout*V1sat))/(T*(P1sat - Vn))

% diff(g,T)%
%.................................................................%
```

Net retention volume

```
% ans = -(R*T*n3*exp(-(P1sat*V1gamma + B11*P1sat - 2*B12*J23*Pout +
J23*Pout*V1sat)/(R*T)))/(P1sat - Vn)^2

% diff(g,Vn)
%.................................................................%
```

Saturated vapour pressure at temperature for the solute T (column)

```
% ans = (n3*exp(-(P1sat*V1gamma + B11*P1sat - 2*B12*J23*Pout +
J23*Pout*V1sat)/(R*T))*(B11 + V1gamma))/(P1sat - Vn) + (R*T*n3*exp(-
(P1sat*V1gamma + B11*P1sat - 2*B12*J23*Pout +
J23*Pout*V1sat)/(R*T)))/(P1sat - Vn)^2

% diff(g,P1sat)
%.................................................................%
```

Second virial coefficient of the solute

```
%ans =(P1sat*n3*exp(-(P1sat*V1gamma + B11*P1sat - 2*B12*J23*Pout +
J23*Pout*V1sat)/(R*T)))/(P1sat - Vn)


% diff(g,B11)
%.................................................................%
```

Cross second virial coefficient of the solute and carrier gas

```
% ans = -(2*J23*Pout*n3*exp(-(P1sat*V1gamma + B11*P1sat - 2*B12*J23*Pout
+ J23*Pout*V1sat)/(R*T)))/(P1sat - Vn)

% diff(g,B12)
%.....................................................................%
```

Outlet pressure (same as the atmospheric pressure)

```
% ans = -(n3*exp(-(P1sat*V1gamma + B11*P1sat - 2*B12*J23*Pout +
J23*Pout*V1sat)/(R*T))*(2*B12*J23 - J23*V1sat))/(P1sat - Vn)

% diff(g,Pout)
%.....................................................................%
```

Pressure correlation term (J23)

```
% ans = (n3*exp(-(P1sat*V1gamma + B11*P1sat - 2*B12*J23*Pout +
J23*Pout*V1sat)/(R*T))*(Pout*V1sat - 2*B12*Pout))/(P1sat - Vn)

% diff(g,J23)
%.....................................................................%
```

Partial molar volume of the solute at infinite dilution (V1sat)

```
% ans = (J23*Pout*n3*exp(-(P1sat*V1gamma + B11*P1sat - 2*B12*J23*Pout +
J23*Pout*V1sat)/(R*T)))/(P1sat - Vn)

% diff(g,V1sat)
%.....................................................................%
```

Molar volume of the solute (V1sat)

```
% ans =(P1sat*n3*exp(-(P1sat*V1gamma + B11*P1sat - 2*B12*J23*Pout +
J23*Pout*V1sat)/(R*T)))/(P1sat - Vn)

% diff(g,V1gamma)
```